

A STUDY OF THE CIS EFFECT OF
SOME PHOSPHORUS DONOR LIGANDS

by

Karen L. Chalk

B.Sc. (Hons., Chem.), Queen's University, 1979

A THESIS SUBMITTED IN PARTIAL FULFILLMENT OF
THE REQUIREMENTS FOR THE DEGREE OF
MASTER OF SCIENCE
in the Department
of
Chemistry

© Karen L. Chalk, 1981

SIMON FRASER UNIVERSITY

November 1981

All rights reserved. This thesis may not be reproduced in whole or in part, by photocopy or other means, without permission of the author

APPROVAL

Name: Karen L. Chalk

Degree: Master of Science

Title of Research Project: A Study of the Cis-Effect of Some Phosphorus Liqands

Supervisory Committee:

Senior Supervisor: R.K. Pomeroy
Assistant
Professor

D. Sutton
Professor

T.N. Bell
Professor

K.E. Newman
Internal
Examiner

Date Approved: November 26, 1981

PARTIAL COPYRIGHT LICENSE

I hereby grant to Simon Fraser University the right to lend my thesis, project or extended essay (the title of which is shown below) to users of the Simon Fraser University Library, and to make partial or single copies only for such users or in response to a request from the library of any other university, or other educational institution, on its own behalf or for one of its users. I further agree that permission for multiple copying of this work for scholarly purposes may be granted by me or the Dean of Graduate Studies. It is understood that copying or publication of this work for financial gain shall not be allowed without my written permission.

Title of Thesis/Project/Extended Essay

"A Study of the Cis-Effect of Some Phosphorus

Donor Ligands"

Author: _____

(signature)

Karen L. CHALK

(name)

December 3, 1981

(date)

Abstract

A kinetic study to investigate the cis-effect exerted by the ligand L in mer-Ru(CO)₃(L)(SiCl₃)₂ (L = phosphine or phosphite) is presented. The cis-effect is defined as the effect of L on the rate of substitution of a group adjacent to it in a metal complex. The rate of substitution by trimethylphosphite of the labile carbonyl, that which is cis to L and trans to SiCl₃, was measured for twenty-five compounds with different L groups. The rate of substitution, for most of the complexes studied, was found to increase as the size of L is increased. The size of L is measured as the ligand cone angle, a measure of the hypothetical solid cone which the ligand occupies in a metal complex. A rate enhancement of three orders of magnitude was observed on going from the smallest ligand, P(OCH₂)₃CC₂H₅ (cone angle 101°) to the largest ligand studied, P(mCH₃C₆H₄)₃ (cone angle 165°). There was no apparent relationship between the electronic properties of L and the rate of carbonyl substitution. The Arrhenius parameters, ΔS[‡] and ΔH[‡], were determined for each of the twenty-five reactions, and a linear relationship was observed between ΔS[‡] and the cone angle of the ligand, L. From these results, it was concluded that the cis-effect of L in this system is mainly steric in origin. Some exceptions were found to this general pattern. In the complexes containing P(OPh)₃, P(CH₂C₆H₅)₃ and some related ligands, very low ΔS[‡] values and reduced ΔH[‡] values were observed. From these activation

parameters, it is proposed that these complexes undergo substitution via an associative type mechanism; one in which the complexed ligand, L, assists in the bond-breaking process. The ligand participates in the reaction by employing the π -electrons of the aromatic ring to stabilize the transition state, which is electron deficient due to the loss of the CO group.

In some of the complexes of the type mer- $\text{Ru}(\text{CO})_3(\text{L})(\text{SiCl}_3)_2$, where L is an asymmetric ligand (e.g., PPh_2Cl), an extra CO stretching band was observed in the infrared spectrum. This is thought to be due to the presence of two rotational conformers in solution.

For Seymour's Fat Lady

Acknowledgments

I wish to express sincere thanks to Roland Pomeroy for his guidance and for his patience throughout the last two years.

Sincere thanks are also extended to:

Dr. D. Sutton, Dr. T. N. Bell and Dr. R.E. Grigg for their helpful discussions.

The technical staff of the Chemistry Department for their co-operation and assistance.

Randy Alex for providing the ^{31}P NMR spectra.

Diana Day (Beak Consultants Ltd.) for the use of her graphics material and equipment.

Leslie Vincent for cheerfully typing the manuscript.

Financial assistance was provided by the Chemistry Department of Simon Fraser University and Research Corporation (New York).

TABLE OF CONTENTS

	Page
Approval	ii
Abstract	iii
Dedication	v
Acknowledgments	vi
Table of Contents	vii
List of Tables	x
List of Figures	xii
List of Abbreviations	xiv
Chapter 1 INTRODUCTION	
1.1.1 General Introduction	1
1.2.1 The Compound <u>cis</u> -Ru(CO) ₄ (SiCl ₃) ₂ and the <u>Cis</u> - Effects of Phosphorus Donor Ligands.	3
1.2.2 Stereospecific Exchange	3
1.2.3 The <u>Cis</u> -Effect of Phosphorus Donor Ligands in <u>mer</u> -Ru(CO) ₃ (L)(SiCl ₃) ₂ .	6
1.3.1 Steric and Electronic Properties of Phosphorus Donor Ligands.	7
1.3.2 The Steric Parameter	11
1.3.3 The Electronic Parameter	16
1.3.4 Some Studies on the Properties of Com- plexes of Phosphorus Ligands: The Rel- ative Importance of Steric and Electronic Effects	18
1.4.1 The <u>Cis</u> -Effect: A Literature Review	23

1.4.2	Cis-Labilization and the Site Preference Model	24
1.4.3	Phosphorus Ligand Dissociation in Bis-Substituted Derivatives of Molybdenum and Chromium Hexacarbonyls	29
Chapter 2	SYNTHESIS AND CHARACTERIZATION OF THE COMPLEXES STUDIED	
	Results and Discussion	
2.1.1	Introduction	32
2.1.2	Infrared Spectra of Complexes with Asymmetrical Ligands	33
2.1.3	Preparation and Characterization of Derivatives of $\text{PCl}_n\text{Ph}_{3-n}$ ($n=0,1,2,3$)	48
	Experimental	
2.2.1	General Procedure	53
2.2.2	Preparation of Complexes of the Type $\text{mer-Ru}(\text{CO})_3(\text{L})(\text{SiCl}_3)_2$	54
2.2.3	Preparation of $\text{mer-Ru}(\text{CO})_3(\text{PF}_3)(\text{SiCl}_3)_2$	54
2.2.4	Preparation of $\text{mer-Ru}(\text{CO})_3(\text{PCl}_3)(\text{SiCl}_3)_2$	58
Chapter 3	PRELIMINARY INVESTIGATIONS TO ESTABLISH THE MECHANISM AND NECESSARY REACTION CONDITIONS	
	Results and Discussion	
3.1.1	Introduction	60
3.1.2	Kinetic Studies	62
3.1.3	Solvent Cage Experiment	64

3.1.4	Other Investigations Related to the Kinetic Measurements	70
3.1.5	Conclusions	71
	Experimental	
3.2.1	General Kinetic Procedure	72
3.2.2	Analysis of Results	72
3.2.3	Kinetic Studies	75
3.2.4	Solvent Cage Experiment	78
Chapter 4	RESULTS OF THE KINETIC STUDY	
	Results and Discussion	
4.1.1	Introduction	80
4.1.2	The Choice of Entering Ligand	80
4.1.3	The Results of The Kinetic Study	82
4.1.4	A Group of Four Exceptions to the General Pattern	98
4.1.5	The Results of the Kinetic Study of <u>mer</u> - $\text{Ru}(\text{CO})_3(\text{PF}_3)(\text{SiCl}_3)_2$	103
	Experimental	
4.2.1	General Kinetic Procedure	109
4.2.2	Kinetic Measurements of the Substitution Reaction of <u>mer</u> - $\text{Ru}(\text{CO})_3(\text{PF}_3)(\text{SiCl}_3)_2$	110
4.2.3	Kinetic Measurements of the Substitution Reaction of <u>mer</u> - $\text{Ru}(\text{CO})_3(\text{ETPB})(\text{SiCl}_3)_2$	116
	Appendices	117
	REFERENCES	120

List of Tables

		Page
1	A Demonstration of the Effect of Electronic Properties on M-P Bond Length	20
2	A Demonstration of the Effect of Size on M-P Bond Length	21
3	Infrared, Analytical and NMR Data for Complexes of the Type <u>mer</u> -Ru(CO) ₃ (L)(SiCl ₃) ₂ which Exhibit a Conformational Effect	44
4	Summary of Complexes of the Type <u>mer</u> -Ru(CO) ₃ (L)(SiCl ₃) ₂ , (L=asymmetric ligand)	46
5	Data for Complexes of the Type <u>mer</u> -Ru(CO) ₃ (L)(SiCl ₃) ₂ (L=PCl _n Ph _{3-n})	49
6	Infrared Data for new Complexes of the Type <u>mer</u> -Ru(CO) ₃ (L)(SiCl ₃) ₂	55
7	Analytical Data for new complexes of the Type <u>mer</u> -Ru(CO) ₃ (L)(SiCl ₃) ₂	56
8	³¹ P Phosphorus NMR Data for Some New Complexes of the Type <u>mer</u> -Ru(CO) ₃ (L)(SiCl ₃) ₂	57
9	Rate of Substitution of CO in Ru(CO) ₃ (PPh ₃)(SiCl ₃) ₂ versus L'.	65
10	Data and Calculations for the NMR Solvent Cage Experiment	69
11	Data and Results from Measurements of the Effect of the Concentration of Entering Ligand and the Effect of Light on the Reaction Rate	77

List of Tables(cont.)

12	Rate constants at 40°C for the Substitution of <u>mer</u> -Ru(CO) ₃ (L)(SiCl ₃) ₂	84
13	Results for the Substitution Reactions of <u>mer</u> - Ru(CO) ₃ [P(<u>p</u> -XPh) ₃](SiCl ₃) ₂	88
14	Arrhenius Parameters for the Substitution Reactions of <u>mer</u> -Ru(CO) ₃ (L)(SiCl ₃) ₂	90
15	The Results of the Kinetic Study of <u>mer</u> - Ru(CO) ₃ (L)(SiCl ₃) ₂ (L=P(CH ₂ Ph) ₃ , P(OPh) ₃ , P(O- <u>o</u> -Tol) ₃ and P(Ph) ₂ (<u>o</u> -MeOPh))	99
16	Results of the Experiment to measure the effect of P _{PF₃} on the rate of Substitution of <u>mer</u> - Ru(CO) ₃ (PF ₃)(SiCl ₃) ₂ at 54°C	105
17	Measured Rate Constants at Various Temperatures for all Ligands Studied	111

List of Figures

		Page
1	The Relationship between the Size of the Substituents and the Hybridization of the Lone Pair Orbital	9
2	The Cone Angle Measurement of a Phosphorus Donor Ligand	11
3	The Cone Angle Measurement for Asymmetric ligands	12
4	The Degree of Substitution (DS) of Carbonyl Groups from $\text{Ni}(\text{CO})_4$ versus cone angle (θ) measured from Molecular Models	13
5	The Process Used to Generate the Ligand Profile	15
6	An Example of a Ligand Profile Generated for Tri-cyclohexyl Phosphine	15
7	A Demonstration of the Effect of Electronic Properties on M-P Bond Length	19
8	The Site Preference Model	26
9	The Vibrational Modes of a Complex of the type $\underline{\text{mer}}\text{-M}(\text{CO})_3\text{L}_3$	34
10	The Infrared Spectrum of $\underline{\text{mer}}\text{-Ru}(\text{CO})_3(\text{PCl}_3)(\text{SiCl}_3)_2$	35
11	The Infrared Spectrum of $\underline{\text{mer}}\text{-Ru}(\text{CO})_2(^{13}\text{CO})(\text{PPh}_3)(\text{SiCl}_3)_2$	37
12	The Infrared Spectrum of $\underline{\text{mer}}\text{-Ru}(\text{CO})_3[\text{PPh}_2(\underline{\text{i}}\text{-Pr)}](\text{SiCl}_3)_2$	39
13	Newman Projections down the Ru-P bond for two Possible conformers of $\underline{\text{mer}}\text{-Ru}(\text{CO})_3(\text{PXY}_2)(\text{SiCl}_3)_2$	42

List of Figures(cont.)	Page
14 A Possible Conformer Which is Stable in the complex $\text{mer-Ru(CO)}_3[\text{P(OMe)}_2\text{Ph}](\text{SiCl}_3)_2$	47
15 Energy Profile for a Dissociative or D Mechanism	61
16 ^{31}P NMR Spectra for the Solvent Cage Experiment	67
17 A Typical Measurement of Absorbance for a Kinetic Run	73
18 An Example of a First Order Plot	76
19 A Plot of Rate Constant at 40°C versus θ , Tolman's Cone Angle	83
20 A Plot of $\ln k$ versus θ	85
21 The Relationship between k at 40°C and ν , Tolman's Electronic Parameter	87
22 ΔH^\ddagger versus ν , (Electronic Parameter)	91
23 ΔS^\ddagger versus θ , (Cone Angle)	92
24 An Illustration of Rate Enhancement due to Steric Labilization	96
25 Two Possible Conformations which may explain the Anomalous Results obtained for the Complexes of $\text{P(CH}_2\text{Ph)}_3$, P(OPh)_3 , $\text{P(O-}\underline{\text{O}}\text{-Tol)}_3$, and $\text{PPh}_2(\underline{\text{O}}\text{-MeoPh)}$	100

List of Abbreviations

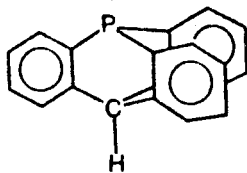
A	Absorbance
Bu ⁿ	n-butyl
Bu ^t	tert-butyl
Bz	benzyl
COD	cyclooctadiene
Δ Cs	coordination chemical shift(δ complex - δ ligand)
Cy	cyclohexyl
Et	ethyl
ETPB	4 ethyl - 2,6,7 trioxa-1-phosphabicyclo[2,2,2]octane
eV	electron volts
G ^o	Gibbs free energy
Δ G [†]	Gibbs free energy of activation
L	any monodentate phosphorus donor ligand
M	any transition metal
Me	methyl
OEt	ethoxy
OMe	methoxy
³¹ P{H}	proton decoupled phosphorus NMR data
Ph	phenyl
<u>i</u> -Pr	iso-propyl
R	alkyl
S	any substituent on phosphorus
T	transmittance
Tol	tolyl (CH ₃ C ₆ H ₅)
ρ	Tolman's electronic Parameter

List of Abbreviations(cont.)

θ Tolman's cone angle

δ NMR chemical shift

$P(\underline{O}-C_6H_4)_3CH$



$P(+)_3$ tri-tertbutyl phosphine

CHAPTER 1

Introduction

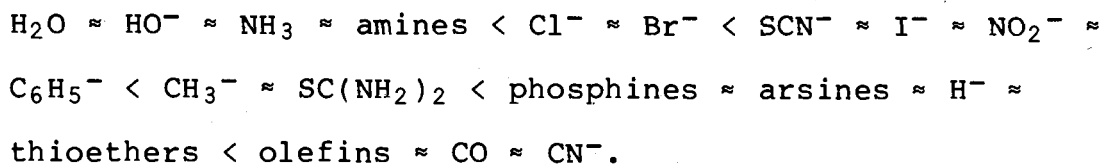
1.1.1 General Introduction

There have been many studies concerning the effect of a ligand in a metal complex on the lability of other ligands in the complex. These types of studies may be broken down into two general groups: (1) those examining the effect of the ligand trans to the leaving group on the rate of substitution (the "trans-effect"), and (2) those examining the effect of the ligand cis to the ligand which is leaving on the rate of substitution (the "cis-effect"). Most experiments have been done on square planar systems and the great majority of these investigations have been concerned with the trans-effect; the cis-effect is thought to be very small and difficult to predict^{1,2}.

Kinetic effects such as trans- or cis-effects must be carefully defined. The cis-effect is the effect of a coordinated group on the rate of substitution of a ligand cis to itself. This should be clearly distinguished from the cis-influence, which is defined as the effect of a coordinated ligand on the ground state properties of another ligand cis to itself. These ground state properties may include infrared stretching frequencies, NMR chemical shifts, or bond lengths and strengths.

In substitution processes of four-coordinate planar complexes, the trans-effect is well established, and has been shown to be more important than the cis-effect. Ligands can be ranked

in sequence according to the relative magnitude of their trans-effects. This series, arranged in order of increasing trans-effects, is as follows³:



A ligand is thought to exert a trans-effect by means of one of two processes. The first process is a ground state effect which causes weakening of a bond. This raises the ground state Gibbs free energy (G°) of the complex, and consequently lowers the activation energy (ΔG^\ddagger) for the reaction. The second process involves stabilization of the transition state for the reaction. Either of these two processes may lead to what is termed the kinetic trans-effect. Therefore, there are two types of ligands which may exert a trans-effect. One type of ligand weakens the bond trans to itself and the other stabilizes the transition state for the substitution reaction. It will be apparent that the first type of ligand has a trans-influence as well as exerting a trans-effect.

The cis-effect has been shown to be more important in substitution reactions of six-coordinate complexes than in substitution reactions of four-coordinate complexes⁴. However, the cis-effect has not been well studied. It has not been established what the basis of the cis-effect is, nor is it even clear which ligands are cis-labilizers in which situations.

Another question which remains inadequately answered is whether the cis-effect is steric or electronic in nature, or some combination of both.

The purpose of this study was to determine whether the cis-effect is steric or electronic in nature for phosphorus donor ligands. The cis-effects of a large number of phosphorus donor ligands in complexes of the type mer-Ru(CO)₃L(SiCl₃)₂ (L = phosphite or phosphine) have been studied to establish the cis-effects of these ligands. The cis-effects determined for the ligands were then compared to the steric and electronic properties of the ligands, and the nature of the cis-effects for phosphorus donor ligands in mer-Ru(CO)₃L(SiCl₃)₂ was established.

1.2.1 The Compound cis-Ru(CO)₄(SiCl₃)₂ and the Cis-Effects of Phosphorus Donors Ligands

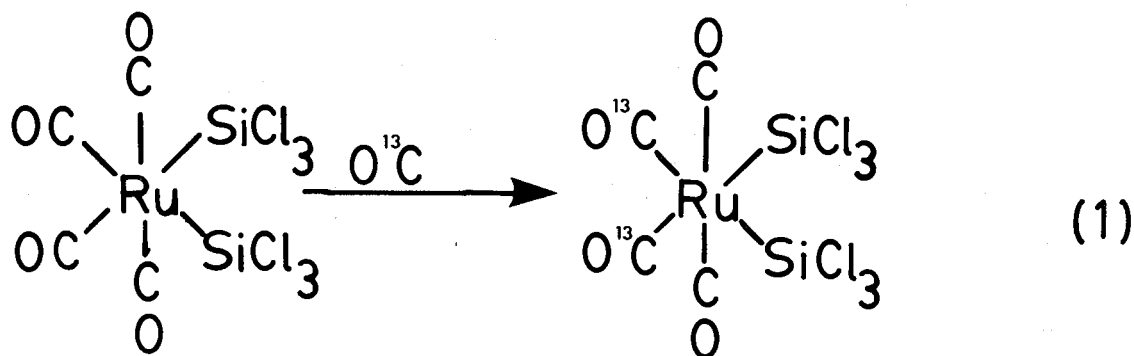
The special properties exhibited by tetracarbonylbis(trichlorosilyl)ruthenium, cis-Ru(CO)₄(SiCl₃)₂, makes this study of the cis-effect of phosphorus donor ligands possible. These special properties will be discussed and will be followed by a brief description of the work on the cis-effect that has been carried out using this complex.

1.2.2 Stereospecific Exchange

When cis-Ru(CO)₄(SiCl₃)₂ was first synthesized, an attempt was made to exchange the carbonyls with ¹³C-labelled CO, to measure the force constants of the equatorial and axial ligands⁵.

A solution of cis-Ru(CO)₄(SiCl₃)₂ was stirred at room

temperature for 18 hours under 1 atm ^{13}CO . The final infrared spectrum revealed that the exchange had been entirely stereospecific; the equatorial carbonyls had exchanged with the labeled ^{13}CO , while the axial carbonyls had not⁵ (Equation 1).

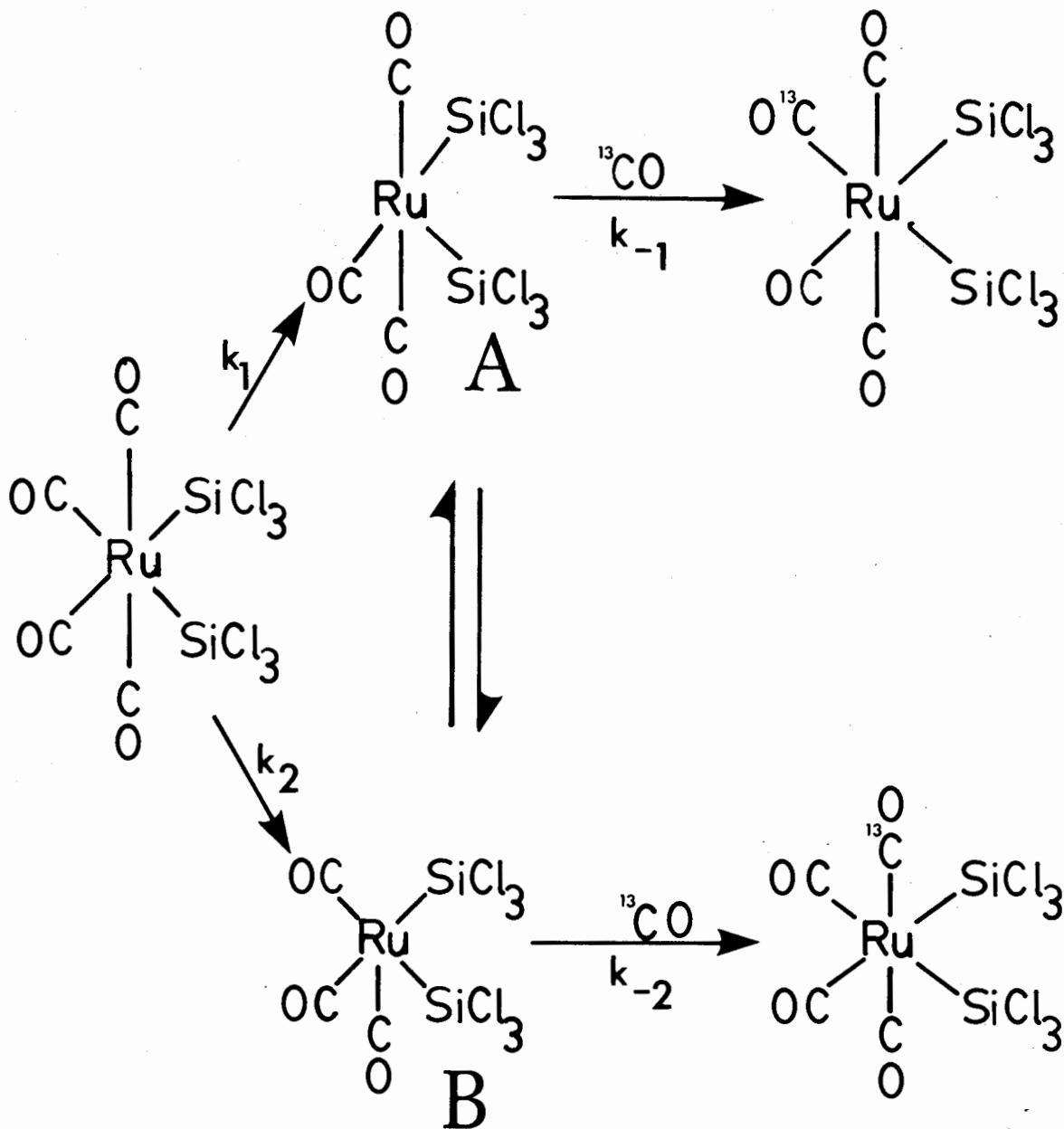


This finding has a number of implications. The first implication of the stereospecific exchange is that the SiCl_3 ligand must be a better trans-director than carbonyl, since those carbonyls trans to SiCl_3 are labile and those trans to carbonyl are not.

The second implication is that the position of carbonyl loss must be equivalent to the position of enrichment, i.e., trans to the SiCl_3 ligand. Scheme 1 outlines this mechanism.

One could imagine another mechanistic possibility, also shown in Scheme 1, involving axial loss, followed by rearrangement of the intermediate B and enrichment to give the observed equatorially substituted product. However, by the principle of microscopic reversibility, axial loss must necessarily lead to axial enrichment, since the transition state for axial enrichment would be of lower energy than that for equatorial enrichment. In other words, if axial loss, with rate constant

k_2 , is preferred to equatorial loss, with rate constant k_1 , then $k_1 < k_2$. This implies that either $k_{-1} < k_{-2}$ for the reincorporation of the carbonyl and, therefore, the axially enriched



Scheme 1

Possible mechanisms for enrichment of cis-Ru(CO)₄(SiCl₃)₂ with ^{13}CO .

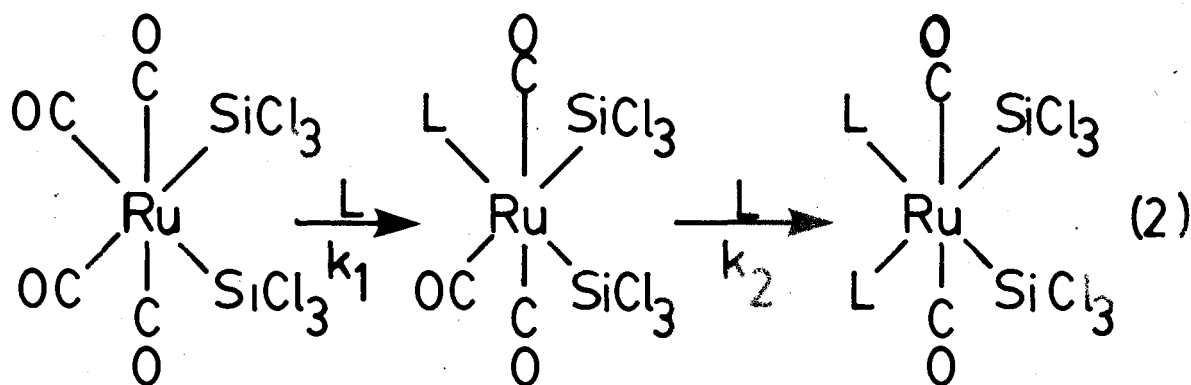
complex would be the preferred product, or scrambling between the intermediates A and B does not occur, due to a kinetic barrier. Therefore, since axial enrichment is not observed, axial loss must not occur, and equatorial enrichment may occur only via equatorial loss.

The third implication of the stereospecific exchange is that the five-coordinate intermediate A in Scheme 1 must be rigid. Since the second enrichment occurs without scrambling of the first ^{13}C O, any rearrangements which involve an intermediate which does not distinguish between axial and equatorial carbonyls throughout the reaction must be ruled out.

In conclusion, the exchange must proceed such that only the equatorial carbonyls are labile, and such that at all times the axial and equatorial carbonyls are distinguishable.

1.2.3 The *Cis*-Effect of Phosphorus Donor Ligands in $\text{mer-Ru}(\text{CO})_3(\text{L})(\text{SiCl}_3)_2$

The compound *cis*- $\text{Ru}(\text{CO})_4(\text{SiCl}_3)_2$ reacts stereospecifically with some two electron donors (L) to form mono- and bis-substituted derivatives⁶. (Equation 2)



In most cases the reaction may be terminated at the stage of mono-substitution, by precipitation of the desired product in the hexane reaction solvent. In the cases where the bis-derivative is desired, it is observed that while the reaction yielding a mono-substituted derivative occurs at the same rate (k_1) regardless of the incoming ligand, the rate of the second substitution (k_2) depends upon the nature of the ligand which has been complexed in the mono-substitution step.

The present study involves the examination of the quantitative relationship between the ligand (L) and the rate of the second substitution step (k_2). The relationship reflects the relative cis-effects of the ligands used in this study.

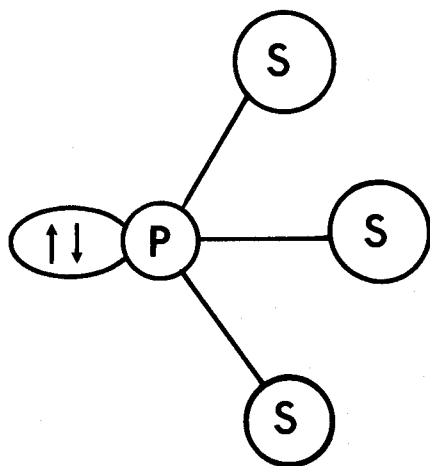
Because SiCl_3 is a stronger trans-directing group than CO, and because the parent compound cis- $\text{Ru}(\text{CO})_4(\text{SiCl}_3)_2$ loses the equatorial carbonyl in exchange reactions, one can be almost completely certain in all cases that the leaving carbonyl will be cis to L and trans to SiCl_3 , regardless of the identity of L.

1.3.1 Steric and Electronic Properties of Phosphorus Donor Ligands

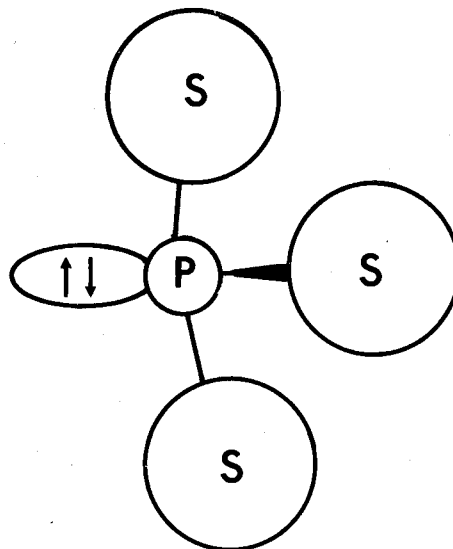
Introduction

The cis-labilizing effects of the phosphorus ligands examined in this study are compared to their steric and electronic properties. It should be noted at this point that however desirable it may be to completely separate steric and electronic

effects for comparison, they are, to some extent, interdependent. The relationship between the two properties is a simple one. The lone pair of electrons on phosphorus will be in a hybridized orbital which will have both s and p character, the relative proportions of which will depend on both the steric and electronic properties of substituents. According to Bent's rule⁷, a more electronegative substituent will prefer a hybridized orbital with more p character, forcing the lone pair orbital to assume greater s character. However, the relative s and p characters of the lone pair orbital will also be affected by the steric properties of the substituents. A larger substituent will force the substituent-phosphorus-substituent angle to open up, thus causing the lone pair orbital to have greater p character (see Fig. 1).



Small Substituents
lone pair and
substituents: sp^3



Large Substituents
lone pair: p, in the limit
substituents: sp^2

Fig. 1

The relationship between the size of substituents and hybridization of the lone pair orbital.

Therefore, it is clear that the electronic properties of the lone pair will be dependent on both the electronegativity and the size of the substituents and, further, that the steric properties of the ligand will depend to some extent on the electronic properties of the substituents.

However careful one must be not to expect complete separation of steric and electronic effects, to a certain extent the two may be examined individually. Tolman⁸ has defined the steric and electronic effects of ligands as follows:

electronic effect: a change in molecular property transmitted along chemical bonds.

steric effect: a change in molecular property resulting from non-bonding forces between parts of a molecule.

Tolman has recently defined and measured two quantities, the "cone angle" and the "electronic parameter", for use as quantitative measures of the steric and electronic properties of phosphorus ligands. These are discussed in Sections 1.3.2 and 1.3.3.

Since Tolman published his review describing these two parameters, the concept of cone angle has been expanded into a more detailed description of the steric properties of phosphorus donor ligands. Ferguson⁹ has developed the concept of ligand profile, which will be discussed in Section 1.3.2.

Finally, a small and certainly not exhaustive group of examples will be given to show how some research workers have used Tolman's two parameters to correlate chemical data such as bond lengths and bond strengths with the properties of phosphorus donor ligands in some complexes.

1.3.2 The Steric Parameter

As it became clear that some properties of phosphorus ligands, such as the ability of ligands to compete for coordination sites, could not be explained solely in terms of electronic effects, Tolman¹⁰ introduced a quantitative measure of the steric effect of phosphorus ligands, the ligand cone angle.

Tolman's measurement of cone angle can be approached in two ways: (1) by physical measurement of space-filling models or (2) by a chemical technique. In the first method, a space-filling model of the ligand is constructed using the smallest cone angle which does not induce substantial strain into the ligand. The cone angle is the apex angle of the cone which encloses the ligand and is centred on a metal atom which is assumed to be 2.28Å away (see Fig. 2).

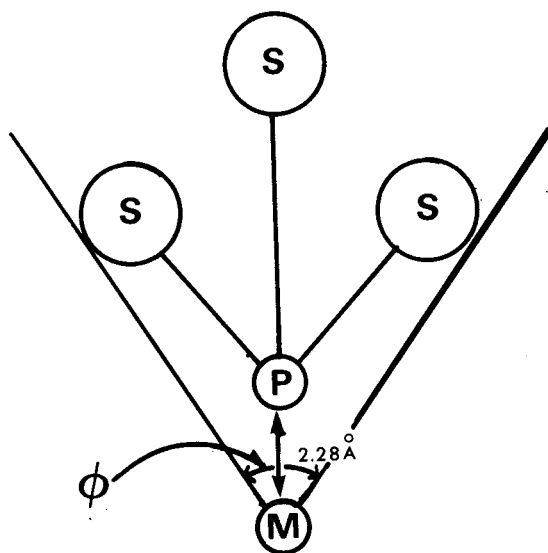


Fig. 2

The cone angle measurement of a phosphorus donor ligand.

In the case of an asymmetrical ligand, Tolman computes the average contribution of each substituent by means of (I) (see Fig. 3).

$$\phi_{\text{asymmetrical ligand}} = \frac{2}{3} \sum_{j=1}^3 \left[\frac{\phi_j}{2} \right] \quad (\text{I})$$

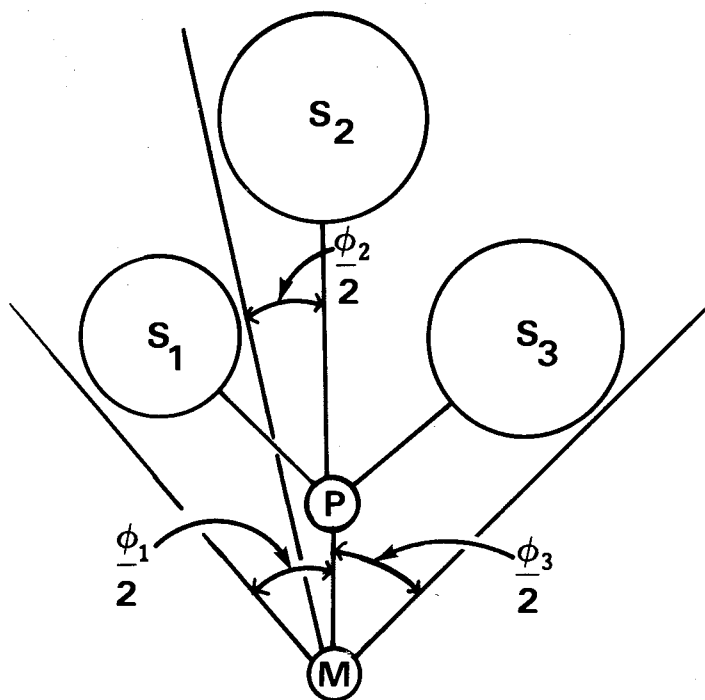


Fig. 3

The cone angle measurement for asymmetrical ligands.

Tolman's second method of measuring cone angle involves determining the degree of substitution of the ligand in $\text{Ni}(\text{CO})_4$ (Equation 3).



This method is useful in the case of ligands where a great deal of difference in cone angles can be measured by introducing various degrees of strain. With the $\text{Ni}(\text{CO})_4$ method one can assume that the ligand will resort to a situation which introduces a "reasonable" amount of strain into the system. An eight-fold excess of ligand L is combined with $\text{Ni}(\text{CO})_4$ in a sealed tube and the mixture is allowed to equilibrate at room temperature for eight days. The value of n, which may be any number from 0 to 4, is determined for each ligand. Since the cone angles of many ligands are available from measurements of space filling models, n, or degree of substitution DS, may be plotted as a function of cone angle (see Fig. 4).

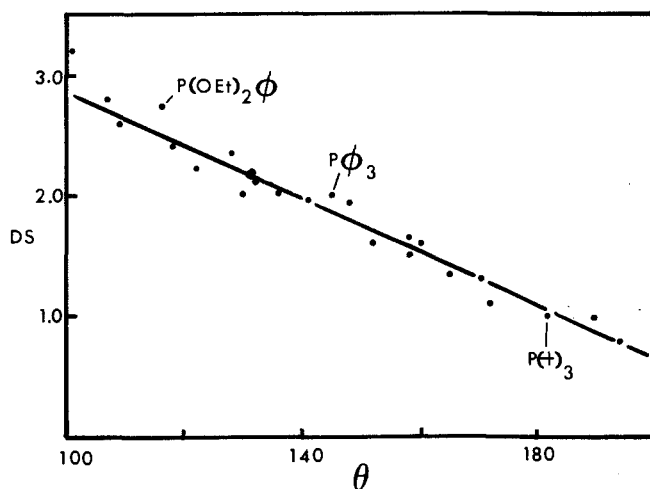


Fig. 4

The degree of substitution (DS) of carbonyl groups from $\text{Ni}(\text{CO})_4$ versus cone angle (θ) measured from molecular models.

A good correlation is obtained, and ligands whose cone angles are difficult to measure with space-filling models can be determined by measuring the degree of substitution in the $\text{Ni}(\text{CO})_4$ system and comparing the results with the known plot.

Since Tolman presented his methods of cone angle measurement, the concept of ligand bulkiness has been developed further. Ferguson⁹ used crystallographic data to measure the cone angle of tricyclohexyl phosphine in two complexes and obtained angles of 181° and 174° , which are in excellent agreement with Tolman's value of $179 \pm 10^\circ$ for tricyclohexylphosphine.

Ferguson introduces the concept of ligand profile^{9,11}, which, like cone angle, is a quantitative measure of ligand bulkiness. However, ligand profile places a greater emphasis on the fact that ligands are not solid cones, but are irregular "conic cogs". The ligand profile is a plot of the angle between the vector A and the ligand centre line, $\theta/2$ (see Fig. 5), as the vector is rotated around the ligand so that it just touches the surface of the van der Waals radii of the atoms in the ligand.

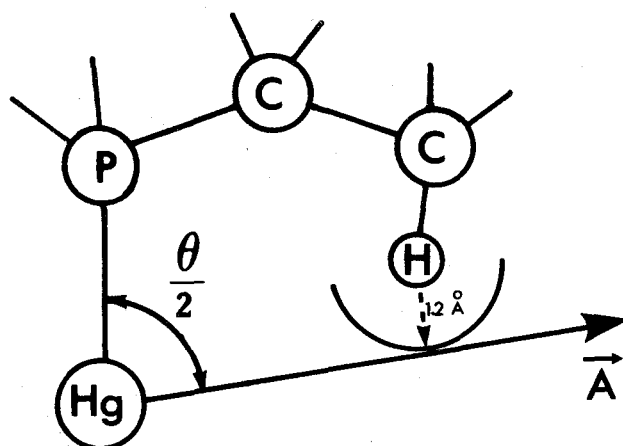


Fig. 5

The process used to generate the ligand profile¹².

The ligand profile clearly demonstrates the gaps between the substituents and the cog-like nature of the ligand (see Fig. 6).

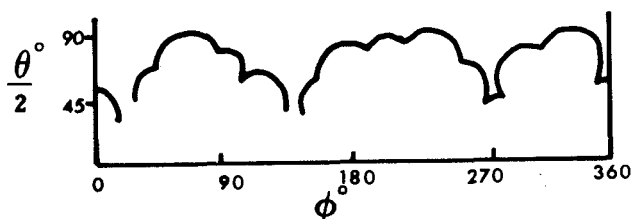


Fig. 6

An example of a ligand profile generated for tricyclohexyl phosphine in $[\text{Hg}(\text{PCy}_3)(\text{NO}_3)_2]_2$ ¹².

Ferguson's work also reveals the dynamic nature of the bulky phosphorus ligands. In compounds where more than one bulky ligand is present, the ligands may be compressed a

substantial amount. For example, in tris(tricyclohexyl phosphine)platinum, the ligand has a cone angle of 164° , whereas in (tricyclohexyl phosphine) mercuric diacetate, $(\text{Cy}_3\text{P})\text{Hg}(\text{OAc})_2$, the ligand has a cone angle of 179° ¹¹. Similar compression has also been observed in tri-tert-butylphosphine and tri-ortho-tolylphosphine in complexes¹¹.

1.3.3 The Electronic Parameter

In a series of complexes $\text{M}(\text{CO})_n\text{L}$ a direct correlation can be observed between the basicity of the ligand and the frequency of the carbonyl stretches in the infrared spectra¹³. The more basic ligand donates more electron density to the metal centre, increasing metal to carbonyl back donation. A greater amount of back donation lowers the force constant of the carbon-oxygen bond, thereby lowering the frequency of the carbonyl stretch.

The first attempt to rank phosphorus ligands according to their effect on carbonyl frequencies was presented by Strohmeier¹⁴. Tolman¹⁰ has expanded this idea to a more extensive series, eventually ranking approximately sixty ligands according to the frequency of the A_1 mode in the infrared spectra of complexes $\text{Ni}(\text{CO})_3\text{L}$ (L = tertiary phosphorus ligand)⁸. The value of the infrared stretching mode, in wavenumbers, is the electronic parameter (ν). The $\text{Ni}(\text{CO})_3\text{L}$ series was chosen principally because of the ease of preparation of the complexes.

However, any mono-substituted carbonyl complex would have been suitable.

Tolman also found that for complexes where the electronic parameter (ν) could not be measured, one could make excellent estimates of ν because of the additive nature of the individual contributions of the substituents on phosphorus to the ν for the whole ligand. The apparent contribution of a substituent to ν in the parent compound $P(S)_3$ is calculated by using (II):

$$\frac{\nu_{Ni(CO)_3[P(S)_3]} - 2056.1}{3} = \text{contribution of S} \quad (\text{II})$$

(ν_S)

The value of ν for a mixed phosphorus ligand can then be calculated from (III):

$$\text{For } P(S_1)(S_2)(S_3) \quad \nu = 2056.1 + \sum_{i=1}^3 (\nu_{S_i}) \quad (\text{III})$$

Perhaps because of the uncrowded nature of the $Ni(CO)_3$ fragment, Tolman's electronic parameter is unaffected by the steric properties of the ligands. This is demonstrated by comparing $P(o\text{-MeC}_6\text{H}_4)_3$ and $P(p\text{-MeC}_6\text{H}_4)_3$. Although these two ligands have cone angles of 194° and 145° , respectively, their electronic parameters are virtually identical. (See Appendix II.)

Since the publication of Tolman's definition of the electronic parameter, further work has correlated ^{13}C NMR data of

carbonyl complexes with ligand basicity¹⁵. The ^{13}C NMR spectra were recorded for a similar series of $\text{Ni}(\text{CO})_3\text{L}$ complexes. Each spectrum consisted of a sharp singlet in the carbonyl region, because the carbonyls in the $\text{Ni}(\text{CO})_3$ fragment are equivalent. Since the carbonyl carbon nuclei are increasingly deshielded as electron density on the metal increases, the greater the basicity of the ligand, the further downfield is the ^{13}C chemical shift. There is a good correlation between stretching force constants calculated from Tolman's infrared values and the ^{13}C chemical shifts for this series of nickel complexes.

Of particular interest to this study is the correlation observed between the carbonyl chemical shifts of $\text{Ni}(\text{CO})_3\text{L}$ complexes and the cis-carbonyl chemical shifts of the corresponding $\text{M}(\text{CO})_5\text{L}$ compounds ($\text{M} = \text{Cr}, \text{Mo}$). The correlation between the carbonyl chemical shifts (δ) in $\text{Ni}(\text{CO})_3\text{L}$ and the trans-carbonyl chemical shifts (δ) in $\text{M}(\text{CO})_5\text{L}$ was much weaker. This implies that the electronic parameter obtained by Tolman and Bodner for $\text{Ni}(\text{CO})_3\text{L}$ complexes best represents the electronic effect of ligand L on carbonyl groups cis to L.

1.3.4 Some Studies of the Properties of Complexes of Phosphorus Ligands: The Relative Importance of Steric and Electronic Effects

Ligand size has been found to have an unexpectedly large effect on many properties of phosphorus ligand complexes. In addition, it has been found that even in the absence of large

steric differences, two phosphorus ligands may produce vastly different properties in complexes because of different electronic properties. These two properties of phosphorus ligands may affect, for example, bond lengths, bond strengths, coordination number, and reactivity. While a comprehensive overview of all the work relating molecular properties to electronic and steric effects of phosphorus ligands is beyond the scope of this introduction, some examples will be given to show the type of investigations which have been pursued¹⁶.

Bond lengths have been shown to be dependent upon both steric and electronic properties of phosphorus ligands. More electronegative substituents direct more s character into the phosphorus lone pair orbital, which would be expected to result in shorter metal-phosphorus bond lengths. This effect has been nicely demonstrated in the complex shown in Figure 7.

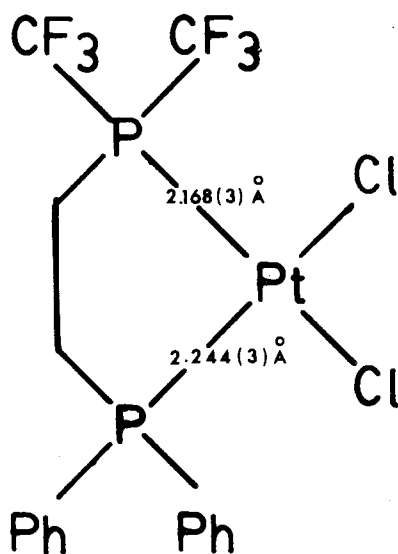


Fig. 7

A demonstration of the effect of electronic properties on M-P bond length.

Table 1: A Demonstration of the Effect of Electronic Properties on M-P Bond Length

Ligand	Electronic ⁸ Parameter ν (cm^{-1})	Steric ⁸ Parameter θ
PPH ₂ Me	2067.0	136°
P(CF ₃)Me	2097.9†	138 ± 3°†

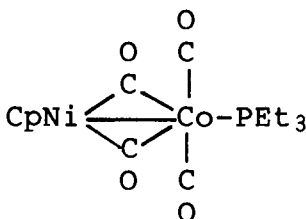
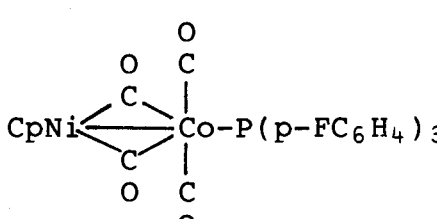
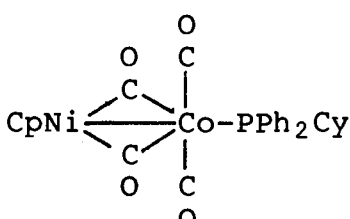
† calculated values.

The CF₃ and phenyl groups on the two phosphorus atoms are similar in size but differ greatly in electronic properties. The more electronegative CF₃ substituent causes the Pt-P bond to be shorter, as expected (see Table 1).

Bond lengthening can be correlated to steric effects in other cases. Table 2 shows three complexes where the substituents on the phosphorus ligand become progressively larger, and the M-P bond lengths become progressively longer¹⁷⁻¹⁹. This effect may be explained as follows: as the substituents on the phosphorus atom become larger, the angles between the substituents increase, conferring a greater p character on the lone pair orbital. This influence, coupled with general arguments of steric repulsion between the carbonyls on the cobalt and the substituents on the phosphorus, explains the observed bond

Table 2

A demonstration of the effect of size on the metal-phosphorus
bond length

	Cone angle ⁸ of phosphorus ligand	Electronic ⁸ parameter (cm ⁻¹)	M-P Bond Length (Å)
	132°	2061.1	2.236(1) ¹⁷
	145°	2071.3	2.242(3) ¹⁸
	155°	2064.8	2.269(2) ¹⁹

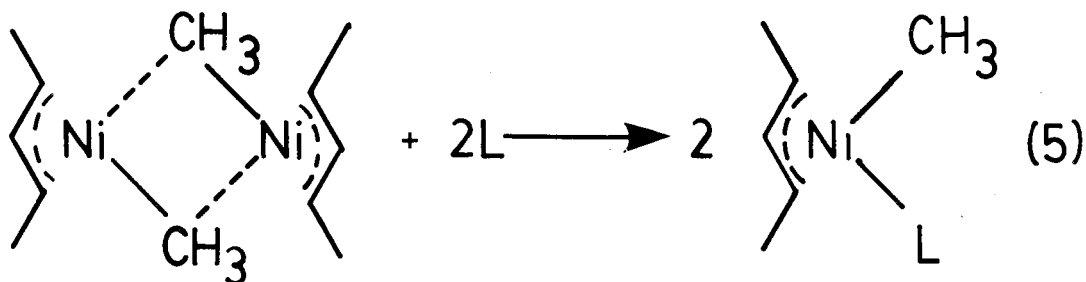
lengthening.

In a study of the replacement reactions of bis-cyclooctadiene nickel, Ni(COD)₂, with phosphines, it was shown that both the coordination number n and the Ni-P bond energy are almost

entirely dependent on the size of the ligand L (Equation 4).



As the cone angle of the ligand increases, the value of n decreases, and the dissociation energy of the Ni-L bond decreases as well²⁰. Similar results were obtained for reaction enthalpies in the production of [methyl-1-3-n(2-butenyl)nickelphosphine]²¹ (Equation 5).



In this reaction ΔH did not correlate with the steric parameter or with the electronic parameter individually. However, the data were shown to fit the following expression:

$$\Delta H_{\text{calc}} = 172.0 + 1.65 X_j - 0.56 \theta_j \text{ kJ/mol}$$

where X_j = Tolman's electronic parameter -2056.1

θ_j = Cone angle

Again one sees that as ligand size increases, bond energy decreases, and that bond energy is also related to Tolman's electronic parameter.

The present study of the cis-effect was undertaken with the intention of relating the cis-effect to Tolman's ligand parameters, in a way that is similar to the above work. It was hoped that either the steric parameter or the electronic parameter would dominate, or that the effect would result from some combination of both parameters.

1.4.1 The Cis Effect: A Literature Review

Introduction

By far the major contribution to research regarding the cis-effect has been made by Brown²²⁻²⁵. Of relevance to the present study is his work with substitution reactions of $\text{Mn}(\text{CO})_5\text{Br}$ and $\text{Re}(\text{CO})_5\text{Br}$ and their mono-substituted derivatives $\text{Mn}(\text{CO})_4\text{LBr}$ and $\text{Re}(\text{CO})_4\text{LBr}$ ($\text{L} = \text{P}(\text{C}_5\text{H}_5)_3$, NC_5H_5 or $\text{P}(\text{OC}_6\text{H}_5)_3$). To accompany these investigations, Brown has proposed a theory to explain the results, the site preference model, which he has supported with molecular orbital calculations. Throughout his work, Brown has emphasized the electronic properties of cis-labilizers, and has tried to explain their behaviour by correlating the ligands' abilities to act as cis-labilizers with their σ - and π -bonding capabilities.

Also related to the present study are investigations of the dissociation of L from complexes of the type $\text{M}(\text{CO})_4\text{L}_2$ ($\text{M} = \text{Cr}$, Mo ; $\text{L} = \text{phosphine}$ or phosphite)^{26,27}. Steric and electronic properties of the ligands and the ligands' conformation, i.e., whether they are cis or trans to each other, are important in

determining the relative rates of the ligand dissociation.

1.4.2 Cis-Labilization and The Site Preference Model

In the first in a series of related papers²², Brown established substitution patterns in $\text{Re}(\text{CO})_5\text{Br}$ and $\text{Mn}(\text{CO})_5\text{Br}$. Using the technique of ^{13}C O exchange and applying the principle of microscopic reversibility, it was found that equatorial dissociation of CO is preferred to axial loss, because the first ^{13}C O enrichment occurs cis to Br.

Equatorial preference can be rationalized using simple arguments of competition for π -bonding electrons. The trans or axial CO group will have stronger π -bonds because it competes for π -electrons with Br, a non π -acceptor. The stronger π -bonding is evidenced by a lower CO bond force constant in the axial carbonyl. However, Brown points out that this argument is faulty, because it would predict that $\text{Mn}(\text{CO})_6^+$ would have labile carbonyls, since all carbonyls are trans to another CO, and it does not.

Brown feels that at this stage one can rule out the possibility of cis-labilization being a ground state effect. In other words, the effect of a cis-labilizer is not to weaken bonds cis to it. He proposes that the ligand stabilizes the transition state leading to cis-carbonyl dissociation, and consequently increases the rate of that dissociation.

In his second paper²³ Brown uses the same technique of ^{13}C O exchange to study substitution patterns in $\text{cis-Mn}(\text{CO})_4\text{LBr}$ (L =

$P(C_6H_5)_3$, NC_5H_5 , $P(OC_6H_5)_3$). It was found that the carbonyl groups cis to both L and Br were labilized preferentially, and that they were more labile than the carbonyl groups of $Mn(CO)_5Br$. Because the labelled carbonyl group was eventually found in other positions after an induction period, it was proposed that the initial dissociation lead to a fluxional intermediate of lower coordination number.

Again, Brown emphasizes the electronic π -acceptor properties of the ligands to explain why triphenylphosphine and pyridine are better cis-labilizers than CO. His contention that cis-labilizers do not act to weaken bonds cis to themselves is supported by observations with cis- $Mn(CO)_4LBr$. PPh_3 is a cis-labilizer but since it is a poorer π -acceptor than CO, it should act to strengthen the π -bonds in the complex $Mn(CO)_4LBr$. Instead, this complex is more labile than the parent complex $Mn(CO)_5Br$.

Brown tries to rule out steric phenomena when rationalizing the cis-effect exerted by these ligands. First, he notes that there is no obvious steric interaction between CO and PPh_3 as indicated in the crystal structure of $Mn(CO)_4Cl(PPh_3)^{28}$. Second, he points out that the cis-effect exerted by pyridine is greater in these complexes than that exerted by PPh_3 , even though PPh_3 has a larger steric requirements. Third, the degree of cis-labilization due to PPh_3 and pyridine are the same in $Re(CO)_4LBr$ and $Mn(CO)_4LBr$, even though Re and Mn have substantially different covalent radii. Brown concludes that the

cis-labilization by PPh_3 and pyridine must be due to a transition state effect, in which the activated complex with L cis to the departing CO is of lower energy than the activated complex with L trans to the departing CO (see Fig. 8).

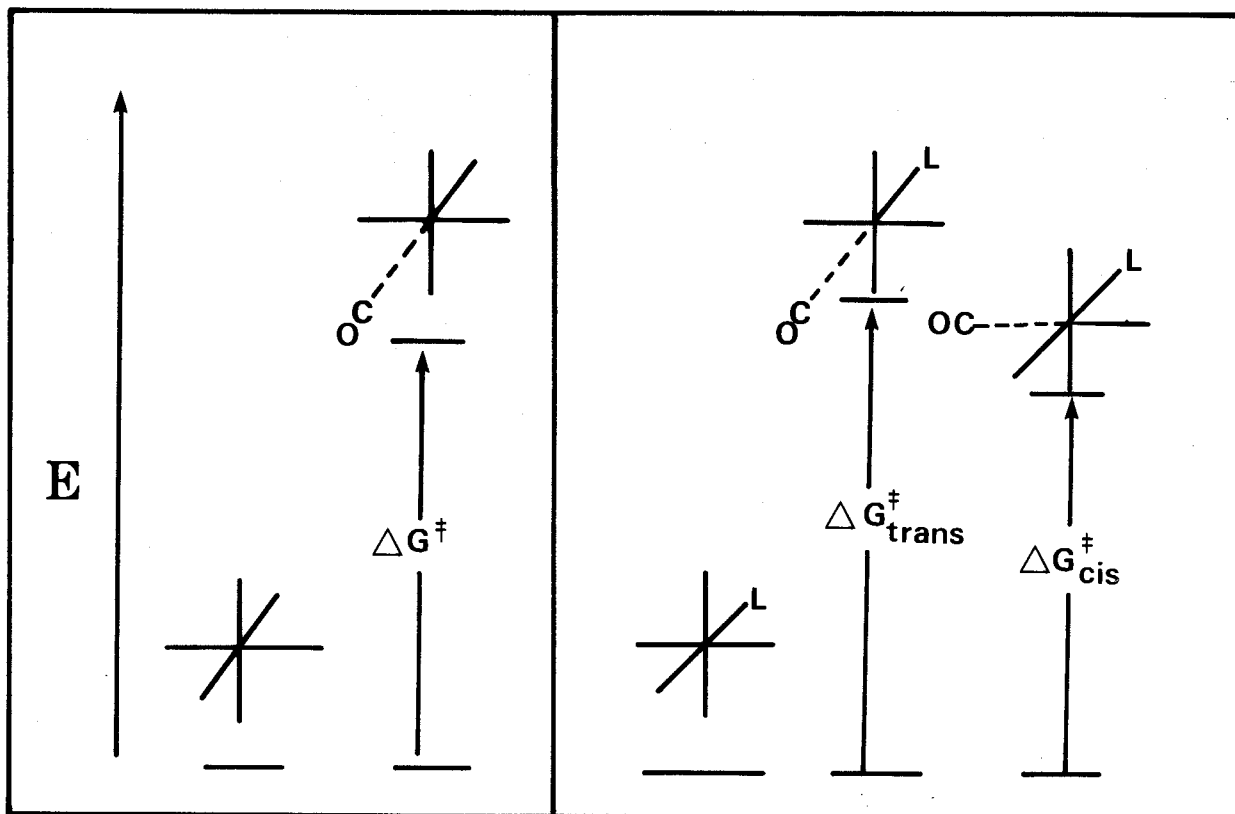


Fig. 8

The Site Preference Model. The energy of the activated complex for cis-labilization is less than the energy for trans-activation, although the ground states for the complexes are the same. Since $\Delta G^\ddagger_{\text{cis}} < \Delta G^\ddagger_{\text{trans}}$, L is a cis-labilizing ligand, in other words, it prefers the sites cis to the labile CO.

Brown fully develops his site preference model in the third paper in his series²⁴. He compares the effect of ligands in the basal position with their effect in the axial position in the square pyramidal intermediate. He assumes that anything which would stabilize the intermediate would also stabilize the transition state for a dissociative mechanism. This assumption is probably a good one for all the complexes Brown studied and, indeed, for most substitution reaction of carbonyls in octahedral complexes because, for these complexes, the dissociation almost always occurs via a SN1 type mechanism. The initial dissociation of CO is the rate-determining step and the reaction involves a discrete five-coordinate intermediate. Because the initial dissociation involves essentially complete M-CO bond rupture, it may be said that the intermediate resembles the transition state.

Ligands which are good cis-labilizers, Brown argues, will stabilize the square pyramid when they are in a basal position, thus favouring that reaction pathway (see Fig. 8). These ligands are predicted to be weak π -acceptors, like triphenylphosphine, for example.

An equivalent argument can be made for a trigonal bipyramidal intermediate instead of a square pyramidal intermediate, as Brown points out²⁴. The only necessary elements for the argument are that there exist two different sites in the intermediate, axial and equatorial, for example, and that the

cis-labilizing ligand shows a preference for one site over the other or, in other words, stabilizes the intermediate for one reaction pathway.

Brown has performed an extensive series of molecular orbital calculations²⁵ on the complexes and intermediates that he has studied, from which he draws two conclusions. First, his calculations support his prior conjecture that the cis-labilization observed is not a ground state effect, but is a transition state effect, such as described in his model. Second, the calculations indicate that ligands which are good electron donors, especially π -donors, tend to stabilize a five-coordinate intermediate representing the transition state when in the basal or equatorial position. The calculations can predict that ligands such as NO_3^- , Cl^- , NCO^- , and NC_5H_5 are potential cis-labilizers, but it is not possible to predict the relative abilities of these ligands to cis-labilize.

Brown concedes that his model does not predict that ligands such as phosphine could cis-labilize and speculates that the observed cis-effect of PPh_3 may be due to steric effects, withdrawing his previous statement regarding the improbability of steric phenomena affecting the cis-labilizing effect.

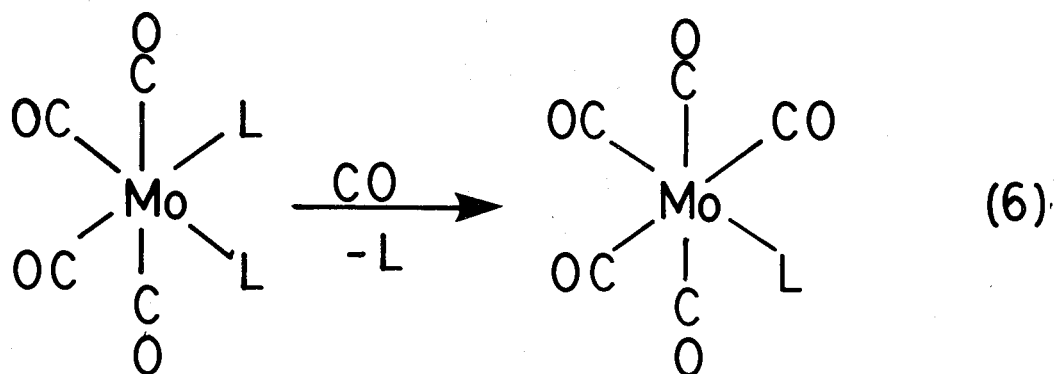
In summary, Brown has examined the systems $\text{Mn}(\text{CO})_5\text{Br}$, $\text{Re}(\text{CO})_5\text{Br}$, and their related derivatives and has established that in these compounds cis-labilization does occur. He has also established that arguments based solely on bond strengths

are not sufficient to explain cis-labilization in complexes. He has therefore proposed that cis-labilization is a transition state effect due to stabilization of the transition state by L, when L occupies certain sites in the complex. He has supported this so-called site preference model with molecular orbital calculations. However, throughout his work, Brown has concentrated on the π -acceptor properties of the ligands he has studied, perhaps because those ligands are of such different electronic character. Finally, after the model he has developed fails to predict that PPh_3 is a potential cis-labilizer, he concedes that PPh_3 may enhance reaction rate by steric means, and that there is possibly both a steric and an electronic component to the cis-effect.

1.4.3 Phosphorus Ligand Dissociation in Bis-Substituted Derivatives of Molybdenum and Chromium Hexacarbonyls

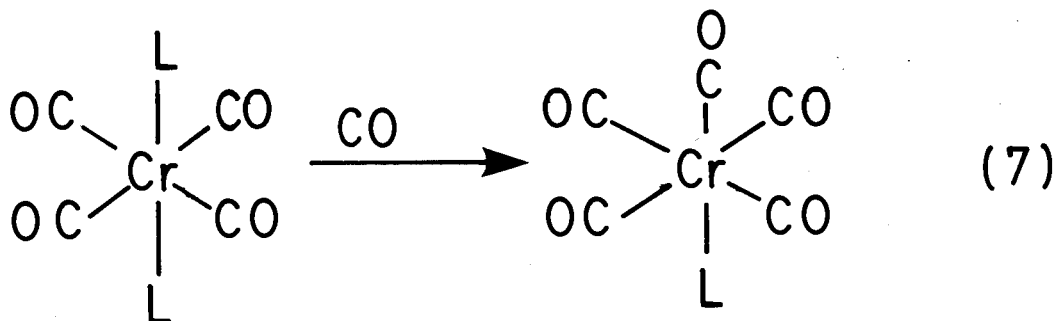
Two separate investigations of ligand dissociation in the substituted metal carbonyls $\text{M}(\text{CO})_4\text{L}_2$ ($\text{M} = \text{Cr}, \text{Mo}$; $\text{L} =$ phosphine or phosphite) have been reported^{26,27}. These are relevant to the present study of the cis-effect of phosphorus donor ligands.

The dissociation of L from cis- $\text{Mo}(\text{CO})_4\text{L}_2$ was reported by Darensbourg²⁶ (Equation 6).



It was found that the rate of dissociation of L was independent of the concentration of the incoming CO, and that the dissociation followed first order kinetics. The rates of dissociation of various ligands L were investigated and it was found that within a series of phosphines or phosphites, the rate increased as the cone angle of L increased. On going from $\text{PN}_3(\text{CH}_2)_6$ (cone angle 102°) to $\text{P}(\text{Cy})_2\text{Ph}$ (cone angle 162°), the rate increased by four orders of magnitude.

In a related experiment²⁷, Atwood investigated the rates of phosphorus ligand dissociation in trans- $\text{Cr}(\text{CO})_4\text{L}_2$ (Equation 7).



The rates spanned five orders of magnitude, depending upon the ligand L. The rates could not be correlated with steric properties of the ligands, perhaps because the trans configuration

minimizes steric interaction, while electronic interaction is maximized because of shared orbitals. However, the dissociation rates could be correlated with bond strengths. This is thought to be due to the different π -acceptor properties of the ligands.

In summary, these two studies showed that in complexes of the type $M(CO)_4L_2$, the rate of dissociation of L is dependent upon both steric and electronic properties of the phosphorus donor ligands. It would appear that when the ligands are in a cis configuration, the steric properties dominate, and when they are trans to each other the electronic or σ -donor/ π -acceptor properties are most important. However, in both studies only a few ligands were investigated, which leaves some doubt about the validity of the authors' conclusions. For example, Atwood²⁷ concluded that phosphines dissociate more rapidly than phosphites although he studied only four phosphorus donor ligands. In addition, from the viewpoint of the cis-effect of phosphorus ligands, too few cases have been studied to clearly differentiate between steric and electronic effects, making further study necessary.

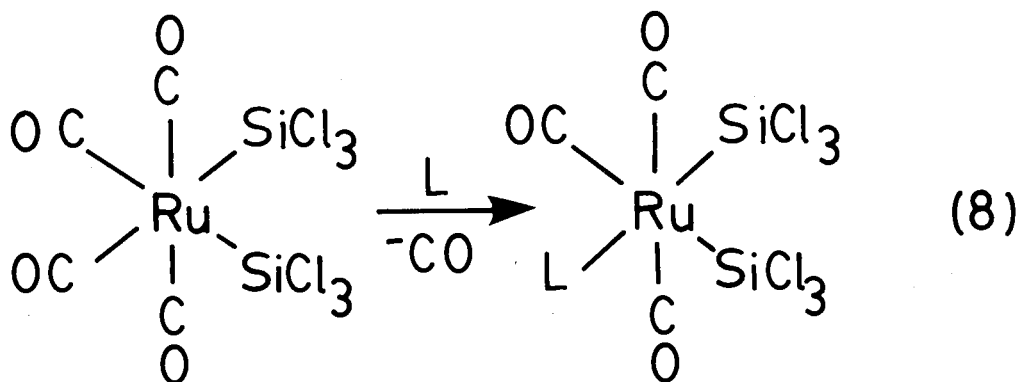
CHAPTER 2

Synthesis and Characterization of the Complexes Studied

Results and Discussion

2.1.1 Introduction

In order to study the kinetics of carbonyl dissociation in complexes of the type mer-Ru(CO)₃(L)(SiCl₃)₂, it was necessary to synthesize the complexes in one-gram quantities. The complexes were made by reacting cis-Ru(CO)₄(SiCl₃)₂ with L (Equation 8).



Most of the complexes have been prepared previously and with the exceptions of the derivatives of PF₃ and PCl₃ the methods of synthesis were routine and have been discussed previously²⁹.

Although this work is a kinetic study, some interesting results were obtained in the process of synthesizing these complexes. First, an interesting case of conformational isomerism was observed in the complexes mer-Ru(CO)₃L(SiCl₃)₂, when L is an asymmetrical ligand, which will be discussed. Second, the

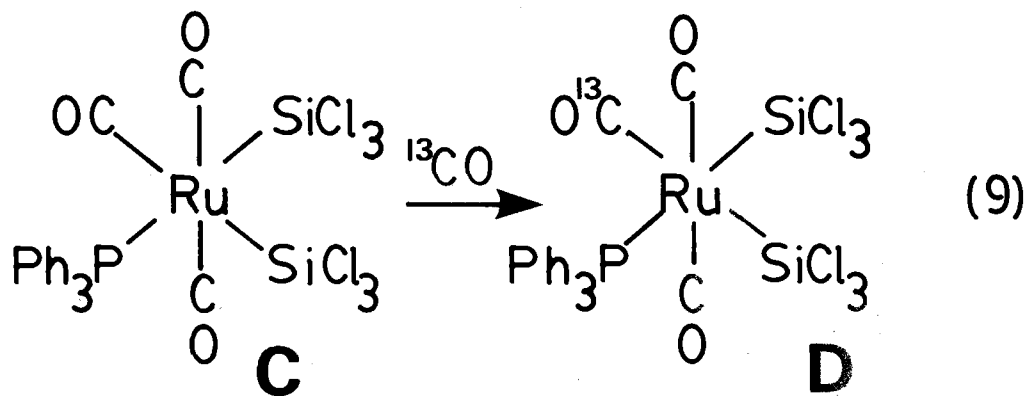
synthesis and characterization of complexes of the type mer- $\text{Ru}(\text{CO})_3(\text{L})(\text{SiCl}_3)_2$ (where $\text{L} = \text{PCl}_n\text{Ph}_{3-n}$; $n = 0, 1, 2, 3$) revealed a marked gradation of chemical and physical properties that also warrants discussion.

2.1.2 Infrared Spectra of Complexes with Asymmetrical Ligands

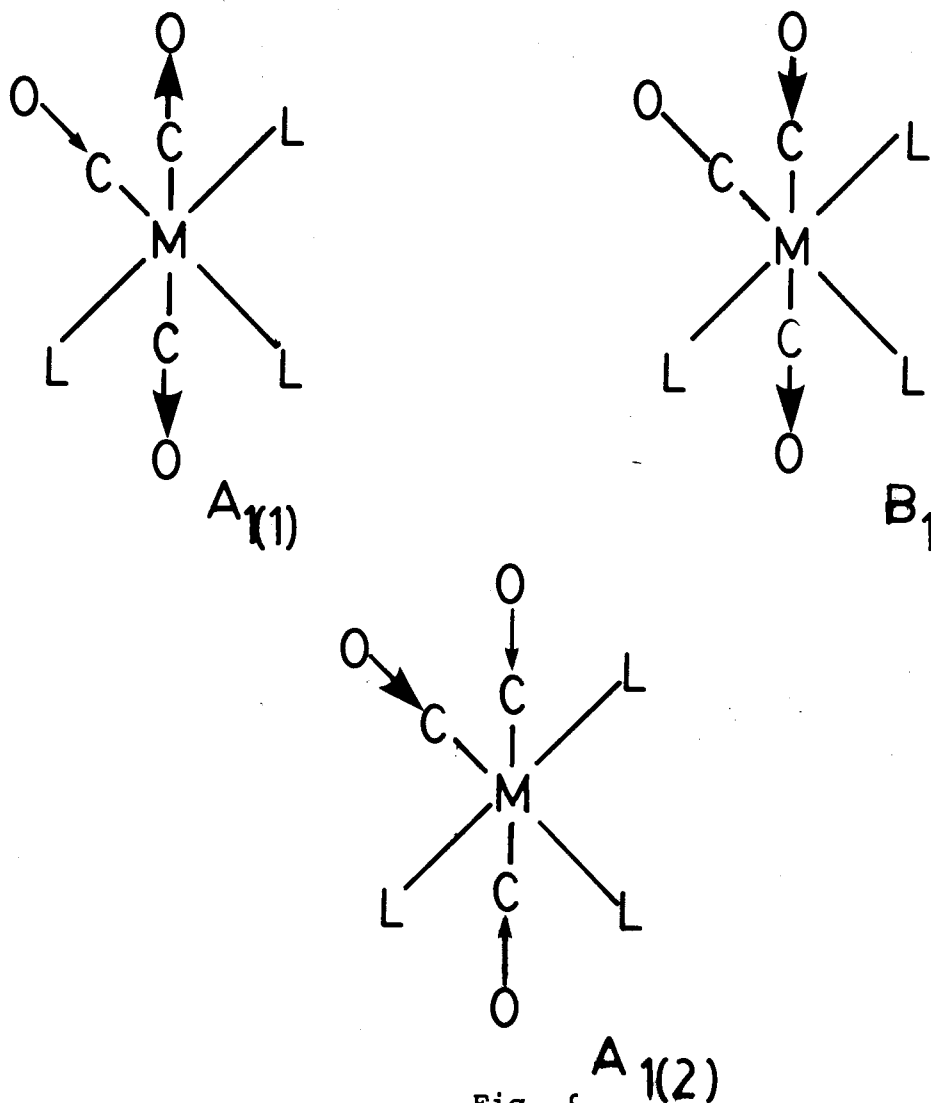
Octahedral complexes of the type mer- $\text{M}(\text{CO})_3\text{L}_3$ are expected to exhibit three fundamental bands in the carbonyl region of their infrared spectra. These bands can be attributed to three vibrational modes with symmetries A_1 (two) and B_1 . These are vibrational modes shown in Fig. 9.

Generally, the $A_1(1)$ band is the highest in energy, but the relative energies of the $A_1(2)$ and B_1 modes depend upon the nature of the complex. In all of the complexes in this study the second $A_1(2)$ mode is of a higher energy than the B_1 mode. An example is provided in Fig. 10.

This assignment has been clearly demonstrated by a simple ^{13}C CO exchange reaction (Equation 9).



The infrared spectra of C is similar to Fig. 10, (2117(w), 2075(m), 2050(s) cm^{-1}). The infrared spectrum of D (2109(vw), 2050(s), 2030(m) cm^{-1}) is shown in Fig. 11. The medium intensity band has shown a characteristic shift to lower frequency of 40-45 wavenumbers, evidence that it has been correctly assigned

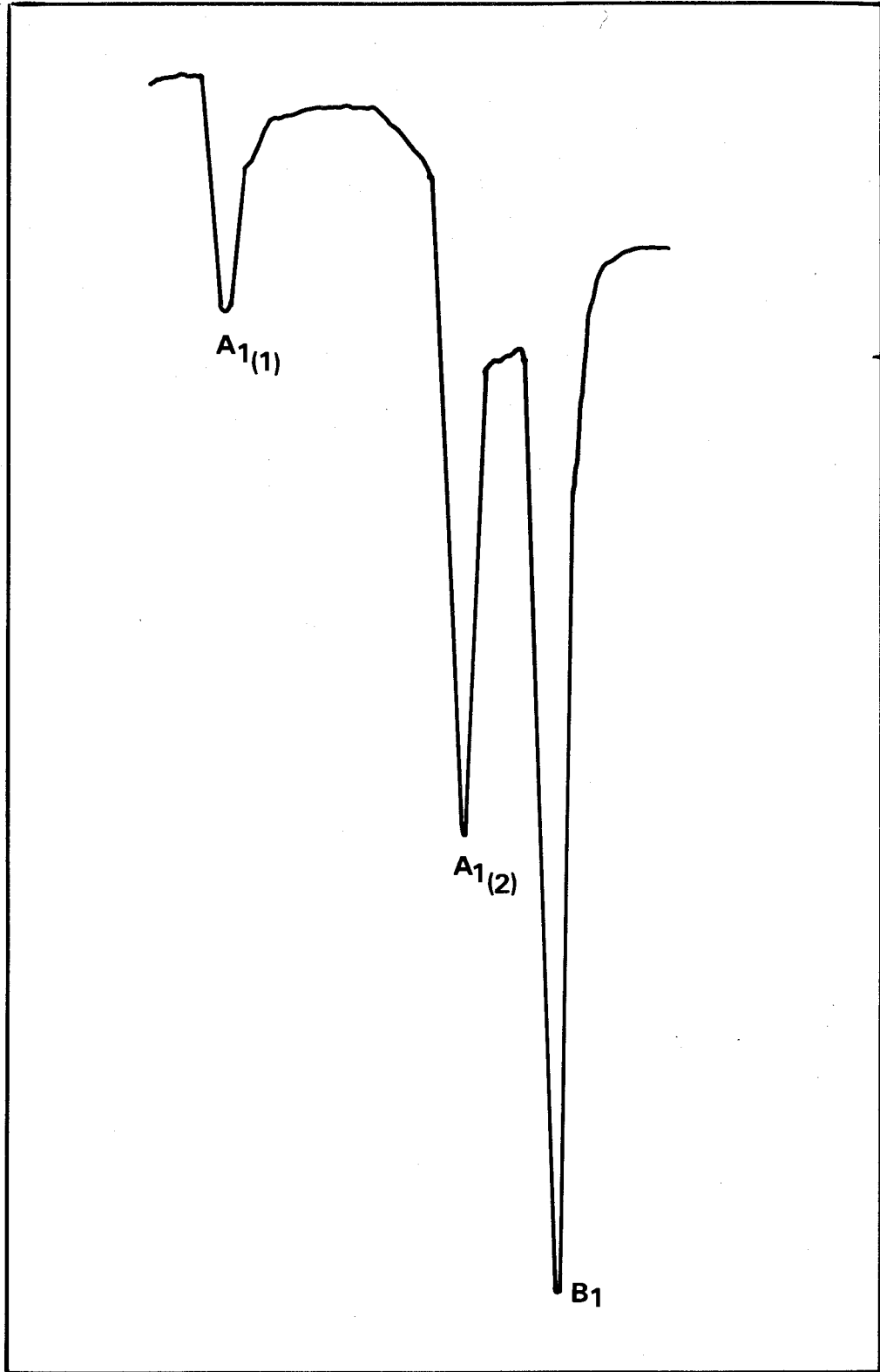


The vibrational modes of a complex of the type
mer-M(CO)₃L₃.

Fig. 10

The infrared spectrum of mer-Ru(CO)₃(PCl₃)(SiCl₃)₂, in
hexane.

% TRANSMITTANCE



2150

2100

2050

WAVENUMBER (cm⁻¹)

Fig. 11

The infrared spectrum of mer-

$\text{Ru}(\text{CO})_2(^{13}\text{CO})(\text{PPh}_3)(\text{SiCl}_3)_2$ in toluene.

·/· TRANSMITTANCE

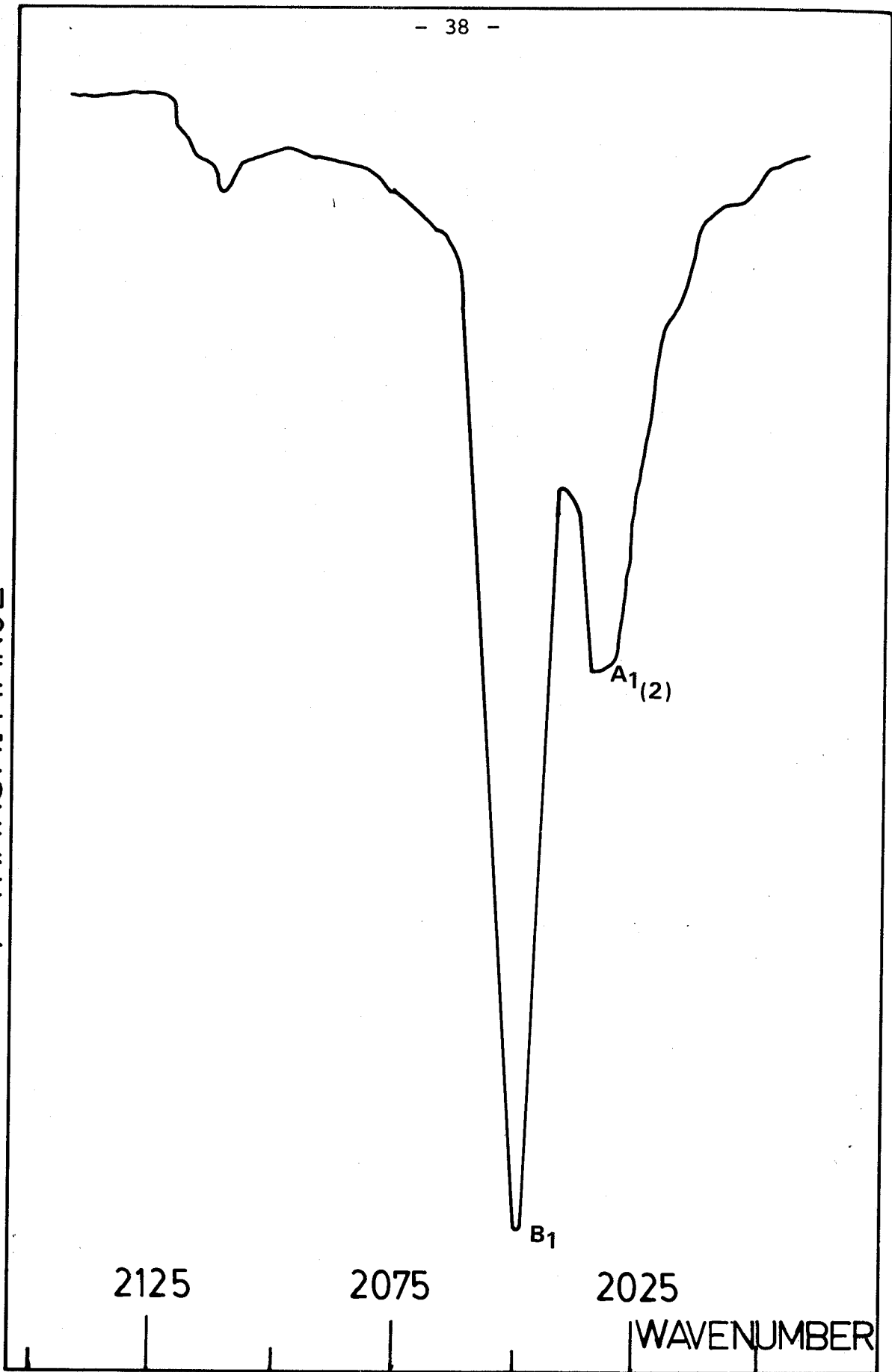
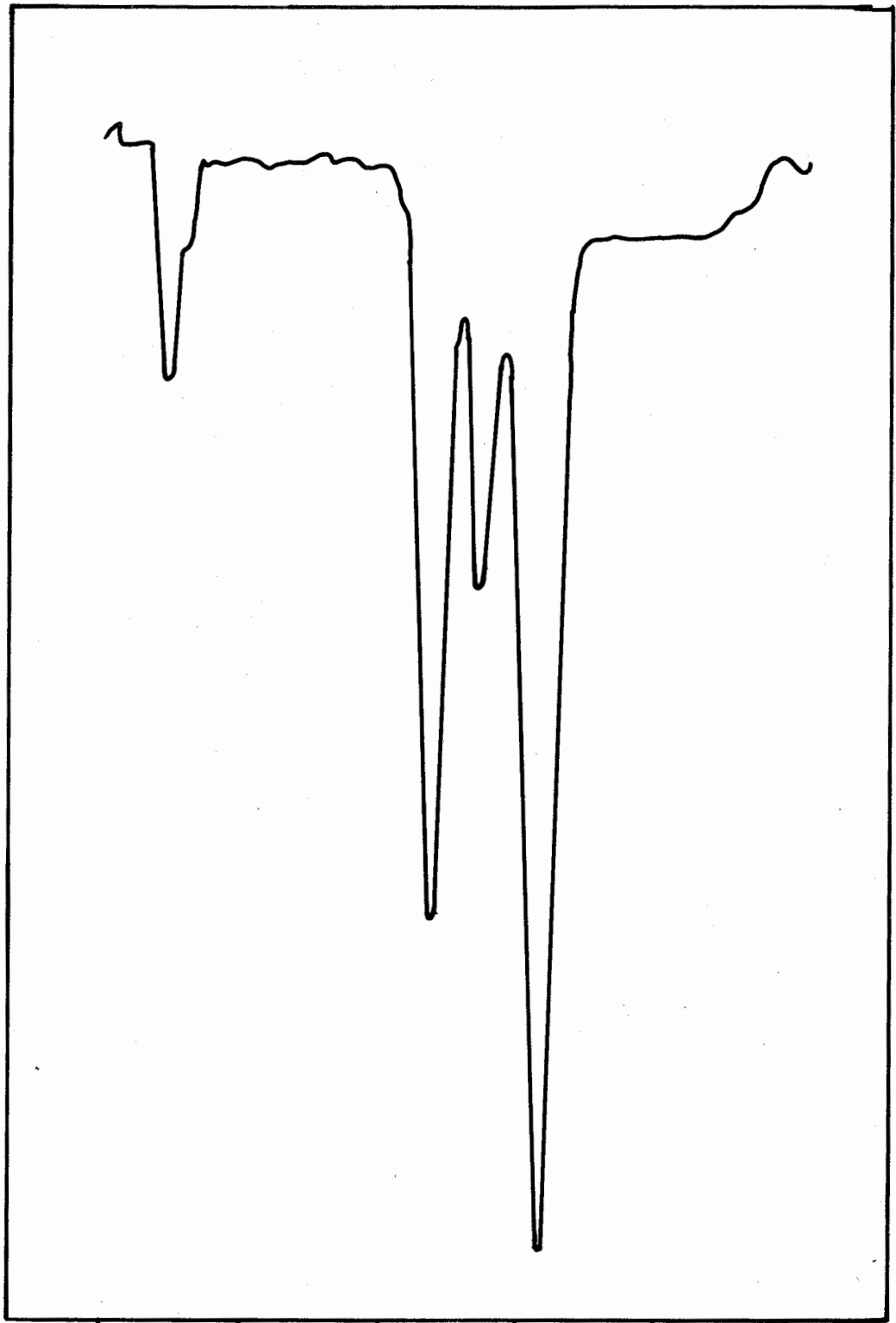


Fig. 12

The infrared spectrum of mer-Ru(CO)₃[PPh₂(i-Pr)](SiCl₃)₂ in hexane.

% TRANSMITTANCE



WAVENUMBER (cm⁻¹)

to the $A_{1(2)}$ mode, since this mode is largely the equatorial stretch. The $A_{1(1)}$ mode loses intensity and also drops in frequency, because the natural frequencies of the A_1 modes have become further separated and the coupling between them is greatly reduced. Since the $A_{1(1)}$ mode is now relatively uncoupled to the $A_{1(2)}$ mode, it is now totally symmetric and the selection rules dictate that it is not allowed. The B_1 mode remains unaffected, as expected, because the ^{13}CO is not involved in that particular mode. Therefore, the assignment as shown in Figs. 10 and 11 are consistent with the expected spectra for complexes of the type mer- $\text{M}(\text{L}_3)(\text{CO})_3$, and mer- $\text{ML}_3(\text{CO})_2(^{13}\text{CO})$.

However, in some complexes of the type mer- $\text{Ru}(\text{CO})_3\text{L}(\text{SiCl}_3)_2$, where L is an asymmetric ligand, another band appeared in the infrared spectrum adjacent to the low energy $A_{1(2)}$ band. An example is shown in Fig. 12. Since the relative intensities of the bands remain unchanged upon repeated recrystallization, the extra band is thought to be due to a conformational effect rather than due to an impurity.

Conformational effects on terminal carbonyl frequencies have been observed before³⁰⁻³³. Dalton has postulated that differences in steric compression of the carbonyl groups in different conformers account for the differences in carbonyl frequencies³². Steric compression of carbonyl groups causes destabilization of the π^* orbital. This will reduce the electron density of the π^* orbital, raising the frequency of the

CO bond vibration.

Examination of the spectra of the affected complexes reveals that while the B_1 and $A_{1(1)}$ bands are either only slightly broadened or unaffected, the $A_{1(2)}$ is split, revealing its greater sensitivity to the nature of the ligand.

Newman projections down the Ru-P bond are presented in Fig. 13 and show two possible conformations of the complex mer- $Ru(CO)_3(PXY_2)(SiCl_3)_2$.

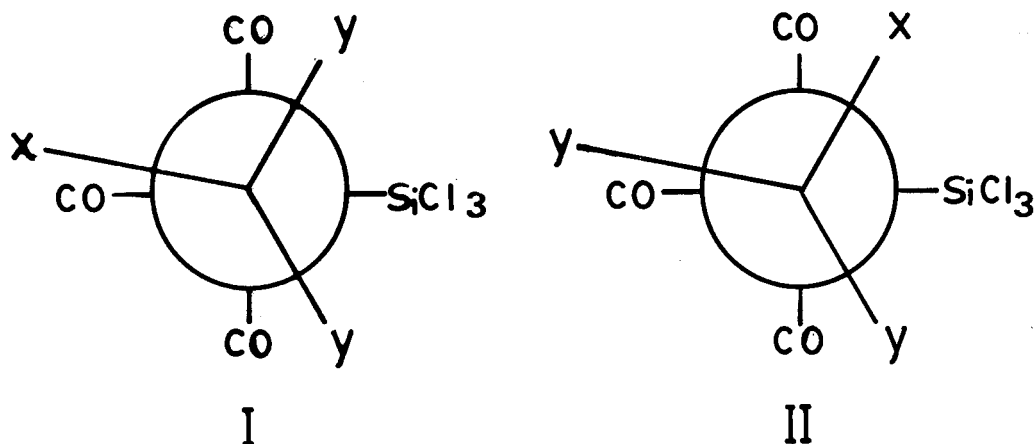


Fig. 13

Newman Projections down the Ru-P bond for two possible conformers of mer- $Ru(CO)_3(PXY_2)(SiCl_3)_2$. Note that one $SiCl_3$ group is directly behind the diagram and is not shown.

Since the $SiCl_3$ group has a larger steric demand than the carbonyl group, one can assume that the substituents on the phosphorus will be staggered with respect to the $SiCl_3$ group and

eclipsed with respect to the carbonyl group trans to the SiCl_3 group. In the case where the phosphorus ligand is of the type PXY_2 , the ligand has three possible orientations and, since two of the three orientations are equivalent, two different rotomers result, each with a different $A_1(2)$ mode frequency. The difference in the steric compression of the axial carbonyls in the two conformers is believed to be less marked than usual since the groups on the phosphorus do not directly eclipse these carbonyl groups. Table 3 contains data for complexes whose spectra exhibited this extra $A_1(2)$ band.

Table 3

Infrared, analytical and NMR data for complexes of the type $\text{mer-Ru(CO)}_3(\text{L})(\text{SiCl}_3)_2$ for complexes which exhibit a conformational effect.

L (cone angle)	Infrared Spectrum (in hexane)	Analysis	^{31}P NMR Chemical Shift ^a
		C H	
$\text{PPh}_2(\underline{i}\text{-Pr})$ (150°)	2113(w), 2066(m) 2056(w), 2048(s) ^b	calc. 31.32 2.48 found 31.37 2.59	55.01 ppm
$\text{P(CH}_3)_2\text{Ph}$ (122°)	2114(w) 2072(m), 2060(m) 2048(s)	c	c
PCl_2Ph (122°)	2126(w), 2087(m) 2081(m), 2065(s)	calc. 17.08 0.80 found 18.33 1.12	-161.4 ppm

a From 85% H_3PO_4 , downfield negative.

b See Fig. 12.

c See Reference 6.

In all complexes with the extra $A_1(2)$ band which were studied, the $A_1(2)$ band of lower frequency was less intense. Since the intensity of an infrared band is directly related to concentration, in all cases the less stable isomer has an $A_1(2)$ mode of lower frequency. This seems to contradict Dalton's observation³² that those conformers which have the greatest steric compression, and subsequently create a greater destabilization of the π^* orbitals of the carbonyl, should have a higher frequency. However, if one assumes that the major steric interaction in mer- $\text{Ru}(\text{CO})_3\text{L}(\text{SiCl}_3)_2$ complexes (L is asymmetrical) is between the groups on the phosphorus and the SiCl_3 group, then those complexes which are most thermodynamically stable will be those where the larger groups on the phosphorus point away from the SiCl_3 group and towards the carbonyl. Therefore, the more thermodynamically stable conformers will have the greater ligand-carbonyl interaction, and will exhibit the higher carbonyl frequencies.

Although all of the complexes which show this conformation effect contain an asymmetric ligand, not all of the complexes containing asymmetric ligands showed this effect. Table 4 shows the complexes (with asymmetric ligands) which do exhibit an extra band and those which do not.

For complexes of PXY_2 where Y is smaller than X, the extra band is observed, but if Y is larger than X, then the conformational effect is not observed. It is thought that when Y is

Table 4

Summary of complexes of the type mer-

Ru(CO)₃(L)(SiCl₃)₂ (L = asymmetrical ligand, PXY₂).

L	X ¹	Y	Predicted Most Stable Conformer
I. Complexes which show a conformational effect:			
PPh ₂ (<u>i</u> -Pr)	<u>i</u> -Pr	Ph	I
PMe ₂ Ph	Ph	Me	I
PCl ₂ Ph	Ph	Cl	I
II. Complexes which do not show effect:			
PClPh ₂	Cl	Ph	II
PMePh ₂	Me	Ph	II
P(OMe)Ph ₂	OMe	Ph	II
P(OMe) ₂ Ph	Ph	OMe	I

¹ X, Y, I, and II all refer to Fig. 13.

larger than X, conformer I (Fig. 13) is much less stable than conformer II, and I does not exist in solution in quantities great enough to be detected in the IR spectrum. There is only one complex which does not follow this general pattern, mer-Ru(CO)₃[P(OMe)₂Ph](SiCl₃)₂. It is possible that all the conformers of Ru(CO)₃[P(OMe)₂Ph](SiCl₃)₂ exhibit the same infrared stretching frequencies. Another possibility is that another conformer (Fig. 14) is more stable in this complex.

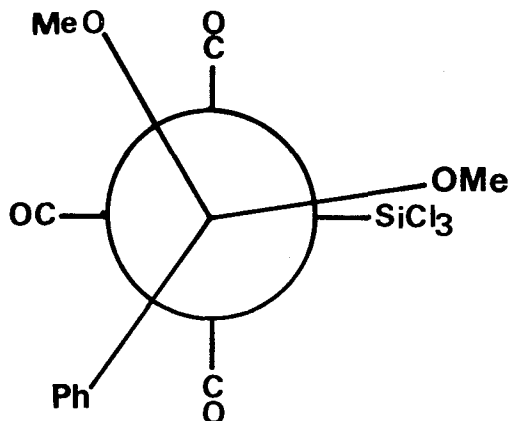


Fig. 14

A possible conformer which is stable in the complex mer-Ru(CO)₃[P(OMe)₂Ph](SiCl₃)₂.

The methoxy substituents were the smallest substituents to be studied, and perhaps the methoxy substituent to SiCl₃ interaction is less than the phenyl to carbonyl interaction in the predicted stable conformer, (I) in Fig. 13. This could introduce the possibility of another conformer (i.e., that illustrated in Fig. 14) being the more stable and only species

observable in the infrared spectrum.

2.1.3 Preparation and Characterization of Derivatives of $\text{PCl}_n\text{Ph}_{3-n}$ ($n = 0, 1, 2, 3$)

In the process of synthesizing the compounds with ligands $\text{PCl}_n\text{Ph}_{3-n}$ ($n = 0, 1, 2, 3$) it was observed that the complexes showed an interesting gradation in chemical properties, and it was decided that it would be worthwhile to fully characterize these compounds. Table 5 summarizes the properties of the ligands and the complexes which will be discussed.

All the CO bands in the infrared spectra of the complexes are progressively shifted to higher wavenumbers along the series of derivatives from PPh_3 to PCl_3 . This is to be expected, considering the parallel increase in the Tolman electronic parameter in the series of ligands.

The $^{31}\text{P}\{\text{H}\}$ NMR spectra of the complexes in the series also follow a distinct pattern, which is notable in itself, since ^{31}P chemical shifts are generally difficult to predict and are poorly understood⁸.

Phosphorus NMR shifts fall within a range of approximately 250 ppm. Many factors are thought to affect the value of the ^{31}P chemical shift, including the electronegativity of the substituents on the phosphorus and the angle between the substituents (i.e., the angle substituent-phosphorus-substituent, S-P-S), as well as less important variables such as solvent,

Table 5: Data for Complexes of The Type $\text{mer-Ru(CO)}_3(\text{L})(\text{SiCl}_3)_2, (\text{L}=\text{PCl Ph}_{3-n})$

Ref.	Ligand	Mp °C	Cone Angle	Electronic Parameter ^a Wavenumbers	IR Data Wavenumbers (hexane)	³¹ P Chemical Shift ^b Ligand	ΔCS^c Complex
-	PCl_3^d	-	124°	2097	2133(w) 2092(m) 2076(s)	-219	-169.4 +48
-	PCl_2Ph^f	90-91	130° ^e	2092	2127(w) 2087(m) 2081(m) 2065(s)	-161.4	-151.3 +10.1
-	PClPh_2	153-154	136° ^e	2080.7	2121(w) 2079(m) 2057(s)	-81.9	-97.6 -15.7
6	PPh_3	204-206	145	2068.9	2113(w) 2068(m) 2047(s)	+6.1	-22.9 -29.0

a Cone angle and electronic parameter as in Reference 8.

b Referenced to H_3PO_4 (85%) $\delta = 0$, downfield is negative (in ppm).

c ΔCS is defined as δ complex- δ ligand, where δ complex and δ ligand are the chemical shifts of the complexed and uncomplexed ligand, respectively.

d $\text{mer-Ru(CO)}_3(\text{SiCl}_3)_2\text{PCl}_3$ is thermally unstable and could not be obtained pure.

e Estimated value.

f Parent peak was observed in mass spectrum.

temperature and ring current effects⁸.

With the free ligands studied in this work, there is a downfield shift when the phenyl groups are replaced by chlorine atoms, which may be explained by electronegativity effects. The more electronegative chlorines withdraw electron density from the phosphorus, thereby deshielding the nucleus. Deshielding of phosphorus by chlorine can also explain the chemical shifts of the complexed ligands, which show a trend similar to the free ligands.

The change in chemical shift upon complexation (Δ CS) is thought to provide information regarding the bonding in phosphorus transition metal complexes⁸. While the electronegativity of the substituents on the phosphorus atom remain unchanged when the free ligand becomes complexed, the change in the electron density on the phosphorus, due to participation of the lone pair in the metal-phosphorus bond, causes the ^{31}P chemical shift value to change upon complexation. For the ligands studied, the Δ CS values are as follows: PPh_3 moves 39 ppm downfield, PCl_3 moves 48 ppm upfield, and the PClPh_2 and PCl_2Ph ligands show intermediate values.

It is felt that the angle of the substituents (S-P-S) and the resultant hybridization of the phosphorus orbitals plays a major role in determining values for chemical shift⁸. It can be argued that the s character of the lone pair on phosphorus is sensitive to the angle between the substituents and that as this

angle increases, the s character of the lone pair decreases. (Also see Section 1.3.1, and Figure 1). The decreased s character and greater p character is thought to contribute to a downfield shift. For example, the chemical shifts of PPh_3 and the tied-back $\text{P}(\text{O}-\text{C}_6\text{H}_4)_3\text{CH}$ are 6.0 and 64.8 ppm, respectively⁸. In this example, PPh_3 has a greater downfield shift and a larger substituent-phosphorus-substituent angle, although the electronegativity of substituents on both ligands are expected to be very similar.

The greatest downfield shift upon complexation in this study is exhibited by PPh_3 , -29 ppm. One can conclude that the lone pair on the phosphorus has a greater p character in complexed PPh_3 than in the free ligand. One can also conclude that the angle between the substituents increases when PPh_3 is complexed, causing a downfield shift. Furthermore, PCl_3 experiences an upfield shift, and one may conclude from the above argument that the substituent-phosphorus-substituent angle closes upon complexation in PCl_3 . This result is contrary to what is expected, namely, that PCl_3 , being the smallest ligand studied, would show the greatest angle opening upon complexation. The simple argument of angle opening and rehybridization upon complexation to explain ΔCS seems to break down for chlorophosphorus complexes.

Other arguments must therefore be invoked to explain the surprising upfield shift in the PCl_3 and PCl_2Ph complexes. Meriwether and Leto³⁴ present a far more more simple argument

for the upfield shift in PCl_3 complexes. They suggest that while PCl_3 is a good π -acceptor (which is supported by the observation that the related PF_3 has a great ability to back-bond), PCl_3 is not a good σ -donor. This results in a net drift of electron density from the metal to phosphorus.

Support for the proposal that PCl_3 is not a good σ -donor comes from the present work. It was found that mer- $\text{Ru}(\text{CO})_3(\text{PCl}_3)(\text{SiCl}_3)_2$ was thermally unstable, decomposing quickly at 50°C . At room temperature it was unstable in solution unless excess PCl_3 was present. This made it difficult to obtain the complex free from excess ligand. Consequently, the ^{31}P NMR spectrum of the complex was recorded from a mixture of complex and ligand and the melting point and analysis of the complex could not be obtained. Also, at no time during the reaction of PCl_3 with cis- $\text{Ru}(\text{CO})_4(\text{SiCl}_3)_2$ did the bis-derivative form in quantities detectable by infrared spectroscopy, perhaps because of an inherent instability of the bis-derivative. These observations suggest that mer- $\text{Ru}(\text{CO})_3(\text{PCl}_3)(\text{SiCl}_3)_2$ has a weak Ru-P bond, which may result from poor σ -donating capability on the part of PCl_3 .

The melting points of the complexes mer- $\text{Ru}(\text{CO})_3(\text{L})(\text{SiCl}_3)_2$ ($\text{L} = \text{PCl}_n\text{Ph}_{3-n}$) were measured and it was observed that this was the temperature at which the complexes decomposed. The decomposition temperature increased as the number of phenyl groups present in the complex increased. One could speculate that the phenyl groups lend stability to the complexes because of a

tendency for such substituents to induce better σ -donation in the ligand.

Therefore, it is felt that the ^{31}P NMR chemical shift data is best explained using electronegativity arguments, and that the ΔCS data is best explained in terms of the increasing σ -donor ability of the ligands as one progresses from PCl_3 to PPh_3 . This causes increased deshielding of the ^{31}P nucleus on going from PCl_3 to PPh_3 , which results in a more negative value for ΔCS .

Experimental

2.2.1 General Procedure

All reactions were carried out under nitrogen using Schlenk techniques. All solvents were dried, distilled, and stored under nitrogen prior to use. Infrared spectra were obtained on a Perkin-Elmer 237 spectrometer fitted with an external recorder, and calibrated with carbon monoxide. Proton decoupled phosphorus NMR spectra were recorded at 40.5 MHz with a Varian XL-100 NMR spectrometer using H_3PO_4 (85%) as an external reference; $\delta = 0$ ppm, downfield is negative. Mass spectra were carried out on a Hewlett-Packard 5985 mass spectrometer, using an ionization voltage of 80 eV. All carbon and hydrogen analyses were performed by Mr. M.K. Yang of the microanalytical laboratory of Simon Fraser University.

2.2.2 Preparation of Complexes of the Type mer- Ru(CO)₃L(SiCl₃)₂

All complexes of the type mer-Ru(CO)₃L(SiCl₃)₂ (where L = phosphine or phosphite) were prepared from cis-Ru(CO)₄(SiCl₃)₂ using a method described previously⁶, except for complexes of PF₃ and PCl₃, whose syntheses are described in Section 2.2.3 and 2.2.4, respectively. In the cases of complexes of P(O-Butⁿ)₃, P(OMe)₂Ph, P(Butⁿ)₃, and P(CH₂-CH=CH₂)₃, where appreciable amounts of the bis-substituted derivative formed during the reaction, the monosubstituted derivative was obtained in a pure form by recrystallization of the crude product from hot hexane. The bis-substituted derivatives were insoluble in hexane. In all other instances kinetic studies were carried out using the crude reaction product. Because many compounds had been prepared previously, in most cases complexes were characterized solely by infrared spectroscopy. Infrared data for new complexes are shown in Table 6. Analytical data for those complexes analyzed are given in Table 7. In some cases, ³¹P NMR spectra were recorded, and these results are given in Table 8.

2.2.3 Preparation of mer-Ru(CO)₃(PF₃)(SiCl₃)₂

A solution of cis-Ru(CO)₄(SiCl₃)₂ (0.50 g, 1.03 mmol) in hexane (15 mL) was placed in a 150 mL round bottom flask fitted with a Teflon valve. The flask was evacuated at -196°C, and the solution was degassed with two freeze/thaw cycles and pressurized with 2 atm of PF₃. The solution was stirred at room

Table 6

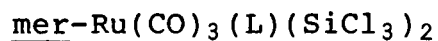
Infrared data for new complexes of the type mer-Ru(CO)₃L(SiCl₃)₂

L	Data	Solvent
P(allyl) ₃	2113(w) 2062(m) 2050(s)	hexane
P(Ph) ₂ (<u>i</u> -Pr)	2113(w) 2066(m) 2056(m) 2047(s) 2116(w) 2069(m) 2048(s)	hexane CH ₂ Cl ₂
P(benzyl) ₃	2115(w) 2065(m) 2047(s)	CH ₂ Cl ₂
PPh ₂ (<u>o</u> -MeOPh)	2116(s) 2076(m) 2047(s)	CH ₂ Cl ₂
P(<u>p</u> -MeOPh) ₃	2110(w) 2066(m) 2045(s)	hexane
P(<u>p</u> -MePh) ₃	2118(w) 2074(m) 2046(s)	hexane
P(<u>m</u> -MePh) ₃	2112(w) 2067(m) 2047(s)	hexane
P(<u>p</u> -FPh) ₃	2116(w) 2066(m) 2049(s) 2118(w) 2075(m) 2049(s)	hexane CH ₂ Cl ₂
P(<u>p</u> -ClPh) ₃	2113(w) 2069(m) 2049(s)	hexane
P(OMe)(Ph) ₂	2118(w) 2075(m) 2052(s) 2120(w) 2077(m) 2053(s)	hexane CH ₂ Cl ₂
P(MeO) ₂ (Ph)	2120(w) 2076(m) 2056(s) 2123(w) 2083(m) 2057(s)	hexane CH ₂ Cl ₂
P(O-But ⁿ) ₃	2121(w) 2080(m) 2053(s)	hexane
P(<u>m</u> -ClPh) ₃	2118(w) 2075(m) 2051(s) 2113(w) 2071(m) 2051(s)	CH ₂ Cl ₂ hexane
PClPh ₂	2123(w) 2083(m) 2058(s) 2121(w) 2079(m) 2057(s)	CH ₂ Cl ₂ hexane
P(O- <u>o</u> -tolyl) ₃	2124(w) 2081(m) 2062(s)	toluene
P(O- <u>p</u> -ClPh) ₃	2124(w) 2080(m) 2063(s) 2125(w) 2079(m) 2066(s)	CH ₂ Cl ₂ hexane
PCl ₂ Ph	2130(w) 2090(m) 2066(s) 2127(w) 2087(m) 2081(m) 2068(s)	CH ₂ Cl ₂ hexane
PCl ₃	2133(w) 2092(m) 2076(s)	hexane

For IR data on complexes previously prepared see Appendix III.

Table 7

Analytical data for new complexes of the type



L	C _{calc}	C _{found}	H _{calc}	H _{found}
PCl ₂ Ph	17.08	18.33	0.80	1.12
PClPh ₂	26.70	27.07	1.49	1.52
P(O-But ⁿ) ₃	25.58	25.92	3.86	3.88
P(<u>m</u> -CH ₃ C ₆ H ₄) ₃	38.02	38.23	2.80	2.92
PPh ₂ (<u>o</u> -MeOPh)	35.40	34.98	2.30	2.28
PPh ₂ (<u>i</u> -Pr)	31.32	31.37	2.48	2.59
P(<u>p</u> -CH ₃ C ₆ H ₄) ₃	38.02	37.80	2.80	2.90

Table 8

³¹P Phosphorus NMR data for some new complexes of the type
mer-Ru(CO)₃(L)(SiCl₃)₂

L	³¹ P Chemical Shift ^a ppm		ΔCS ^b
	Complex	Ligand	
PClPh ₂	-97.6	-81.9	-15.7
PCl ₂ Ph	-151.3	-161.4	+10.1
PCl ₃	-169.0	-219.0 ^c	+47.1
PPh ₂ (<u>i</u> -Pr)	+55.0	+28.1	-26.9

^a measured using H₃PO₄ (85%) as an external reference, δ = 0, downfield negative.

^b ΔCS is defined as δ complex - δ ligand, where δ ligand and δ complex are the chemical shifts in ppm of the ligand and the complex, respectively.

^c Previously reported at 216 (Reference 34).

temperature. Periodically, the carbon monoxide that had evolved in the reaction was removed by freezing the solution to -196°C and evacuating the flask. After 18 h, the solution contained very little parent compound, as determined by infrared spectroscopy. The hexane was removed by evaporation, leaving a clear colorless oil. All remaining cis- $\text{Ru}(\text{CO})_4(\text{SiCl}_3)_2$ was removed by sublimation at room temperature onto a probe cooled to -78°C . The samples for kinetic study were obtained by subliming the remaining mixture at 40°C onto a probe cooled to -78°C . It was not possible to obtain mer- $\text{Ru}(\text{CO})_3(\text{PF}_3)(\text{SiCl}_3)_2$ free of the bis-substituted product cis- $\text{Ru}(\text{CO})_2(\text{PF}_3)_2(\text{SiCl}_3)_2$, the presence of which was indicated by a shoulder on the infrared band at 2078 cm^{-1} of mer- $\text{Ru}(\text{CO})_3(\text{PF}_3)(\text{SiCl}_3)_2$.

2.2.4 Preparation of mer-Ru(CO)₃(PCl₃)(SiCl₃)₂

A solution of cis- $\text{Ru}(\text{CO})_4(\text{SiCl}_3)_2$ (0.356 g, 0.73 mmol) in hexane (25 mL) was placed in a round bottom flask, fitted with a Teflon valve. The ligand PCl_3 (1.0 mL, 7.2 mmol) was added, the flask was evacuated at -196°C , and the solution was degassed with two freeze/thaw cycles. The evacuated flask was left to stir at room temperature. Over the course of 2 hours, the flask was reevacuated every thirty minutes, and then over the succeeding 48 hours, every 6 hours. After 48 hours cis- $\text{Ru}(\text{CO})_4(\text{SiCl}_3)_2$ remained in small quantities, as detected by IR. The infrared spectrum of the final product, mer- $\text{Ru}(\text{CO})_3(\text{PCl}_3)(\text{SiCl}_3)_2$, was obtained by diluting the reaction

mixture approximately ten times with hexane. The IR spectrum in hexane showed bands at 2133(w), 2092(m), and 2076(s). A ^{31}P NMR spectrum was recorded using the undiluted solution.

The ligand and the complex were the only species present according to the ^{31}P NMR. It was concluded that under these conditions only the mono-substituted derivative was formed.

The hexane was removed and the colorless oil that remained behind was sublimed, but the complex could not be obtained free of the starting material cis- $\text{Ru}(\text{CO})_4(\text{SiCl}_3)_2$. The white oil decomposed in the Schlenk tube in two hours under vacuum and at room temperature. The decomposition was rapid when the temperature was raised at 40°C. In both instances a dark oil remained. Because of the thermal instability of the compound, it was not further characterized.

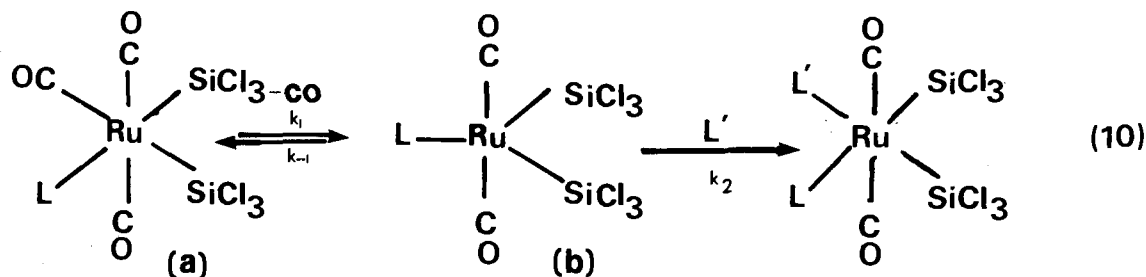
CHAPTER 3

Preliminary Investigations to Establish the Mechanism and
Necessary Reaction Conditions

Results and Discussion

3.1.1 Introduction

Some preliminary investigations are necessary in a kinetic study such as this to clearly establish the mechanism of the reaction. Previous work⁵ indicated that the rate of the reaction to be studied showed first order dependence on the concentration of the starting complex only. This kinetic evidence is usually indicative of a dissociative reaction, one which proceeds via a discrete intermediate (b) of lower coordination number (Equation 10).



This type of mechanism is common in organometallic chemistry, and forms the basis of Tolman's 16-18 electron postulate³⁵. Tolman's postulate is that ligand exchange processes involve discrete steps in which 16- and 18-electron species alternate. In Reaction 10, the Ru in the starting complex (a) has 18 valence electrons, the intermediate (b) has 16 valence

electrons, and the product has 18 electrons in the valence shell of ruthenium.

In order to study the effect of L on Reaction 10, it is necessary to establish that the rate of the reaction depends only on L, and not on L', the incoming ligand. This would be true only if the mechanism of the reaction was dissociative.

Langford and Gray have established a classification system for ligand substitution mechanisms, in which Reaction 10 would be designated type "D"³⁶. The essential feature of a type D reaction is a reaction intermediate of lower coordination number which survives long enough for its solvation sphere, otherwise known as the outer- or second coordination sphere, to rearrange.

An energy profile for a reaction exhibiting a dissociative mechanism is shown in Figure 15.

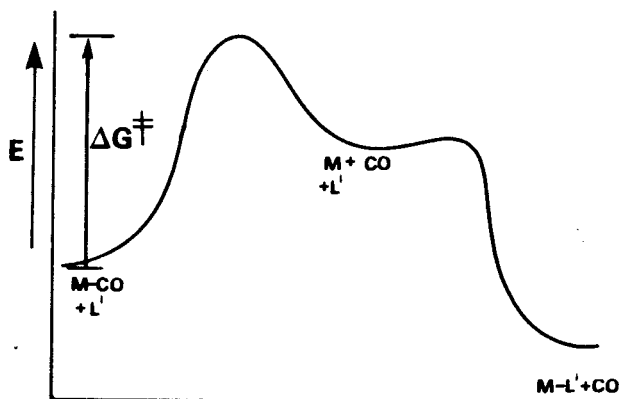


Fig. 15

Energy Profile for a dissociative or D mechanism.

The essential characteristics of a D mechanism are apparent in Fig. 15. The entering ligand, L', plays no role in the energetics of the reaction rate since ΔG^\ddagger will be unaffected by the

nature of L'. Therefore, the reaction rate depends only upon the nature of the complex which is reacting.

This chapter deals with experiments that were performed to establish the mechanism of Reaction 10 as well as to establish the acceptability of the techniques that were used to study this reaction.

3.1.2 Kinetic Studies

In order for a substitution reaction to be termed dissociative, or D, the rate of the reaction should not be sensitive to the nature and concentration of the incoming ligand. The rate law for Reaction 10 can be written as follows:

$$\begin{aligned} \text{rate of disappearance} &= -\frac{\partial}{\partial t} [\text{Ru}(\text{CO})_3(\text{L})(\text{SiCl}_3)_2] \\ \text{of starting material} & \\ &= \frac{k_1 k_2 [\text{Ru}(\text{CO})_3(\text{L})(\text{SiCl}_3)_2] [\text{L}']}{k_2 [\text{L}'] + k_{-1} [\text{CO}]} \end{aligned}$$

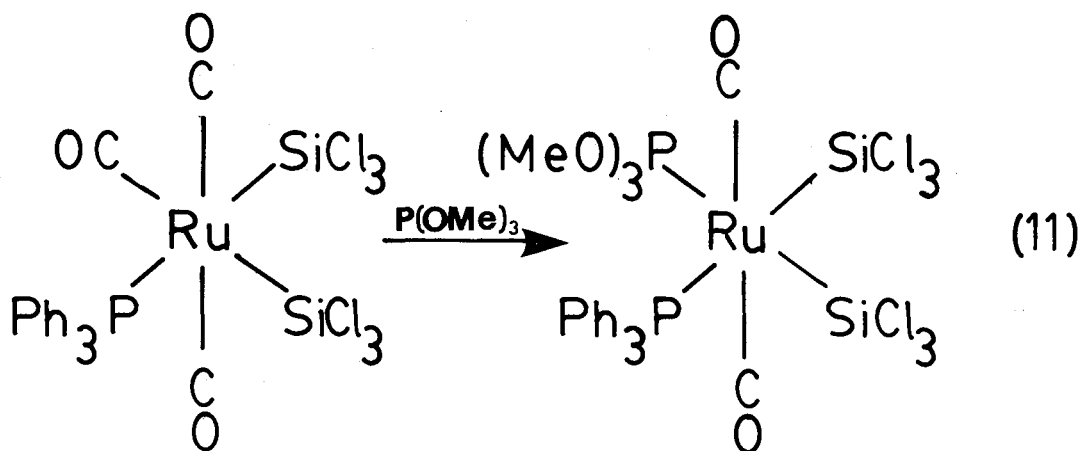
(The rate constants are defined in Equation 10).

If L' is added in excess, causing $k_2 [\text{L}']$ to be much greater than $k_{-1} [\text{CO}]$, then the rate law reduces to a simple expression:

$$\text{rate} = k_1 [\text{Ru}(\text{CO})_3(\text{L})(\text{SiCl}_3)_2]$$

Experiments were performed to determine how the reaction rate depended on the concentration of L', by varying the ratio of $[\text{Ru}(\text{CO})_3(\text{L})(\text{SiCl}_3)_2]$ to L'. This was done using $\text{Ru}(\text{CO})_3(\text{PPh}_3)(\text{SiCl}_3)_2$ as starting complex and $\text{P}(\text{OMe})_3$ as

entering ligand, L'. The reaction rate was observed to follow first order kinetics at 40.2°C for two half-lives with ligand:-complex ratios of 3.3:1, 9.5:1, and 21:1 (Equation 11).



The rate constant was found to be $8.7 \times 10^{-4} \text{ s}^{-1}$ under these conditions.

In the case where the complex to ligand ratio was 1:1, the initial rate constant was $7.6 \times 10^{-4} \text{ s}^{-1}$, but fell after about one half-life, indicating that the condition $k_{-1}[\text{CO}] \ll k_2[\text{L}']$ no longer held or, in other words, that the carbon monoxide produced in the reaction was now competing with L' for the intermediate because the concentration of L' was no longer overwhelming. This indicated that in order to maintain strict first order kinetics for all the reactions, a ten-fold excess of P(OMe)₃ should be maintained at all times.

The rate of Reaction 11 was also shown to be insensitive to the nature of the incoming ligand, L', for the series of

phosphorus donor ligands shown in Table 9. It can be seen that the rate remains constant as long as the entering ligand has a low steric requirement, but the rate decreases for $P(OPh)_3$ (cone angle 128°) and PPh_3 (cone angle 145°). The reactions with bulkier ligands are slower because the second step (Reaction 10) becomes slow, due to steric crowding in the transition state of that step.

Therefore, as long as the first step, with rate constant k_1 , is rate determining, the rate will never be larger than the rate of CO loss, and will be less than the rate of CO loss only when the steric requirements of the incoming ligand make access to the vacant position difficult.

3.1.3 Solvent Cage Experiment

To establish that a reaction has a D mechanism, proof is required that the reaction proceeds via a discrete five-coordinate intermediate, where the carbonyl that has dissociated is totally removed from the outer-sphere solvent cage of the intermediate. An experiment to show that the reaction does proceed via a five-coordinate intermediate was performed as follows. A reaction mixture was prepared which contained known quantities of E and F (Equation 12).

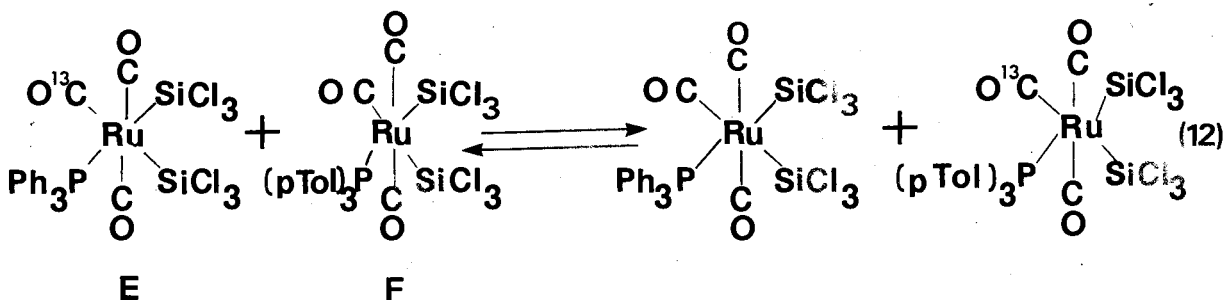
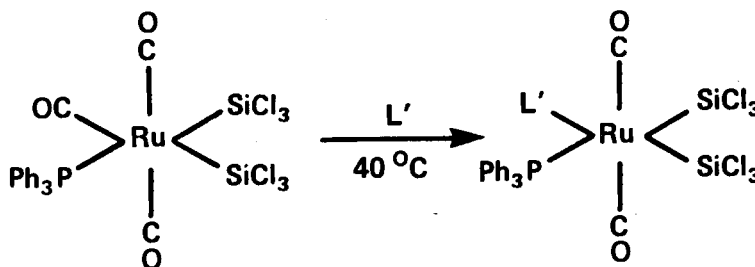


Table 9

Rate of substitution of CO in mer-Ru(CO)₃(PPh₃)(SiCl₃)₂ versus

L'.

Rate of substitution is independent of the concentration and, provided it is small, the identity of L'

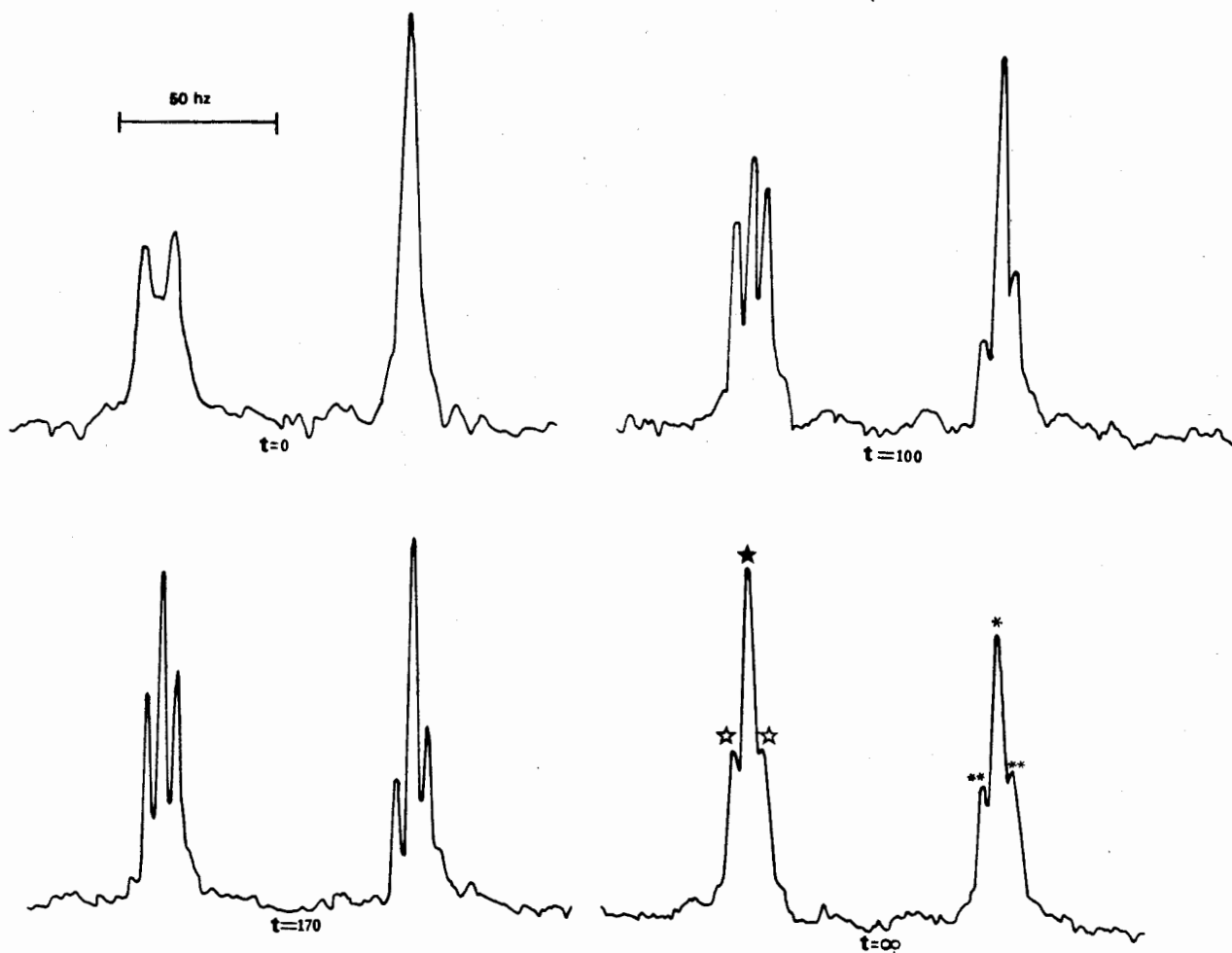


L'	Cone Angle ^o	k ±.5 sec ⁻¹ X 10 ⁴
P(OCH ₂) ₃ CC ₂ H ₅	101	9.2
P(OMe) ₃	107	9.1
P(OEt) ₃	109	9.0
P(OMe) ₂ Ph	115	9.2
PMe ₂ Ph	122	8.7
P(n - Bu) ₃	132	9.6
P(OPh) ₃	128	5.0
PPh ₃	145	no reaction

The rate of carbonyl dissociation at 30°C of E was known, and F was chosen because it was thought that it would exhibit a similar rate of carbonyl dissociation, since P(p-CH₃C₆H₄)₃ and PPh₃ have identical cone angles and very similar electronic properties. By extrapolating the Arrhenius plot for the carbonyl dissociation of E the rate constant is determined to be $2.1 \pm 0.2 \times 10^{-4} \text{ s}^{-1}$ at 30°C, and it was later found that the rate constant at 30°C for carbonyl dissociation of F is $1.9 \pm 0.2 \times 10^{-4} \text{ s}^{-1}$, so the prediction that they would turn out to be very similar was correct.

The proton decoupled ³¹P NMR spectra of the complexes were measured. The chemical shifts of E and F differed by 2 ppm, which allowed total separation of the two signals in the NMR spectrum of the mixture. The labelled species, E, can be readily distinguished from the unlabelled species due to the ³¹P-¹³C coupling. This was observed to be 10.1 Hz, which is in the range expected for cis coupling³⁷. The mixture was prepared in toluene, the normal reaction solvent in this study, and the ³¹P {¹H} spectrum was recorded immediately, at 100 minutes, and at 170 minutes. It was also recorded eight days later when the system had reached equilibrium. These four NMR spectra are shown in Figure 16.

The temperature of 30°C was chosen to best represent the highest reasonable mean temperature. The temperature in the NMR probe was known to be higher than room temperature, especially



t = time in minutes

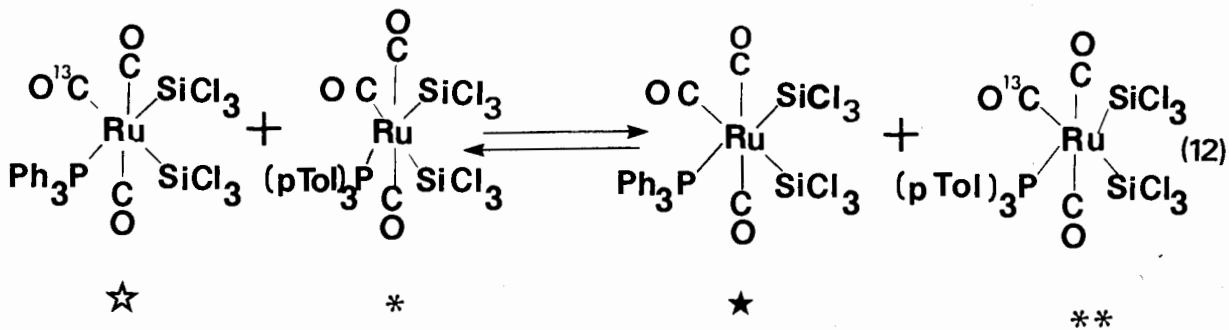


Figure 16: NMR experiment over time to measure the ^{13}C CO exchange rate in reaction 12.

since the proton decoupler was on. Because it is impractical to measure the temperature of the solution when the decoupler is on, the mean temperature over the course of the experiment cannot be determined. A temperature of 30°C was chosen as a highest reasonable average between the temperature in the probe and room temperature.

Table 10 summarizes the results of the experiment. The expected half-life of the reaction was calculated to be 60 minutes. Spectrum 3, which was recorded at 170 minutes, is the spectrum at approximately three half-lives. Since 45% enrichment is observed, it can be concluded that the rate of exchange in this experiment is very close to the rate of dissociation.

Since E and F equilibrated at a rate very close to the rate of carbonyl dissociation, it is definitely established that the reaction proceeds via a D mechanism. Carbonyl exchange between E and F requires that a certain amount of carbon monoxide, both labelled and unlabelled, must build up in solution and react with the five-coordinate intermediate.

If the reaction proceeded via what Gray and Langford term an Id mechanism³⁶, in which the entering ligand enters the solvation sphere of the complex and then the entering ligand and leaving group simply exchange sites, then the rate of reaction would be greatly retarded, because the concentration of entering ligand would be very low, since there is no excess carbon monoxide in solution. In addition, the carbonyl exchange would

Table 10

Data and calculations for the NMR solvent cage experiment

Spectrum Number	Peak Height ^a of		% enrichment ^c	time minutes
	<u>mer</u> -Ru(CO) ₃ [P(<u>p</u> -CH ₃ C ₆ H ₄) ₃](SiCl ₃) ₂ unlabelled (h ₁)	labelled ^b (h ₂)		
1	1	0	0	0
2	1	0.213	30	100
3	1	0.406	45	170
4	1	0.490	49	

a Peak heights are relative and have no absolute meaning.

b Measured peak height from one peak of doublet.

c Calculated from the equation:

$$\% \text{ enrichment} = \frac{2 \times h_2}{h_1 + 2h_2} \times 100$$

and estimated to be good to \pm 5%.

occur much more slowly if the carbon monoxide that had dissociated was trapped in the outer solvation sphere, or was still intimately associated with the intermediate, since the intermediate would preferentially react with the same CO.

Therefore, in conclusion, the available evidence supports the D mechanism for this reaction: the carbonyl dissociation from $\text{Ru}(\text{CO})_3(\text{L})(\text{SiCl}_3)_2$ proceeds via a discrete five-coordinate intermediate, where the leaving group is completely removed from the solvent cage of the intermediate.

3.1.4 Other Investigations Related to the Kinetic Measurement

It is important in any experiment in kinetics to ensure that experimental methods and apparatus used to determine the rate constants give precise results, and it is likewise important to establish the degree of precision that is possible.

The value for the reaction rate constant was consistently measured to within four percent. This value is taken from rate constants measured on different days, under dark and light conditions, with varying amounts of entering ligand, and with varying initial concentration of complex.

A kinetic run was performed at 40.2°C in toluene to observe the dissociation of CO from $\text{Ru}(\text{CO})_3(\text{PPh}_3)(\text{SiCl}_3)_2$ when no entering ligand was added. No observable drop in the concentration of complex due to decomposition was found, nor was there any apparent increase in concentration due to evaporation of toluene.

over the period of measurement.

Another simulated run was performed at 70°C using $\text{Ru}(\text{CO})_3(\text{ETPB})(\text{SiCl}_3)_2$ and again the concentration remained unchanged. It was concluded that toluene was an appropriate solvent for the temperature range in which all measurements were made, and that at these temperatures no decomposition of the complexes in solution occurred over the period of time necessary for kinetic measurements.

To check if the rate of reaction was sensitive to light, one Schlenk tube was painted black and the reaction was carried out in dark conditions. The rate of reaction in the dark was equal to the rate when the reaction was performed in normal indoor light, within the allowed experimental error of four percent.

3.1.5 Conclusions

At the completion of these preliminary studies, it was concluded that it is possible to measure the rate of the reaction using any small ligand as L', at a ligand:complex ratio of 10:1. Trimethylphosphite ($\text{P}(\text{OMe})_3$) was chosen as the entering ligand because it is inexpensive, has a small cone angle, is easy to handle, and does not absorb in the infrared region where measurements were taken. It was also concluded that the reaction proceeds via a dissociative mechanism, type D, and that different lighting conditions do not affect the rate of reaction. The measurement of the rate of reaction is reproducible within a range of $\pm 4\%$.

Experimental

3.2.1 General Kinetic Procedure

All reactions were carried out in a temperature bath kept at $40.2^{\circ} \pm 0.5^{\circ}\text{C}$. Solutions of $\text{Ru}(\text{CO})_3(\text{PPh}_3)(\text{SiCl}_3)_2$ in toluene (6 mL) were added to the reaction vessel under nitrogen and left stirring to attain thermal equilibrium. Trimethyl phosphite was added to the vessel and the reaction was monitored by infrared spectroscopy by periodically removing aliquots (0.2 mL) and measuring the decrease in the absorbance of the $A_{1(1)}$ CO stretching mode. Sodium chloride cells (1 mm) were used throughout. The $A_{1(1)}$ band was recorded and measured three times and the mean values were used in subsequent calculations. The infrared spectrum of the final mixture was recorded and calibrated with carbon monoxide. The product was identified as $\text{Ru}(\text{CO})_2(\text{PPh}_3)[\text{P}(\text{OMe})_3](\text{SiCl}_3)_2$ in all cases, by means of its IR spectrum.

3.2.2 Analysis of Results

The results of all kinetic experiments were analyzed in the same fashion. The recorded infrared spectra were measured as shown in Figure 17. The first order plot was constructed by plotting

$\ln \frac{A_{t_i}}{A_{t=0}}$ vs time, where $A_{t=0}$ is the initial absorbance and A_{t_i} is the absorbance at some later time t_i .

Fig. 17

A typical measurement of absorbance for a kinetic run.

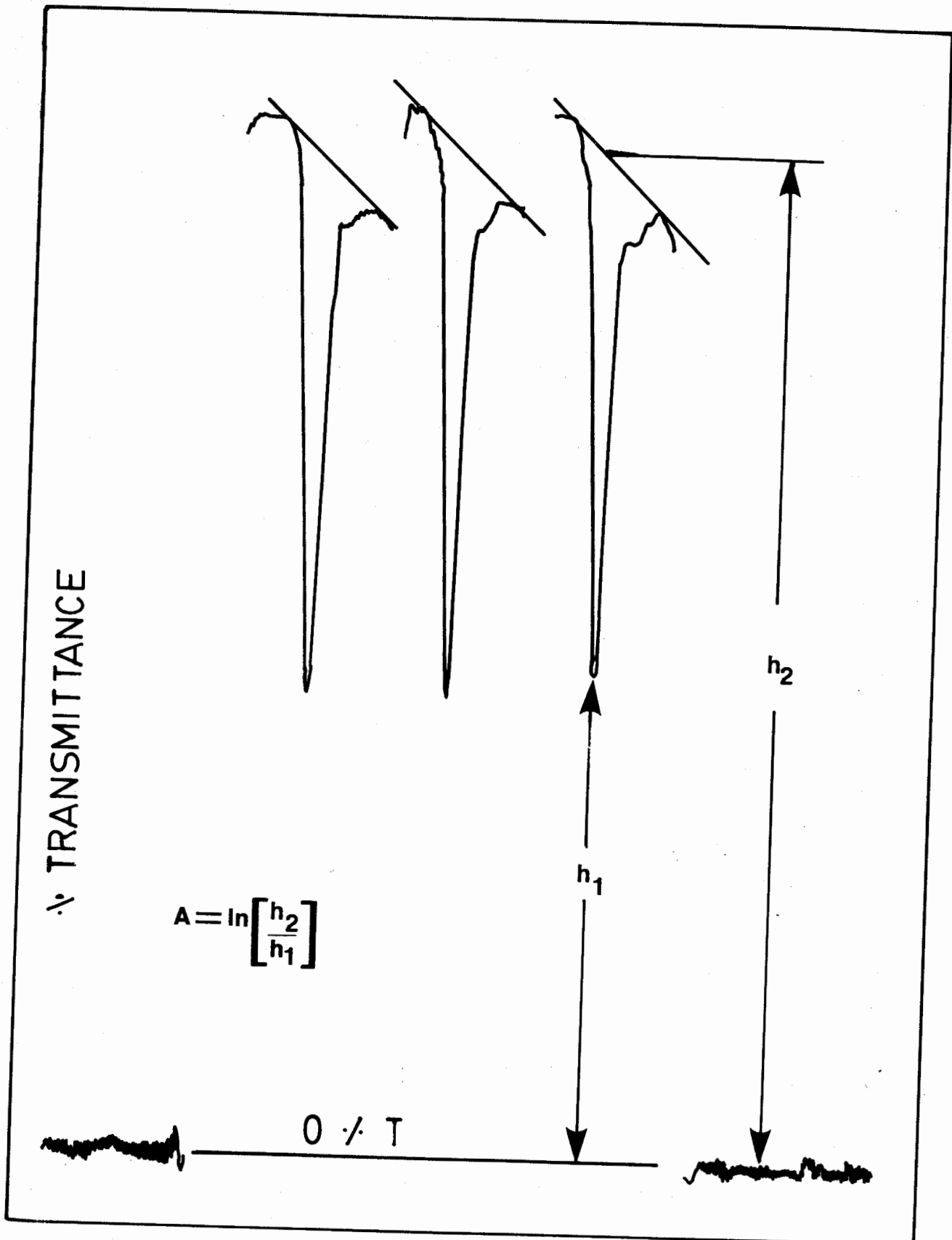
· TRANSMITTANCE

$$A = \ln \left[\frac{h_2}{h_1} \right]$$

0 · T

h_1

h_2



An example of a first order plot is given in Fig. 18. The slope of the line was calculated by means of a least squares linear regression, yielding the value of the rate constant. The rate constants were reproducible to within 4% over different ratios of complex:ligand, as long as there was at least a ten-fold excess of ligand.

3.2.3 Kinetic Studies

- a) Measuring the effect of the concentration of entering ligand on the rate of reaction

All procedures followed the general procedures of Sections 2.2.1 and 3.2.1, except that the varying amounts of entering ligand, $P(OMe)_3$, were used. Solid $Ru(CO)_3(PPh_3)(SiCl_3)_2$ was weighed in the reaction vessel, 6 mL of toluene was added and $P(OMe)_3$ was introduced to the vessel by means of a calibrated syringe. The results are given in Table 11, experiment numbers 1 to 5.

- b) Measuring the effect of light on the reaction rate

All measurements followed the general procedure as described in Sections 2.2.1 and 3.2.1. Two separate reaction vessels were set up in the temperature bath: one was a regular reaction vessel and the other was painted black to protect the solution from indoor lighting. Both solutions were made to a similar concentration and were run simultaneously, under identical conditions. The results appear as experiment numbers 2 and 5 in Table 11.

Figure 18

An example of a first order plot for the reaction of
mer-Ru(CO)₃(PPh₃)(SiCl₃)₂ with P(OMe)₃ at 40°C

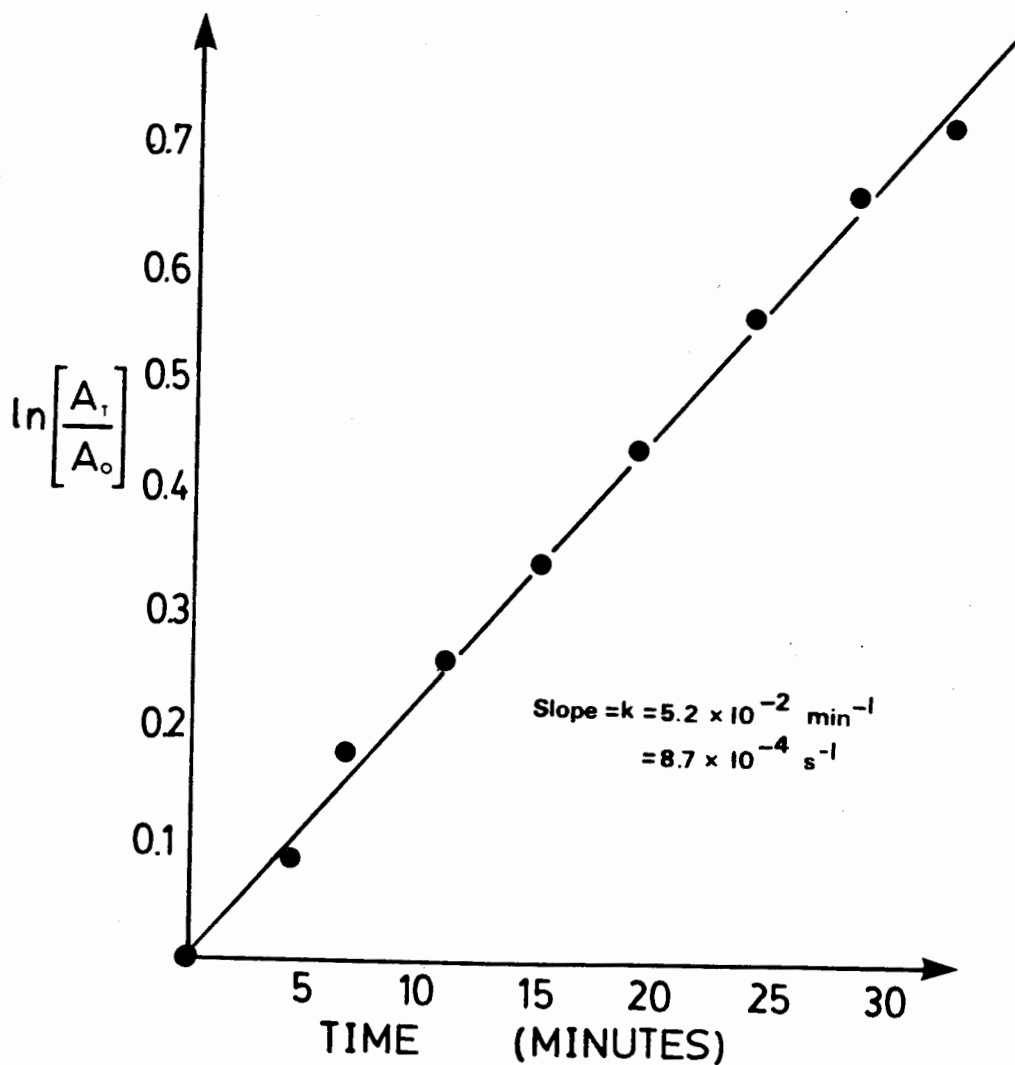


Table 11

Data and results from measurements of the effect of the concentration of entering

ligand and the effect of light on reaction rate

Experiment Number	g of $\text{Ru}(\text{CO})_3(\text{PPh}_3)(\text{SiCl}_3)_2$	Moles of $\text{Ru}(\text{CO})_3(\text{PPh}_3)(\text{SiCl}_3)_2$ $\times 10^4$	mL $\text{P}(\text{OMe})_3$	Moles $\text{P}(\text{OMe})_3$ $\times 10^4$	Ligand: Complex Ratio	Rate s^{-1} $\times 10^4$
1	0.076	1.1	0.012 ^c	1.0	1:1	7.6
2 ^a	0.171	2.4	0.10	7.9	3.3:1	8.8
3	0.107	1.5	0.20	15.8	9.5:1	8.7
4	0.054	0.75	0.20	15.8	21:1	8.6
5 ^b	0.186	2.6	0.10	7.9	3.3:1	8.6

a in normal indoor lighting, run simultaneously with experiment 5.

b in dark conditions, run simultaneously with experiment 2.

c 0.12 mL of a solution of 0.10 mL $\text{P}(\text{OMe})_3$ in 0.90 mL toluene.

- c) Measuring the effect of the nature of the entering ligand on the rate

All measurements followed the general procedure as described in Sections 2.2.1 and 3.2.1, except that the entering ligand (L') varied. The initial quantities of $[\text{Ru}(\text{CO})_3(\text{PPh}_3)(\text{SiCl}_3)_2]$ also varied slightly: from 0.11 g to 0.18 g in toluene (6 mL) (2.5×10^{-2} to 4.2×10^{-2} M). Most of the ligands were liquids (0.15 to 0.20 mL) and were introduced to the flask with a syringe. ETPB and PPh_3 were solids (0.1 to 0.2 g) and were introduced directly to the vessel. The results are reported in Table 9 in Section 3.1.2

3.2.4 Solvent Cage Experiment

- a) Preparation of $\text{Ru}(\text{CO})_2(^{13}\text{CO})(\text{PPh}_3)(\text{SiCl}_3)_2$

A solution of $\text{Ru}(\text{CO})_3(\text{PPh}_3)(\text{SiCl}_3)_2$ (0.20 g, 0.28 mmol) in CH_2Cl_2 (15 mL) was placed into a round bottom flask fitted with a Teflon valve. The solution was frozen (-196°C) and the vessel was evacuated. The solution was thawed and frozen and the flask was reevacuated to eliminate any gas in the system. The labelled gas ^{13}CO (2 atm) was introduced into the flask and the system was left stirring at room temperature for 72 hours. The IR spectrum of the reaction mixture at 72 hours showed very little starting material and the labelled product $[\text{Ru}(\text{CO})_2(^{13}\text{CO})(\text{PPh}_3)(\text{SiCl}_3)_2]$ (2109(vw), 2050(s), 2030(m) cm^{-1}). The CH_2Cl_2 was removed, leaving a white solid which was not purified

further. The $^{31}\text{P}\{\text{H}^1\}$ NMR spectrum in toluene was recorded and consisted of a singlet at 50.6 ppm due to the unlabelled product and a doublet centered on 50.6 ppm split by 10.1 Hz, due to the labelled product. The ^{31}P NMR spectrum indicated that the compound was approximately 90% enriched.

b) Exchange experiment

A solution of $\text{Ru}(\text{CO})_2(^{13}\text{CO})(\text{PPh}_3)(\text{SiCl}_3)_2$ (0.168 g, 0.23 mmol) was prepared in toluene (2.5 mL). A solution of $[\text{Ru}(\text{CO})_3(\text{P}(\text{p-tolyl})_3)(\text{SiCl}_3)_2]$ (0.134 g, 0.176 mmol) was also prepared in toluene (2.5 mL). The $^{31}\text{P}\{\text{H}^1\}$ spectrum of this compound showed a singlet at 48.5 ppm.

A mixture of 0.50 mL of each solution was prepared in a 5 mm NMR tube under nitrogen and the $^{31}\text{P}\{\text{H}^1\}$ spectrum was recorded immediately. The mixture was left standing at room temperature and spectra were recorded at 100 min, 170 min, and at 8 days, by which time equilibrium had presumably been reached. The results are given in Table 10 and Figure 16.

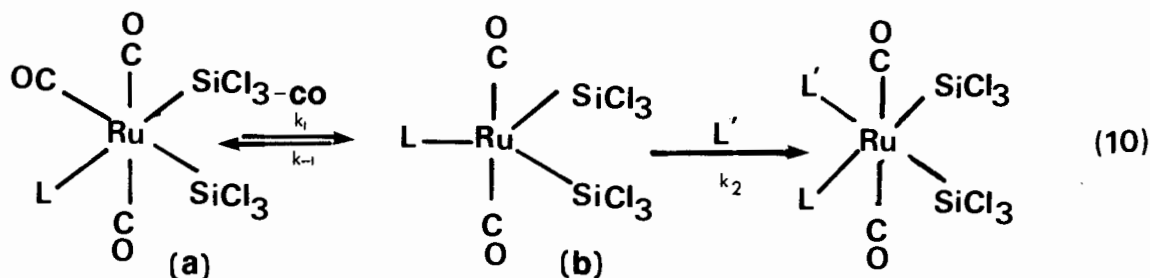
CHAPTER 4

Results of the Kinetic Study

Results and Discussion

4.1.1 Introduction

The kinetics of the substitution reactions of twenty-five complexes of the type mer-Ru(CO)₃(L)(SiCl₃)₂ containing different L groups is presented in this chapter. The reaction studied is the CO substitution of mer-Ru(CO)₃(L)(SiCl₃)₂ (Equation 10).



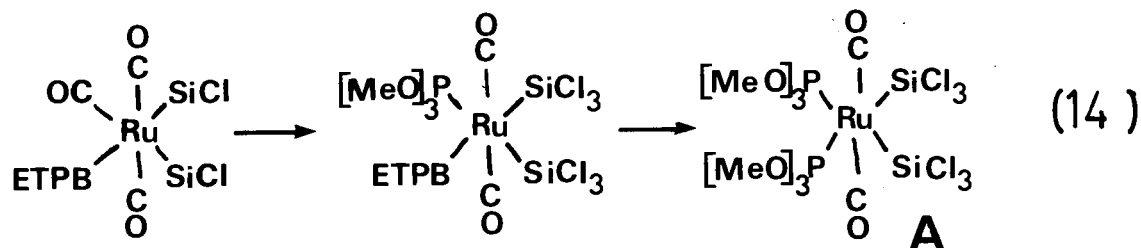
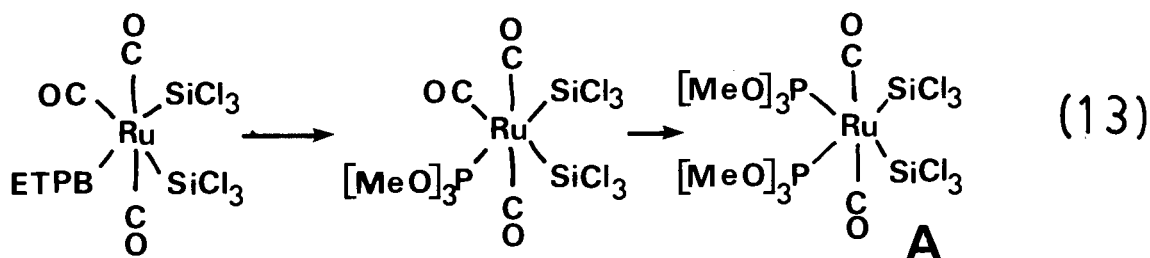
In Chapter 3 the mechanism of this reaction was shown to be dissociative, so that variation of rate (k_1) with L depends only on the properties of L and not on the properties of L', the entering ligand. The different rates of the reaction can then be attributed to the cis-effect of L in this system.

4.1.2 The Choice of the Entering Ligand

In Section 3.1.1 an experiment was discussed which proved that the reaction under study is dissociative in nature, and that the rate is independent of the concentration and nature of

the entering ligand. It was shown that, under pseudo-first order conditions, the CO dissociation was rate determining. First order dependence on the concentration of complex was observed and P(OMe)₃ was used as the entering ligand because it has a small cone angle, is easy to handle, is inexpensive and is very soluble in the reaction solution.

However, during the study of the kinetics of the substitution of mer-Ru(CO)₃(ETPB)(SiCl₃)₂, the compound Ru(CO)₂[P(OMe)₃]₂(SiCl₃)₂ was detected in the mixture. The compound could have been produced by one of two processes (Equations 13 and 14).



If the unexpected product (A) was produced via Equation 14, then the rate of loss of mer-Ru(CO)₃(ETPB)(SiCl₃)₂ would remain unaffected by this reaction and detection of the bis-substituted P(OMe)₃ complex would be of no consequence. However, if the

bis-substituted derivatives were produced via Equation 13, the rate of loss of mer-Ru(CO)₃(ETPB)(SiCl₃)₂ would not be a true reflection of the cis-effect of ETPB. This is because the rate would be higher than it should be, since mer-Ru(CO)₃(ETPB)(SiCl₃)₂ is consumed via two pathways. It was very possible that Reaction 13 was occurring, because the elevated temperatures that were necessary to induce CO dissociation could have also induced Ru-ETPB bond rupture.

To eliminate the problem of competing phosphite dissociation, ETPB was used as the entering ligand for the mer-Ru(CO)₃(ETPB)(SiCl₃)₂ rate measurements. In this way, if ETPB was lost at the elevated temperatures necessary to induce CO dissociation, it would be immediately replaced by ETPB, and no loss of mer-Ru(CO)₃(ETPB)(SiCl₃)₂ would be observed due to the dissociation of phosphite.

The policy of keeping the entering and leaving phosphorus ligands the same was maintained for the study of PF₃, P(OMe)₂Ph and P(o-Butⁿ)₃ complexes. In all three cases the temperature was high for the kinetic study, possibly inducing phosphorus ligand dissociation. Also, the ligands were small enough so that it was assured that pseudo-first order kinetics could easily be attained.

4.1.3 The Results of the Kinetic Study

The rate of each reaction was measured over a range of temperatures and the rate constant at 40°C was calculated by

extrapolating the Arrhenius plot in each case. These constants are presented in Table 12, along with θ , the ligand cone angle, and ν , Tolman's electronic parameter for the ligand⁸.

Figure 19 is a plot of k_{40° versus θ , and it is readily apparent that these two quantities are related.

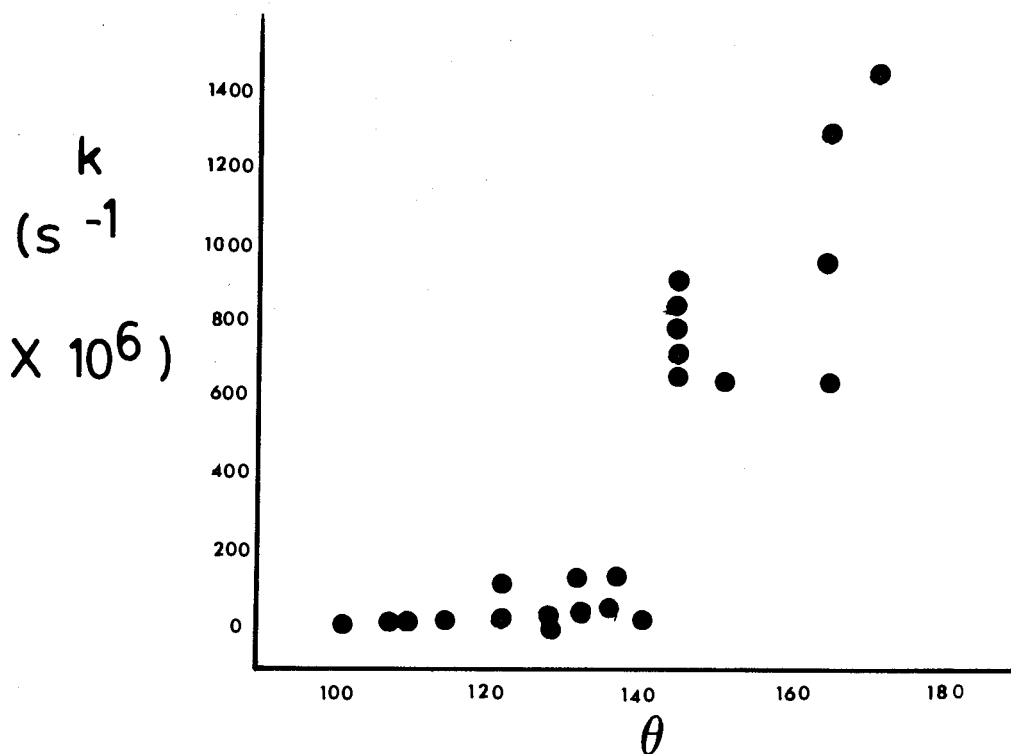


Fig. 19

A plot of the rate constant k ($s^{-1} \times 10^6$) at $40^\circ C$ versus θ , Tolman's cone angle, for the substitution of $mer-Ru(CO)_3(L)(SiCl_3)_2$.

In the region where θ is small, the relationship between k_{40} and θ is difficult to assess.

Table 12: Rate constants at 40°C for the substitution of mer-Ru(CO)₃(L)(SiCl₃)₂ complexes.

L	θ°	ν cm^{-1}	k $\times 10^6 \text{ s}^{-1}$
ETPB	101	2087.3	1.1
P(OMe) ₃	107	2079	7.3
P(OBut ⁿ) ₃	109	2076 *	6.7
P(OMe) ₂ Ph	115	2075.8	11.3
PCl ₂ Ph	122*	2092.1	110
PMe ₂ Ph	122	2065.3	19.0
P(OPh) ₃	128	2085.3	20.0
P(O-p-ClPh) ₃	128	2089.3	13.0
P(CH ₂ CH=CH ₂) ₃	132*	2065.0	21.0
P(But ⁿ) ₃	132	2060.0	140
P(OMe)Ph ₂	132	2072.0	23.0
P(Me)Ph ₂	136	2067	71
PClPh ₂	137*	2080.7	166
P(O-oMeC ₆ H ₄) ₃	141	2084.1	15.8
P(p-MeOPh) ₃	145	2066.1	755
P(p-CH ₃ Ph) ₃	145	2066.7	840
PPh ₃	145	2068.9	900
P(p-FPh) ₃	145	2071.3	750
P(p-ClPh) ₃	145	2072.8	670
PPh ₂ (i-Pr)	150	2065.7	640
P(m-ClPh) ₃	165*	2075.6	963
P(m-CH ₃ Ph) ₃	165*	2067.2	1300
P(CH ₂ Ph) ₃	165	2066.4	640
PPh ₂ (o-MeOPh)	171	2066.1	1470

* values for these parameters have been calculated using information in Tolman's work.

A plot of $\ln k$ versus θ clarifies this region (Figure 20).

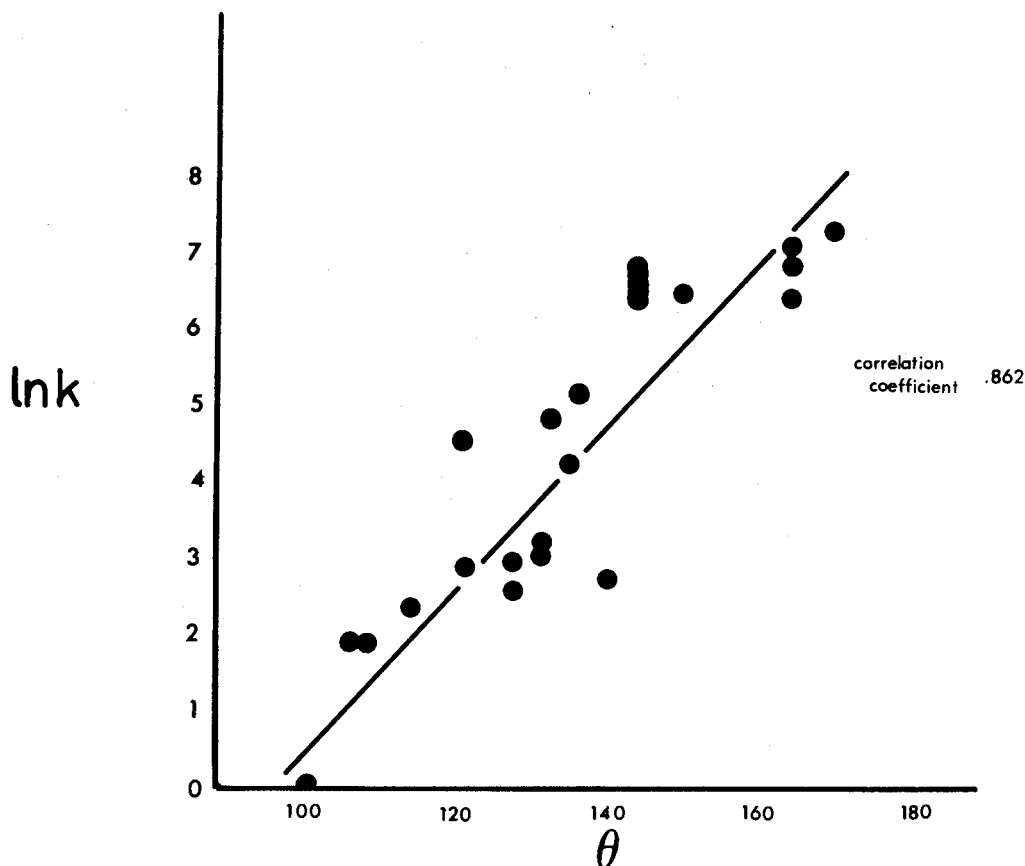


Fig. 20

A plot of $\ln (k \times 10^{+6})$ at $40^{\circ}\text{C s}^{-1}$ versus θ , for the substitution of mer- $\text{Ru}(\text{CO})_3(\text{L})(\text{SiCl}_3)_2$.

The value of $\ln k$ appears to show a linear relationship with θ , the ligand cone angle. This type of behaviour is characteristic of a linear free energy relationship, (LFER), and is commonly found when studying substituent effects in reaction kinetics³⁸. The LFER relates free energy of activation, ΔG^\ddagger ,

(or $\ln k$) to the equilibrium constant for the reaction. In this case the reaction to be considered is Step 1, the loss of CO to yield the five-coordinate intermediate. This is an example of an empirical LFER, which is a relationship between ΔG^\ddagger and a defined ground state parameter, such as the nucleophilicity of a ligand³⁹. The LFER demonstrated in Figure 20 relates ΔG^\ddagger to θ the cone angle, in the dissociation step in the substitution of CO in mer-Ru(CO)₃(L)(SiCl₃)₂.

The pattern for all complexes in Figure 20 is that the rate of substitution of the carbonyl group cis to the ligand (L) increases as the cone angle of the ligand increases. There is considerable variation in the rate constants for two complexes with ligands of the same cone angle, so that the relationship between the substitution reaction rate and cone angle is only a general trend.

The relationship between the rate constants for the reactions and ν , the electronic parameter of the ligands is shown in Figure 21. As can be seen, there is no apparent relationship between the electronic parameter and k_{40}° .

Table 13: Results for the substitution reaction of mer-
 $\text{Ru}(\text{CO})_3(\text{P}(\text{p-XPh})_3)(\text{SiCl}_3)_2$.

Ligand	ν cm^{-1}	k $\times 10^6 \text{ s}^{-1}$
$\text{P}(\text{p-MeOPh})_3$	2066.1	755
$\text{P}(\text{p-MePh})_3$	2066.7	840
$\text{P}(\text{Ph})_3$	2068.9	900
$\text{P}(\text{p-FPh})_3$	2071.3	750
$\text{P}(\text{p-ClPh})_3$	2072.8	670

The data in Table 13 indicate that the rate is not proportional to ν , the electronic parameter. In other words, it does not appear that the large steric effect is obscuring a small electronic effect; rather, there is no measurable electronic effect. The spread in k values in Table 13 is slightly larger than can be expected for simple random error in measurement. However the variation is difficult to rationalize.

The Arrhenius parameters exhibit a pattern of variation with θ and ν similar to the patterns seen with k (see Table 14). The ΔS^\ddagger values for most reactions studied were positive, as expected for a dissociative reaction.

In a dissociative reaction ΔH^\ddagger can be related to the bond-strength of the metal-ligand bond undergoing cleavage²⁶. In the present study the ΔH^\ddagger values measure the strength of the Ru-CO bond. Any variation in ΔH^\ddagger due to changing the ligand L may be interpreted as the effect of L on the bond-strength of the metal-carbonyl bond. Because the electronic parameter of L has been shown to affect the ^{13}C chemical shift and the infrared stretching frequencies of the carbonyl cis to L, it was felt that the electronic properties of L might affect the bond strength of the Ru-CO bond, and that this would be reflected in the ΔH^\ddagger values for the substitution reactions.

The enthalpy of activation for the reactions studied showed very little variation and can be considered to be essentially constant.

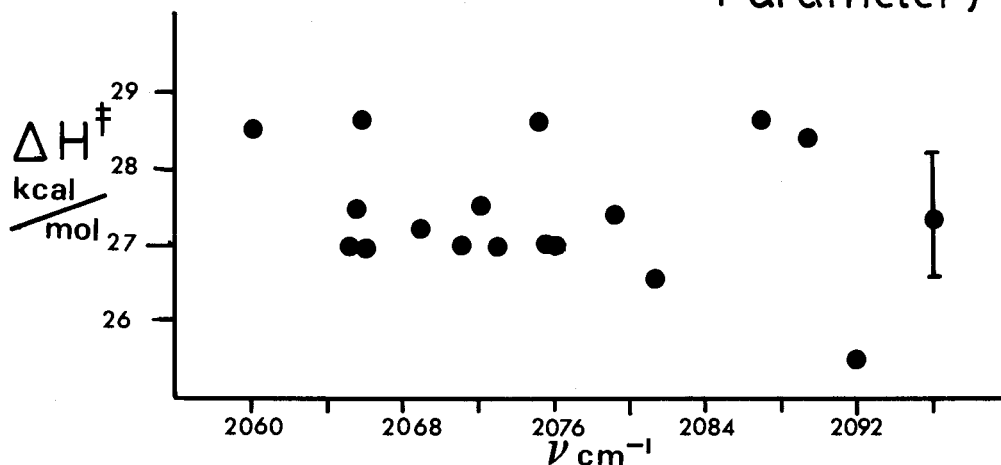
Table 14

Arrhenius parameters for the substitution reactions of
mer-Ru(CO)₃(L)(SiCl₃)₂.

Ligand	θ°	$\Delta S^\ddagger_{\pm 3}$ cal/mol deg	$\Delta H^\ddagger_{\pm 1}$ kcal/mol
ETPB	101	5	28.4
P(OMe) ₃	107	5	27.4
P(OBut ⁿ) ₃	109	4	27.0
P(OMe) ₂ Ph	115	5	26.9
PCl ₂ Ph	122	4	25.5
PMe ₂ Ph	122	7.5	27.5
P(O-p-ClPh) ₃	128	10	28.5
P(CH ₂ CH=CH ₂) ₃	132	7	27.2
P(But ⁿ) ₃	132	11	28.7
P(OMe)Ph ₂	132	8	27.5
PMePh ₂	136	10	27.4
PClPh ₂	137	9	26.5
PPh ₃	145	14	27.1
P(p-FPh) ₃	145	13	27.0
P(p-ClPh) ₃	145	13	27.0
P(p-MeOPh) ₃	145	13	26.8
P(p-MePh) ₃	145	13	26.9
PPh ₂ (i-Pr)	150	14	28.7
P(m-CH ₃ Ph) ₃	165	16	27.5
P(m-ClPh) ₃	165	19	28.7

The mean ΔH^\ddagger value is 27.4 kcal/mol. The standard deviation is calculated to be 0.8 kcal/mol, which is less than the expected experimental error of 1 kcal/mol. Therefore, the variation in measured ΔH^\ddagger values could be attributed to random error. A plot of ΔH^\ddagger versus ν , the electronic parameter, is shown in Figure 22. No trend is visible and the distribution of points appears to be completely random.

FIGURE 22
 ΔH^\ddagger versus ν (Electronic Parameter)

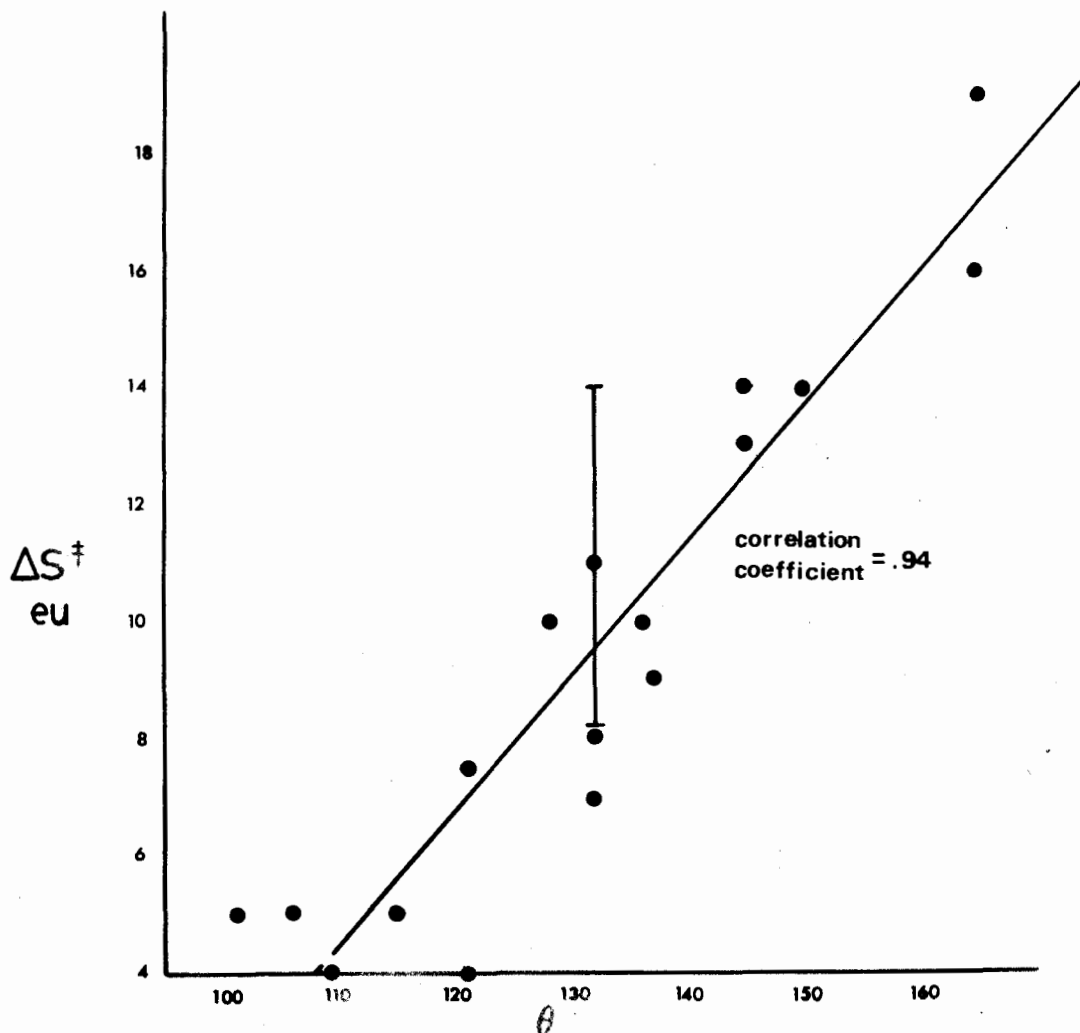


On careful examination of the data in Table 14 it appears possible that there is a trend in ΔH^\ddagger values in the series PPh_3 ($\nu = 2068.9$), PClPh_2 ($\nu = 2080.7$) and PCl_2Ph ($\nu = 2092.1$ cm^{-1}), as ΔH^\ddagger decreases from 27.1 to 26.5 to 25.5 kcal/mol. It is felt that this trend is probably coincidental, because a similar trend is not observed for the $\text{P}(\underline{p}\text{-X-Ph})_3$ group discussed previously. Also, the complexes of the ligand $\text{P}(\text{But}^n)_3$ ($\nu = 2060.0$) and ETPB ($\nu = 2087.3$ cm^{-1}) have ΔH^\ddagger values of 28.7 kcal/mol and 28.4 kcal/mol, respectively, even though they

differ widely in electronic properties.

The most striking relationship that appears when comparing ΔH^\ddagger and ΔS^\ddagger to θ and ν is a direct correlation between ΔS^\ddagger and θ . This linear correlation, which is illustrated in Figure 23, is reasonably strong, considering the larger error associated with the value of ΔS^\ddagger (also illustrated in Figure 23).

FIGURE 23
 ΔS^\ddagger versus θ Cone Angle



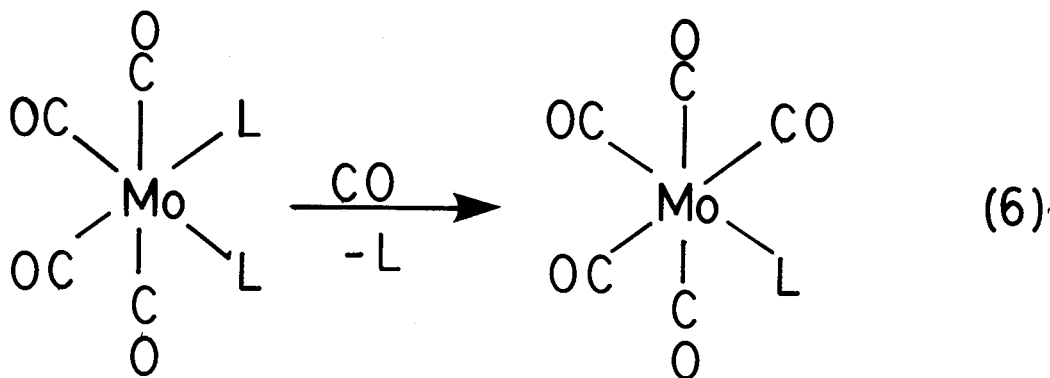
There are five components to entropy of activation values. These are due to rotational, vibrational, electronic and translational changes in the transition state, as well as a component which accounts for different symmetries in the transition state and the ground state. The most important contribution to the large change in entropy for large ligands is thought to be rotational entropy. The internal rotations of the phosphorus ligands are expected to be less hindered in the five-coordinate transition state. The barrier to rotation of large ligands is expected to be greater, which leads to larger ΔS^\ddagger values. Also the moment of inertia of the rotor is proportional to the change in entropy. Again this will be larger for large ligands, and will lead to larger ΔS^\ddagger values.

In conclusion, in substitution reactions of mer- $\text{Ru}(\text{CO})_3(\text{L})(\text{SiCl}_3)_2$, the cis-effect exerted by L (where L = phosphine or phosphite) is largely steric in origin. If the effect exerted by L on the rate of the substitution also has an electronic component, it must be smaller than the random error associated with the measurement of the rate constant.

Throughout this argument no assumption has been made concerning the nature of the five-coordinate intermediate. Whilst a trigonal bipyramidal intermediate is favoured because the large ΔS^\ddagger values imply that substantial rearrangement has occurred on going from reactants to intermediate, a square pyramidal intermediate cannot be ruled out. The large ΔS^\ddagger values could be attributed to a greater degree of freedom in the less hindered

phosphine in this type of intermediate.

This work supports Darensbourg's conclusions about the rate of substitution of L in cis-Mo(CO)₄L₂ complexes, which were discussed in Section 1.3.2. Darensbourg found that the rate of substitution increased as the size of the phosphorus donor ligand, L, increased²⁶. However, Darensbourg's study tends to overemphasize the steric influence of L since, in his series of reactions, both the leaving group, L, and the ligand cis to it, also L, are changed (Equation 6).



Thus, Darensbourg is really measuring the cis-effect exerted by L on different phosphorus donor ligands. The present study does not have this problem, since in all cases the leaving group is CO and the cis-effect exerted by L on CO is what is always measured.

Because the substitution of CO in mer-Ru(CO)₃(L)(SiCl₃)₂ is a dissociative process, the measured ΔH[‡] may be, as mentioned previously, related to the M-CO bond-strength²⁶. However, since Darensbourg changes the leaving group, the ΔH[‡] value always changes. Therefore, it is unclear to what extent the changes in

ΔH^\ddagger are due to the different leaving group, and to what extent they are due to the cis-influence of L, the other phosphine. In the present study it was possible to clearly state that any change in ΔH^\ddagger would be due to the effect of L on the Ru-CO bond-strength.

On the surface, the results of the present study seem to contradict Brown's ideas regarding the cis-effect, namely, that the electronic properties of the cis-labilizer play the most important role²²⁻²⁴. However, Brown's work involved comparing the cis-effects of ligands with greater differences in electronic character than the ligands studied in the present work. It may be that because only phosphorus donor ligands have been examined, the electronic parameter may not have changed sufficiently to produce a measurable effect.

Brown's site preference model regards cis-labilizers as ligands which stabilize the transition state when occupying that site which is cis to the vacant site. Brown proposes that the cis-effect is mainly a transition state effect, and is not due to destabilization of the ground state.

The present work does not support this view. The effect that is observed in the present study is steric labilization, which is illustrated in Figure 24.

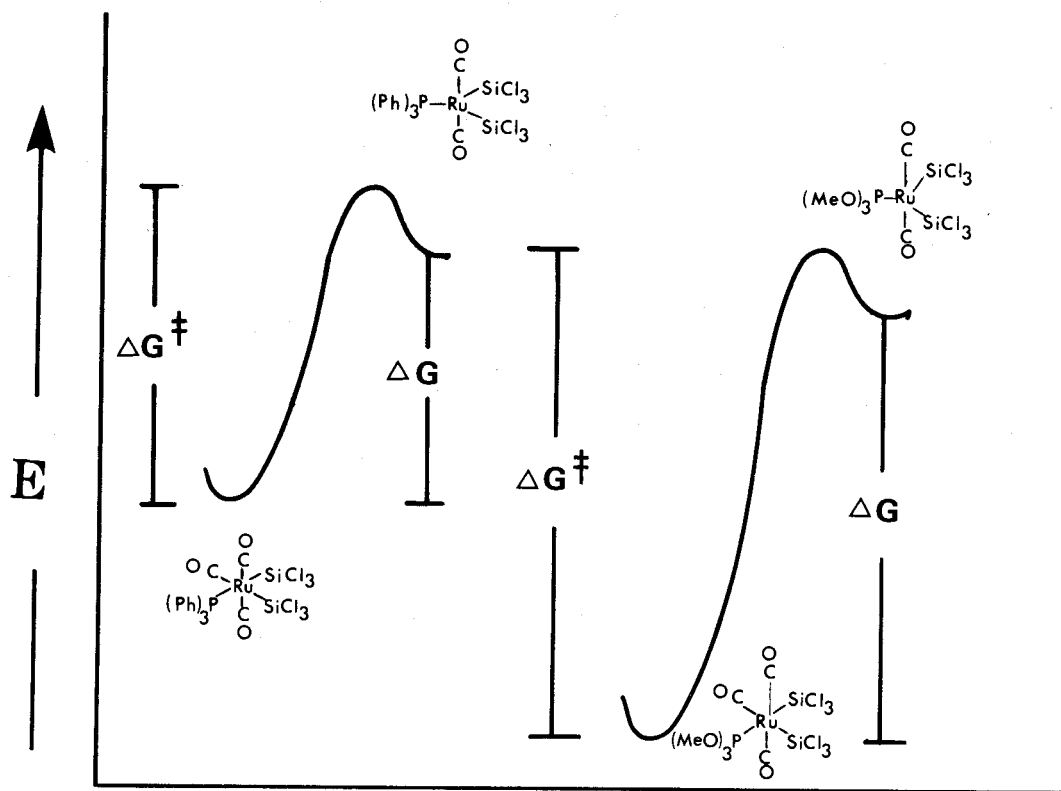


Fig. 24

An illustration of rate enhancement due to steric la-
bilization. The PPh_3 ligand destabilizes both the
ground state and the transition state, but because the
ground state is more destabilized, ΔG^\ddagger is reduced.

The large ligand (PPh_3 in Figure 24) destabilizes both the
ground state and the transition state of the complex relative to
a smaller ligand $P(OMe)_3$ in Figure 24. This destabilization is
due to steric interactions. Further, the destabilization is
more pronounced in the ground state than in the transition
state, because the ground state is six-coordinate,

while the transition state is closer to being five-coordinate. Therefore, the steric interactions in the ground state are relieved to some extent in the transition state. This is assumed to cause $\Delta G^\ddagger_{\text{PPh}_3} < \Delta G^\ddagger_{\text{P(OMe)}_3}$, as illustrated in Figure 24.

As a more general statement, rate enhancement is observed for larger ligands because the Gibbs free energy of the ground state is increased relative to the ground state of smaller ligands. Therefore, the effect observed is properly labelled a ground state effect, and the rate enhancement with larger ligands is due to relief of steric interactions in the ground state.*

* By similar arguments, Figure 24 reveals that $\Delta G_{\text{PPh}_3} < \Delta G_{\text{P(OMe)}_3}$, for the overall reaction. This relationship between ΔG for the overall reaction (from reactants to intermediate) and θ for the ligand explains the seemingly empirical relationship described earlier between $\ln k$ (ΔG^\ddagger) and θ . If θ is related to ΔG^\ddagger , as shown graphically in Figure 20, and θ is related to ΔG , as described in Figure 24, then there must exist a relationship between ΔG^\ddagger and ΔG . Therefore, this may indicate that we are measuring a true linear free energy relationship, and not an empirical LFER as was suggested previously.

It may be possible that the cis-effect, in the general case, is actually a combination of steric and electronic effects, and that only the steric effect is observed here, because the electronic properties of the ligands were not altered sufficiently. If this is the case, when the effect is electronic, Brown's transition state site preference model could be useful in explaining observations of rate enhancement. However, when the cis-effect is steric in origin, as in the system examined in the present work, the results are best explained in terms of a ground-state effect.

4.1.4 A Group of Four Exceptions to the General Pattern

Most of the ligands used in this study followed the general pattern, namely, that ΔS^\ddagger increased as the size of L increased. There were four exceptions to this pattern: the complexes of $P(OPh)_3$, $P(CH_2C_6H_5)_3$, $P(O-\underline{O}-Tol)_3$ and $PPh_2(\underline{O}-MeOPh)$. The kinetic parameters for these complexes are given in Table 15.

The strikingly different activation parameters observed for these complexes, compared to the other twenty complexes, leads one to consider other reaction pathways. One property which these ligands have in common is a structure which allows them to easily adopt, without excessive twisting or strain, a configuration where a site of electron density on the ligand may come in close proximity to the electron deficient ruthenium centre in the transition state. This configuration is illustrated in

Table 15

The results of the kinetic study of mer-Ru(CO)₃(L)(SiCl₃)₂
(where L= (P(CH₂Ph)₃, P(OPh)₃, P(O-o-Tol)₃, and PPh₂(oMeOPh))

Ligand	$k_{40^\circ\text{C}}$ $\text{s}^{-1} \times 10^6$	ΔS^\ddagger eu	ΔH^\ddagger kcal/mol	θ°	ν cm^{-1}
PPh ₂ (<u>o</u> -MeOPh)	1470	4	23.6	171	2066.1
P(CH ₂ Ph) ₃	637	1	23.0	165	2066.0
P(OPh) ₃	19.8	0	25.2	128	2085.1
P(O- <u>o</u> -Tol) ₃	15.8	-6.5	23.5	141	2084.1

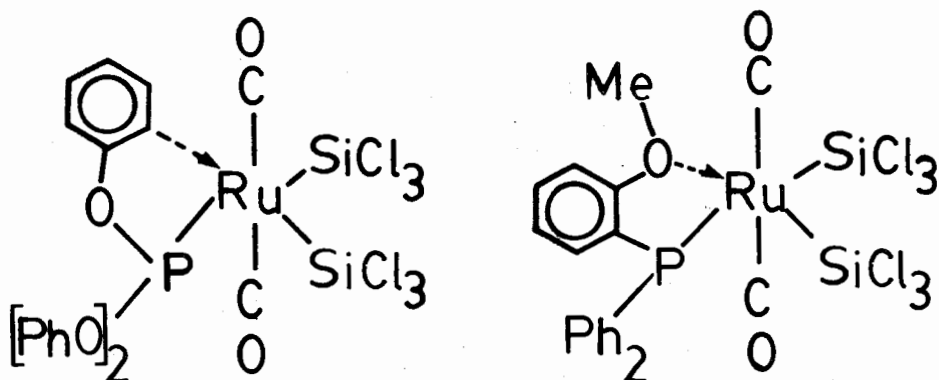


Fig. 25

Two possible conformations which may explain the anomalous results obtained for the complexes of $P(\text{CH}_2\text{C}_6\text{H}_5)_3$, $P(\text{OPh})_3$, $P(\text{O}-\underline{\text{O}}-\text{Tol})_3$ and $\text{PPh}_2(\text{o-MeOPh})$.

Figure 25.

ΔH^\ddagger for the reaction is lowered from 27.4 kcal/mol to approximately 23 kcal/mol. This suggests that the ligand is assisting in the bond-breaking process. It is significant that in each complex where this lowering of ΔH^\ddagger did occur, there is significant electron density on an atom which can act as a potential electron donor in the transition state. The ruthenium centre in the transition state will be electron deficient, because the leaving carbonyl removes two electrons from the valence shell of the metal. Therefore, it is feasible that the ligand does assist in the bond-breaking process, by stabilizing the transition state for dissociation.

The lower ΔS^\ddagger values also support this proposal. They

would be expected to be lower than that for the normal dissociation, since there is a greater degree of order in the transition state of the assisted dissociation. If the transition state incorporates a ring-like structure as in Figure 25, then the rotation about the Ru-P bond would be expected to be restricted. These stereochemical restraints would be expected to lower the value for ΔS^\ddagger .

The rate of the reaction at 40°C, calculated by extrapolating the Arrhenius curve, was within the normal range expected for these reactions. It is expected that the rate should not be less than the rate would be if there was no ligand assistance, because if there are two mechanisms open to a reactant, it is expected that the reaction will follow the pathway with lower activation energy, or a higher rate constant. Since the rates of the unassisted reactions, predicted using the results of this study, are close to the observed rate, it can be concluded that the two pathways are close in energy. It is therefore possible that the reaction proceeds via both ligand-assisted and ligand-unassisted pathways, since both supposedly have similar ΔG^\ddagger values.

Working on the hypothesis that the ligand does participate in the reaction by donating electrons to the electron deficient transition state, it was reasoned that the reaction intermediate might also be stabilized, and attempts were made to isolate the intermediate in the reaction of mer-Ru(CO)₃(L)(SiCl₃)₂ where L =

$P(OPh)_3$ and $P(\underline{o}\text{-MeOPh})_3$. The complexes were dissolved in hexane and left stirring under a closed vacuum for three days. The solution was monitored periodically by recording its IR spectrum but no products were observed. Mild irradiation was employed in the case of the $P(\underline{o}\text{-MeOPh})_3$ complex, but no products were recovered except a dark green oil which showed no CO bands in the IR spectrum and was attributed to decomposition.

Isolation of an intermediate for the ligand-assisted reaction would have been excellent support for the reaction mechanism. However, failure to isolate it does not rule out the proposed mechanism, but it does suggest that the proposed intermediate is unstable and reactive.

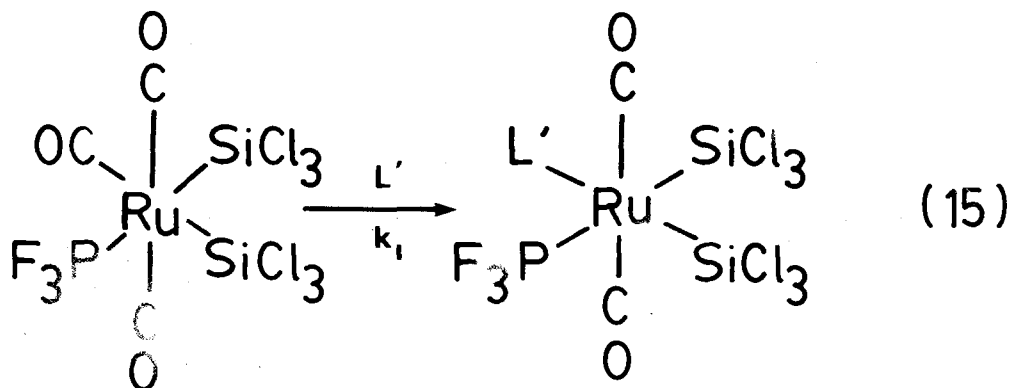
One ligand studied, $P(\underline{o}\text{-p-ClPh})_3$ has a structure which makes the ligand-assisted dissociation possible, but mer- $Ru(CO)_3[P(\underline{o}\text{-p-ClPh})_3](SiCl_3)_2$ followed the general pattern and did not show anomalous behaviour like the four complexes discussed above. The compound mer- $Ru(CO)_3[P(\underline{o}\text{-p-ClPh})_3](SiCl_3)_2$ is thought to be an exception because of the low π -electron density on the aromatic ring due to the presence of the chlorine, a strong electron-withdrawing group. This argument is supported by the fact that synthesis of bis(arene)chromium complexes is difficult when the arene is substituted by a halogen, presumably because of the lower π -electron density on the aromatic ring⁴⁰. Also, the strong electron-withdrawing ability of Cl is demonstrated in the electrophilic substitution patterns of aromatic

compounds. Halogenated aromatics are less reactive than benzene in electrophilic aromatic substitution and this is thought to be due to an inductive effect⁴¹.

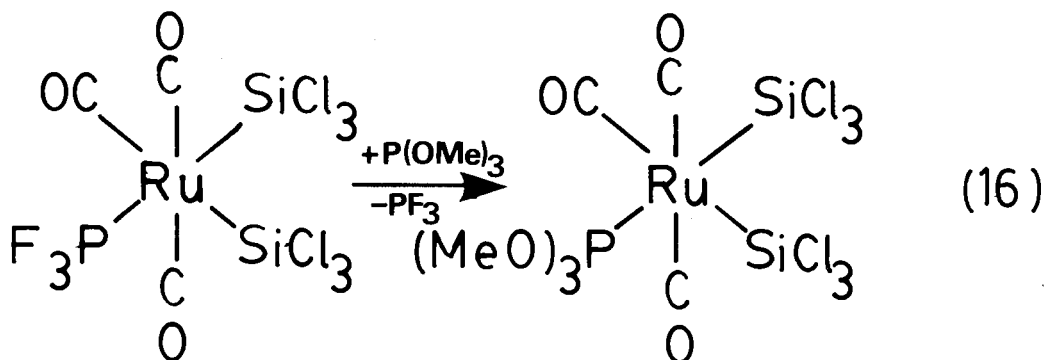
In conclusion, the anomalous kinetic results obtained with mer-Ru(CO)₃(L)(SiCl₃)₂ (L = P(CH₂C₆H₅)₃, P(OPh)₃, P(O-O-Tol)₃ and PPh₂(O-MeOPh)) can be explained by proposing that the reaction in these complexes proceeds via an associative type mechanism, one in which the complexed ligand, L, assists in the bond-breaking process. This is supported by values for the rate constants and the activation parameters, and by the observation that when the phenyl group which is thought to donate electrons to the electron-deficient metal centre is substituted by chlorine, anomalous results are not obtained, because the chlorine withdraws electrons from the aromatic ring.

4.1.5 The Results of the Kinetic Study of mer-
Ru(CO)₃(PF₃)(SiCl₃)₂

An unsuccessful attempt was made to study the rate of substitution of mer-Ru(CO)₃(PF₃)(SiCl₃)₂ (Equation 15).



At first an attempt was made to study the reaction of the PF_3 complex using $\text{P}(\text{OMe})_3$ as the entering ligand. The reaction proceeded to completion in 50 minutes at 27.5°C . The products, as determined by infrared spectroscopy, were mer- $\text{Ru}(\text{CO})_3[\text{P}(\text{OMe})_3](\text{SiCl}_3)_2$ and $\text{Ru}(\text{CO})_2(\text{PF}_3)(\text{P}(\text{OMe})_3)(\text{SiCl}_3)_2$. This indicated that mer- $\text{Ru}(\text{CO})_3(\text{PF}_3)(\text{SiCl}_3)_2$ was disappearing in two ways: (1) via Equation 15 to yield the mixed bis-substituted derivative and (2) via Equation 16 to yield the mono-substituted $\text{P}(\text{OMe})_2$ derivative.



As in Section 4.1.2, the occurrence of both reactions lead to the conclusion that PF_3 would have to be used as the entering ligand, so that Equation 16 would not contribute to the rate of disappearance of starting material and lead to falsely high values for the rate constants. In other words, the effect of the dissociation of PF_3 would be negated by using PF_3 as the entering ligand.

A special reaction vessel was designed so that PF_3 , which is a gas at room temperature, could be used as the entering ligand. The aliquots for IR spectra were withdrawn with a syringe

Table 16

Results of the experiment to measure the effect of P_{PF_3} on the rate of substitution of $mer-Ru(CO)_3(PF_3)(SiCl_3)_2$ at $54^\circ C$.

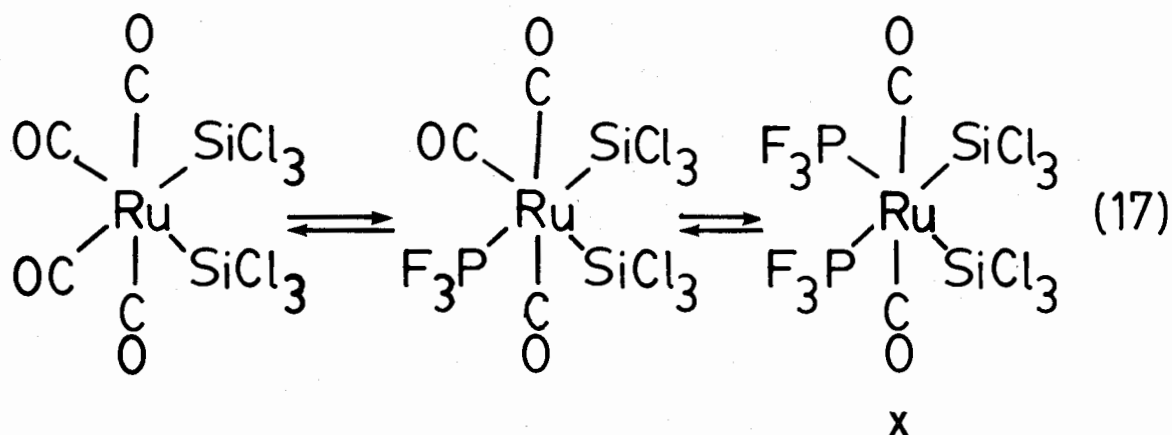
P_{PF_3} (atm)	concentration complex(mol/L)	moles PF_3	moles complex	molar ratio ligand:complex	k $s^{-1} \times 10^4$
1.3	0.052	0.0050	0.0002	25:1	4.6
1.5	0.026	0.0055	0.0001	55:1	3.7
1.5	0.026	0.0055	0.0001	55:1	5.7
1.7	0.013	0.0062	0.00005	125:1	3.3

from the closed reaction vessel which was under a positive pressure of PF_3 .

An experiment was performed to establish the pressure of PF_3 necessary to maintain pseudo-first order kinetics. A solution with a known amount of mer- $\text{Ru}(\text{CO})_3(\text{PF}_3)(\text{SiCl}_3)_2$ was reacted with a known amount of PF_3 . The amounts of PF_3 and complex were varied to alter the ligand:complex ratio, and the results are given in Table 16.

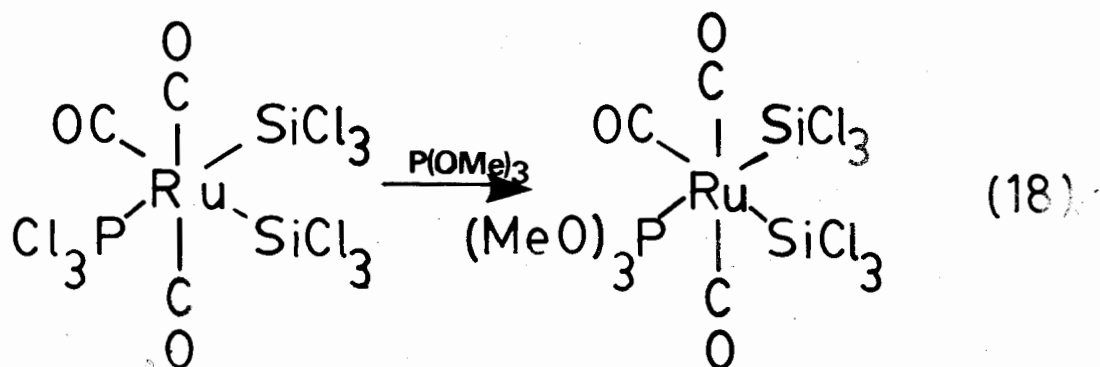
The results in Table 16 show that the rate constants are not very reproducible. In fact, even when the conditions were identical, the rate constants for the reactions differed by as much as 50%. It is unclear why the results are not reproducible. Because the method designed could not measure the rate constants at pressures higher than those in Table 16, and because the concentration of ligand could not be lowered and still measured accurately over the required time period, it was concluded that the method was not suitable for measuring the rate constant of this substitution reaction. The experiment was abandoned after repeated attempts to establish reproducibility failed.

One explanation for the non-reproducible results is that a complex equilibrium may be set up between mer- $\text{Ru}(\text{CO})_3(\text{PF}_3)(\text{SiCl}_3)_2$, $\text{Ru}(\text{CO})_2(\text{PF}_3)_2(\text{SiCl}_3)_2$ and cis- $\text{Ru}(\text{CO})_4(\text{SiCl}_3)_2$ (Equation 17).



Perhaps because the system was closed, so that CO could not escape, the PF₃ in the system could not completely drive the reaction towards X. One way to overcome this problem would be to set up a reaction vessel which was open to 1 atm pressure, and to bubble PF₃ through the solution.

Although the kinetics of the substitution of mer-Ru(CO)₃(PCl₃)(SiCl₃)₂ were not studied, a similar situation is anticipated in this system. The complex mer-Ru(CO)₃(PCl₃)(SiCl₃)₂ reacted quickly at room temperature with P(OMe)₃ to form mer-Ru(CO)₃[P(OMe)₃](SiCl₃)₂ as the only product (Equation 18).



In addition, mer-Ru(CO)₃(PCl₃)(SiCl₃)₂ did not react with PCl₃ to form Ru(CO)₂(PCl₃)₂(SiCl₃)₂. Since it is desired to study the rate of substitution of the remaining equatorial carbonyl, and since PCl₃ is more labile than CO, the cis-effect of PCl₃ could not be studied using this method.

In general, then, the cis-effect of a ligand cannot be measured in this system if it is more labile than CO. However, as in the case of ETPB, where evidence showed that the phosphorus ligand was somewhat labile, the effect of dissociation could be negated by adding excess ETPB as the entering ligand.

Experimental

4.2.1 General Kinetic Procedure

All kinetic experiments were performed according to the general procedures outlined in Sections 2.2.1 and 3.2.1, except for the study of mer-Ru(CO)₃(PF₃)(SiCl₃)₂, which will be described in Section 4.2.2. The results were analyzed according to the procedure described in Section 3.2.2. The preparation of all complexes studied has been described in Section 2.2.2.

For each complex studied, P(OMe)₃ was used as the entering ligand, except with complexes of P(O-Butⁿ)₃, P(OMe)₂Ph, ETPB, and PF₃, where the coordinated phosphorus ligand and the entering ligand were the same. Toluene was used as the reaction solvent, except in the case of mer-Ru(CO)₃(ETPB)(SiCl₃)₂, where 1,2-dichlorobenzene was used for reasons of solubility. The Arrhenius parameters, ΔH^\ddagger and ΔS^\ddagger , were calculated for each complex studied using a computer program which generates the activation parameters using the Arrhenius equation. The errors associated with these parameters are estimated to be ± 1 kcal/mol for ΔH^\ddagger and ± 3 cal/mol deg for ΔS^\ddagger . Because all the measurements were performed over a temperature range of 25°C to 80°C, it was considered unnecessary to make temperature corrections to ΔH^\ddagger and ΔS^\ddagger . Marked variation of ΔH^\ddagger with temperature, or a non-linear Arrhenius plot, is unusual for reactions of metal complexes, so that ΔH^\ddagger and ΔS^\ddagger can be compared for a series of related reactions, even if the data are obtained from different

temperature ranges⁴². The rate constants were calculated at 40°C for each complex by extrapolation of the Arrhenius plot. The results are given in Section 4.1.2, and in Table 17.

4.2.2 Kinetic Measurements of the Substitution Reaction of mer-Ru(CO)₃(PF₃)(SiCl₃)₂

All procedures followed the general procedure outlined in Section 2.2.1, except that the infrared measurements were performed on a Perkin-Elmer 599B infrared spectrometer.

A solution of cis-Ru(CO)₄(SiCl₃)₂ (0.50 g, 0.0010 mmol) in toluene (20.0 mL) was prepared in a 90 mL round bottom flask equipped with a Teflon stopper and a side arm (10 cm) to which a rubber syringe cap could be firmly attached. The solution was frozen to -196°C and the vessel was evacuated. The solution was warmed to allow any trapped gas to escape and the degassing procedure was repeated. When the vessel returned to room temperature PF₃ (1.6 atm) was added. The solution was left stirring overnight. When no cis-Ru(CO)₄(SiCl₃)₂ remained, as shown by infrared spectroscopy, the reaction was stopped by purging the flask with N₂. The solution was removed and left under N₂ in another vessel.

Known volumes of the solution, assumed to be 0.0052 M in mer-Ru(CO)₃(PF₃)(SiCl₃)₂, were delivered to the reaction vessel described above. When necessary, the solution was made up to 4 mL using known volumes of toluene. The solution was again degassed, using two freeze-thaw cycles as described above and PF₃ was added to the flask. The flask was left stirring in a

Table 17

Measured rate constants at various temperatures for all ligands studied, in the order in which they were measured.

Ligand	T°C±0.3°C	k s ⁻¹ × 10 ⁴ ± 4%	Activation Parameters
ETPB	69.8	0.82	$\Delta H^\ddagger = 28.4 \pm 0.8 \frac{\text{kcal}}{\text{mol}}$ $\Delta S^\ddagger = 5.4 \pm 2.3 \text{ eu}$ correlation coefficient = 0.999
	65.5	0.49	
	75.5	1.7	
	72.3	1.2	
	79.2	2.6	

P(OMe) ₃	71.5	4.9	$\Delta H^\ddagger = 27.4 \pm 1.3 \frac{\text{kcal}}{\text{mol}}$ $\Delta S^\ddagger = 5.4 \pm 4 \text{ eu}$ correlation coefficient = 0.994
	55.8	0.65	
	68.0	2.8	
	63.1	1.7	
	60.1	1.2	
	65.5	1.9	
	69.8	3.8	

P(OBut ⁿ) ₃	59.8	0.94	$\Delta H^\ddagger = 27.0 \pm 0.8 \frac{\text{kcal}}{\text{mol}}$ $\Delta S^\ddagger = 3.8 \pm 2 \text{ eu}$ correlation coefficient = 0.999
	68.9	2.9	
	71.9	3.8	
	64.3	1.55	
	76.9	7.2	

P(OMe) ₂ Ph	74.6	9.2	$\Delta H^\ddagger = 27.0 \pm 0.3 \frac{\text{kcal}}{\text{mol}}$ $\Delta S^\ddagger = 4.7 \pm 1 \text{ eu}$ correlation coefficient = 0.999
	77.6	13.0	
	68.7	4.6	
	64.1	2.7	

PCl ₂ Ph	55.3	7.8	$\Delta H^\ddagger = 25.2 \pm 1.1 \frac{\text{kcal}}{\text{mol}}$ $\Delta S^\ddagger = 3.8 \pm 4 \text{ eu}$ correlation coefficient = 0.996
	50.5	3.9	
	52.8	5.6	
	56.6	8.7	
	58.5	10.2	
	47.3	2.7	

Table 17 (cont.)

Ligand	T °C ± 0.3 °C	k s ⁻¹ × 10 ⁴ ± 4%	Activation Parameters
PMe ₂ Ph	66.9	6.8	$\Delta H^\ddagger = 27.5 \pm 0.4 \frac{\text{kcal}}{\text{mol}}$ $\Delta S^\ddagger = 7.5 \pm 1 \text{ eu}$ correlation coefficient = 0.999
	71.0	1.08	
	64.0	4.7	
	59.8	2.8	
	55.5	1.6	
P(O-p-ClPh) ₃	70.6	8.3	$\Delta H^\ddagger = 28.5 \pm 1.3 \frac{\text{kcal}}{\text{mol}}$ $\Delta S^\ddagger = 10 \pm 4 \text{ eu}$ correlation coefficient = 0.996
	59.2	1.8	
	63.0	3.3	
	69.6	6.9	
	65.6	4.3	
	61.1	2.5	
P(OPh) ₃	53.0	0.92	$\Delta H^\ddagger = 25.2 \pm 0.6 \frac{\text{kcal}}{\text{mol}}$ $\Delta S^\ddagger = 0.2 \pm 2 \text{ eu}$ correlation coefficient = 0.999
	66.7	4.4	
	69.9	6.8	
	60.0	2.2	
	63.0	3.0	
P(CH ₂ CH=CH ₂) ₃	59.0	2.7	$\Delta H^\ddagger = 27.2 \pm 0.9 \frac{\text{kcal}}{\text{mol}}$ $\Delta S^\ddagger = 7 \pm 2.5 \text{ eu}$ correlation coefficient = 0.999
	64.6	5.5	
	55.7	1.8	
	60.7	3.6	
	67.1	7.4	
P(nBut) ₃	59.5	2.3	$\Delta H^\ddagger = 28.8 \pm 0.8 \frac{\text{kcal}}{\text{mol}}$ $\Delta S^\ddagger = 11 \pm 2.5 \text{ eu}$ correlation coefficient = 0.998
	71.6	10.8	
	64.8	4.6	
	65.0	4.7	
	62.0	3.2	
	66.9	5.8	
	67.0	6.5	

Table 17 (cont.)

Ligand	T°C±0.3°C	k s ⁻¹ x10 ⁴	Activation Parameters
P(OMe)Ph ₂	57.1	2.4	$\Delta H^\ddagger = 27.5 \pm 1.3 \frac{\text{kcal}}{\text{mol}}$ $\Delta S^\ddagger = 8 \pm 4 \text{ eu}$ correlation = 0.996 coefficient
	64.1	6.1	
	66.6	8.6	
	60.3	3.7	
	68.3	9.3	
PMePh ₂	51.7	3.7	$\Delta H^\ddagger = 27.4 \pm 0.2 \frac{\text{kcal}}{\text{mol}}$ $\Delta S^\ddagger = 10 \pm 1 \text{ eu}$ correlation = 0.999 coefficient
	54.6	5.3	
	44.7	1.4	
	48.0	2.2	
	57.5	7.8	
PClPh ₂	50.3	6.7	$\Delta H^\ddagger = 26.5 \pm 0.6 \frac{\text{kcal}}{\text{mol}}$ $\Delta S^\ddagger = 8.5 \pm 2 \text{ eu}$ correlation = 0.999 coefficient
	46.2	4.0	
	53.8	1.0	
	42.0	2.1	
P(o-o-Tol) ₃	54.1	0.82	$\Delta H^\ddagger = 23.2 \pm 1.6 \frac{\text{kcal}}{\text{mol}}$ $\Delta S^\ddagger = -6.5 \pm 5 \text{ eu}$ correlation = 0.985 coefficient
	67.7	3.1	
	72.6	5.9	
	69.9	4.6	
	65.2	2.0	
	60.6	1.4	
	57.4	1.15	
65.6	2.7		
PPh ₃	44.5	16.1	$\Delta H^\ddagger = 27.2 \pm 0.68 \frac{\text{kcal}}{\text{mol}}$ $\Delta S^\ddagger = 14 \pm 2 \text{ eu}$ correlation = 0.999 coefficient
	39.5	8.6	
	30.0	2.0	
	35.1	4.3	
P(p-CH ₃ Ph) ₃	30.0	1.9	$\Delta H^\ddagger = 27.0 \pm 1.0 \frac{\text{kcal}}{\text{mol}}$ $\Delta S^\ddagger = 13 \pm 3 \text{ eu}$ correlation = 0.998 coefficient
	40.7	8.4	
	37.5	5.7	
	34.2	3.6	
	44.6	1.7	

Table 17 (cont.)

Ligand	T °C ± 0.3 °C	k s ⁻¹ × 10 ⁴	Activation Parameters
P(<u>p</u> -ClPh) ₃	41.2	8.2	$\Delta H^\ddagger = 27.0 \pm 2 \frac{\text{kcal}}{\text{mol}}$ $\Delta S^\ddagger = 13 \pm 6 \text{ eu}$ correlation = 0.988 coefficient
	37.6	4.6	
	43.1	10.8	
	39.9	6.4	
	34.8	3.7	
	38.0	4.6	
	31.9	2.0	

P(<u>p</u> -MeOPh) ₃	30.8	2.1	$\Delta H^\ddagger = 26.8 \pm 1 \frac{\text{kcal}}{\text{mol}}$ $\Delta S^\ddagger = 13 \pm 4 \text{ eu}$ correlation = 0.997 coefficient
	37.0	5.0	
	42.0	1.0	
	34.5	3.2	
	39.5	7.0	

P(<u>p</u> -FPh) ₃	46.0	1.7	$\Delta H^\ddagger = 27.0 \pm 1 \frac{\text{kcal}}{\text{mol}}$ $\Delta S^\ddagger = 13 \pm 3 \text{ eu}$ correlation = 0.999 coefficient
	40.0	7.4	
	36.5	4.9	
	31.5	2.1	

PPh ₂ (<u>i</u> -Pr)	51.5	3.4	$\Delta H^\ddagger = 28.7 \pm 0.8 \frac{\text{kcal}}{\text{mol}}$ $\Delta S^\ddagger = 14 \pm 2 \text{ eu}$ correlation = 0.998 coefficient
	56.5	6.3	
	59.2	9.4	
	47.2	1.8	
	58.7	9.7	
	54.1	4.7	
	56.5	6.7	
	59.9	11.0	
	49.8	2.8	

P(<u>m</u> -CH ₃ Ph) ₃	30.7	3.2	$\Delta H^\ddagger = 27.5 \pm 0.4 \frac{\text{kcal}}{\text{mol}}$ $\Delta S^\ddagger = 16 \pm 2 \text{ eu}$ correlation = 0.999 coefficient
	36.4	7.4	
	40.8	14.0	
	27.2	1.8	

Table 17 (cont.)

Ligand	T°C±0.3°C	k s ⁻¹ x10 ⁴	Activation Parameters
P(<u>m</u> -ClPh) ₃	39.0	8.7	$\Delta H^\ddagger = 28.7 \pm 1 \frac{\text{kcal}}{\text{mol}}$ $\Delta S^\ddagger = 19 \pm 3 \text{ eu}$ correlation=0.998 coefficient
	25.0	0.85	
	31.0	2.5	
	35.2	4.5	
	42.5	1.3	
P(CH ₂ Ph) ₃	51.5	25.5	$\Delta H^\ddagger = 23.1 \pm 1 \frac{\text{kcal}}{\text{mol}}$ $\Delta S^\ddagger = 0.7 \pm 3 \text{ eu}$ correlation=0.997 coefficient
	39.0	5.4	
	35.5	3.3	
	29.0	1.7	
	44.0	10.8	
PPh ₂ (<u>o</u> -MeOPh)	28.0	3.2	$\Delta H^\ddagger = 23.6 \pm 0.3 \frac{\text{kcal}}{\text{mol}}$ $\Delta S^\ddagger = 4 \pm 1 \text{ eu}$ correlation= 0.999 coefficient
	32.1	5.4	
	38.5	12.2	
	24.9	2.0	
	35.2	8.2	

constant temperature bath. Aliquots of solution were removed with a syringe periodically to measure the rate of disappearance of mer-Ru(CO)₃(PF₃)(SiCl₃)₂ by infrared spectroscopy. By altering the number of moles of complex delivered to the vessel and the pressure of PF₃, the ligand:complex ratio was varied from 25:1 to 125:1. The results are given in Section 4.1.4.

4.2.3 Kinetic Measurements of the Substitution Reaction of mer-Ru(CO)₃(ETPB)(SiCl₃)₂

Because of solubility problems, mer-Ru(CO)₃(ETPB)(SiCl₃)₂ was studied in 1,2-dichlorobenzene, rather than toluene. It was necessary to test that this did not affect the results, and the rate of substitution of mer-Ru(CO)₃[PPh₂(i-Pr)](SiCl₃)₂ was measured in toluene and in 1,2-dichlorobenzene at the same temperature. At 52.3°C the rate of substitution of mer-Ru(CO)₃(PPh₂(i-Pr))(SiCl₃)₂ was found to be $4.59 \times 10^{-4} \text{ s}^{-1}$ in 1,2-dichlorobenzene and $4.54 \times 10^{-4} \text{ s}^{-1}$ in toluene. It was concluded that 1,2-dichlorobenzene did not produce a detectable change in the reaction rate.

APPENDIX I

Tolman's Cone Angle, θ , for Phosphorus Donor Ligands

Ligand	θ°
PH_3	87
$\text{P}(\text{OCH}_2)_3\text{CC}_2\text{H}_5$	101
PF_3	104
$\text{P}(\text{OMe})_3$	107
$\text{P}(\text{OC}_2\text{H}_5)_3$	109
$\text{P}(\text{OMe})_2\text{Ph}$	115
$\text{P}(\text{OEt})_3\text{Ph}$	116
PMe_3	118
PMe_2Ph	122
PCl_3	124
$\text{P}(\text{OPh})_3$	128
$\text{P}(\text{O-}p\text{-CH}_3\text{C}_6\text{H}_4)_3$	128
$\text{P}(\underline{i}\text{-Pr})_3$	130
$\text{P}(\text{But}^n)_3$	132
$\text{P}(\text{OMe})\text{Ph}_2$	132
$\text{P}(\text{OEt})\text{Ph}_2$	133
PMePh_2	136
$\text{P}(\text{CF}_3)_3$	137
$\text{P}(\text{O-}o\text{-MeC}_6\text{H}_4)_3$	141
PPh_3	145
$\text{PPh}_2(\underline{i}\text{-Pr})$	150
$\text{PPh}_2(\text{But}^t)$	157
$\text{P}(\underline{i}\text{-Pr})_3$	160
PBz_3	165
PCy_3	170
$\text{P}(\text{But}^t)_3$	182
$\text{P}(\underline{o}\text{-Tol})_3$	194

Cone angles of Ligands not bound by a group 5 atom

H	75
Me	90
CO	95
Ph	105

APPENDIX II

Tolman's Electronic Parameter for Phosphorus Donor Ligands

Ligand	ν cm ⁻¹
P(But ^t) ₃	2056.1
P(<u>o</u> -MeOC ₆ H ₄) ₃	2058.3
P(But ⁿ) ₃	2060.3
PMe ₃	2064.1
PMe ₂ Ph	2065.3
P(<u>p</u> -MeOPh) ₃	2066.1
PPh ₂ (<u>o</u> -MeoPh)	2066.1
PBz ₃	2066.4
P(<u>o</u> -Tol) ₃	2066.6
P(<u>p</u> -Tol) ₃	2066.7
PMePh ₂	2067.0
P(<u>m</u> -Tol) ₃	2067.2
PPh ₃	2068.9
P(CH=CH ₂) ₃	2069.5
P(<u>p</u> -FPh) ₃	2071.3
P(OEt)Ph ₂	2071.6
P(OMe)Ph ₂	2072.0
P(<u>p</u> -ClPh) ₃	2072.8
P(OEt) ₂ Ph	2074.2
P(O- <u>i</u> -Pr) ₃	2975.9
P(OEt) ₃	2076.3
P(OMe) ₃	2079.5
PClPh ₂	2080.7
PH ₃	2083.2
P(O- <u>o</u> -Tol) ₃	2084.1
P(OPh) ₃	2085.3
P(OCH ₂) ₃ CEt	2086.8
P(<u>p</u> -ClC ₆ H ₄) ₃	2089.3
P(C ₆ F ₅) ₃	2090.9
PCl ₂ Ph	2092.1
PCl ₃	2097.0
PF ₃	2110.8

Appendix III
Infrared Data for $\text{LRu}(\text{CO})_3(\text{SiCl}_3)_2$ Complexes²⁹

L $\nu(\text{CO})\text{cm}^{-1}$
 CH_2Cl_2 soln.

PF_3^{a}	2138w, 2096m, 2081s
ETPB	2133w, 2089m, 2068s
$\text{P}(\text{OPh})_3$	2124w, 2077m, 2064s
$\text{P}(\text{OMe})_3$	2123w, 2082m, 2055s
$\text{P}(\text{OEt})_3$	2122w, 2081m, 2054s
PPh_3	2117w, 2075m, 2050s
AsPh_3	2118w, 2072m, 2049s
SbPh_3	2114w, 2070m, 2047s
PPh_2Me	2115w, 2072m, 2046s
PPhMe_2	2117w, 2075m, 2049s
$\text{P}(\text{o-C}_6\text{H}_4\text{CH}_3)_3$	2111w, 2066m, 2041s
$\text{P}(\text{n-C}_4\text{H}_9)_3$	2112w, 2062m, 2044s
$\text{P}(\text{C}_6\text{H}_{11})_3$	2106w, 2056m, 2037s

a = in hexane solution

References

- 1 Wilkins, R.G. "The Study of Kinetics and Mechanism of Reactions of Transition Metal Complexes"; Allyn and Bacon:Boston, 1974,p.229.
- 2 Tobe, M.L. " Inorganic Reaction Mechanisms";Nelson:Southampton, Great Britain, 1972, pp. 58,88.
- 3 ibid., p.55.
- 4 Huheey, J.E. "Inorganic Chemistry, 2nd Ed.";Harper and Row:New York, 1978, pp. 498-503.
- 5 Pomeroy, R.K.; Gay, R.S.; Evans. G.O.; Graham, W.A.G. J. Am. Chem Soc. 1972, 94, 272.
- 6 Wijesekera, K.S.; Pomeroy, R.K. Inorg. Chem. 1980,19,3729.
- 7 Bent, H.A. Chem. Rev. 1977, 1961,61,275. See also Huheey, J.E. "Inorganic Chemistry" Harper and Row:New York, 1972, pp. 132-133, 162-163.
- 8 Tolman, C.A. Chem. Rev. 1977, 77, 313.
- 9 Alyea, E.C.; Dias, S.A.; Ferguson, G.; Restivo, R.J. J. Chem. Soc., Dalton. Trans. 1977, 1845.
- 10 Tolman, C.A. J. Am. Chem. Soc. 1970, 92,2956.
- 11 Ferguson, G.; Roberts, P.J.; Alyea, E.C.; Khan, M. Inorg. Chem. 1978, 17, 2956.
- 12 Alyea, E.C.; Dias, S.A.; Ferguson, G.;Restivo, R.J. Inorg. Chem. 1978, 16, 2329.
- 13 Huheey, J.E. "Inorganic Chemistry, 2nd Ed."; Harper and Row:New York, 1978, pp. 405-406.
- 14 Strohmeier, W.; Muller, F.J. Chem. Ber. 1967, 100,2812.
- 15 Bodner, G.M.; May, M.P.; McKinney, L.E. Inorg. Chem. 1980, 19, 1951.
- 16 For more comprehensive reviews see ref. 8 or Mason,R.; Meek, D.W. Angew. Chem. Int. Ed. Eng. 1978, 78,183.
- 17 Stephens, F.S. J. Chem. Soc., Dalton Trans. 1974,1067.
- 18 Campbell, I.C.S.; Stephens, F.S. J. Chem. Soc. ,Dalton, Trans.1975,340.
- 19 Campbell, I.C.S.; Stephens, F.S. J. Chem. Soc. , Dalton Trans. 1975, 337.
- 20 Tolman, C.A. et al J. Organomet. Chem. 1976, 117, C30.
- 21 Schenkluhn, H.; Scheidt, W.; Weirman, B.; Zahres, M. Angew. Chem Int.

Ed. Eng. 1979, 18, 401.

- 22 Atwood, J.D.; Brown, T.L. J. Am. Chem. Soc. 1975, 97, 3380.
- 23 Atwood, J.D.; Brown, T.L. J. Am. Chem. Soc. 1976, 98, 3155.
- 24 Atwood, J.D.; Brown T.L. J. Am. Chem. Soc. 1976, 98, 3160.
- 25 Lichtenberger, D.L.; Brown, T.L. J. Am. Chem. Soc. 1978, 100, 366.
- 26 Darensbourg, D.J.; Graves, A.H. Inorg. Chem. 1979, 18, 1254.
- 27 Woukulich, M.J.; Feinberg, S.J.; Atwood, J.D. Inorg Chem. 1980, 19, 2608.
- 28 Varenkamp, H. Chem. Ber. 1971, 104, 449.
- 29 Wijesekera, K.S. M.Sc. Thesis, Simon Fraser University, 1980.
- 30 Jetz, W.; Graham, W.A.G. J. Am. Chem. Soc. 1967, 89, 2773.
- 31 Cotton, F.A.; Marks, T.J. J. Am. Chem. Soc. 1969, 91, 7323.
- 32 Dalton, J. Inorg. Chem. 1972, 11, 915.
- 33 Wilkinson, G.; Cotton, F.A. "Advanced Inorganic Chemistry, 4th Ed." Wiley: Interscience: New York, 1981, p.1077.
- 34 Meriwether, L.S.; Leto, J.R. J. Am. Chem. Soc. 1961, 83, 3192.
- 35 Tolman, C.A. Quart. Rev. 1972, 337.
- 36 Langford, C.H.; Gray, H.B. "Ligand Substitution Processes"; W.A. Benjamin: New York, 1965, Chapter 1.
- 37 Gill, D.F.; Mann, B.E.; Shaw, B.L. J. Chem. Soc., Dalton Trans. 1973, 312. Also see Bodner, G.M. Inorg. Chem. 1975, 14, 2694.
- 38 Wilkins, R.G. "The Study of Kinetics and Mechanism of Reactions of Transition Metal Complexes; Allyn and Bacon: Boston, 1974, pp. 88-96.
- 39 An example of an empirical LFER is the Swain-Scott relationship which relates nucleophilicity of ligands to the rate of substitution in square planar complexes, ibid., p. 96.
- 40 Skell, P.S.; Williams-Smith, D.L.; McGlinchey, M.J. J. Am. Chem. Soc. 1972, 93, 3337.
- 41 Morrison, R.; Boyd, R. "Organic Chemistry, 3rd Ed."; Allyn and Bacon: Boston, 1973, p. 365.
- 42 Wilkins, R.G. "The Study Of Kinetics and Mechanism of Reactions of Transition Metal Complexes"; Allyn and Bacon: Boston, 1974, p.84.